

**DESIGN AND DEVELOPMENT OF MECHANICALLY
CONTROLLED ABOVE KNEE PROSTHESIS**

MD. SAYEM HOSSAIN BHUIYAN

**THESIS SUBMITTED IN FULFILLMENT OF THE
REQUIREMENTS FOR THE DEGREE OF DOCTOR OF
PHILOSOPHY**

**FACULTY OF ENGINEERING
UNIVERSITY OF MALAYA
KUALA LUMPUR**

2017

UNIVERSITY MALAYA

ORIGINAL LITERARY WORK DECLARATION

Name of Candidate: **Md. Sayem Hossain Bhuiyan**

Registration/Matric No: **KHA120107**

Name of Degree: **Doctor of Philosophy**

Title of Project Paper/Research Report/Dissertation/Thesis ("this work"): **Design and Development of Mechanically Controlled Above Knee Prosthesis**

Field of Study: **Automation, Control & Robotics**

I do solemnly and sincerely declare that:

- (1) I am the sole author/writer of this Work;
- (2) This Work is original;
- (3) Any use of any work in which copyright exists was done by way of fair dealing and for permitted purposes and any excerpt or extract form, or reference to or reproduction of any copyright work has been disclosed expressly and sufficiently and the title of the Work and its authorship have been acknowledged in this Work;
- (4) I do not have any actual knowledge nor do I ought reasonably to know that the making of this work constitutes an infringement of any copyright work;
- (5) I hereby assign all and every rights in the copyright of this Work to the University of Malaya ("UM"), who henceforth shall be owner of the copyright in this Work and that any reproduction or use in any form or by any means whatsoever is prohibited without the written consent of UM having been first had and obtained;
- (6) I am fully aware that if in the course of making this Work I have infringed any copyright whether intentionally or otherwise, I may be subjected to legal action or any other action as may be determined by UM.

Candidate's Signature

Date:

Subscribed and solemnly declared before,

Witness's Signature

Date:

Name:

Designation:

ABSTRACT

A mechanically controlled prosthesis is designed and developed to enhance the controllability of the conventional passive type prosthesis within an affordable price. Unlike to the typical mechanical prosthesis, the new design has made the prosthesis to follow the residual limb movements without having any intricate guiding arrangement. A gear based knee joint has made the prosthesis to move according to the residual limb movement. A spring based ankle joint, on the other hand, helped the amputee to overcome the difficulties in producing required flexion and extension in their prosthetic feet. It also expedited the energy storing and returning quality of the prosthetic ankle. A torsion spring has enabled the ankle joint to rotate in a controlled way to any desired angle without demanding any additional setup. The gear based knee joint is designed to improve the performance of mechanical type above-knee prostheses. The gear set with some bracing, and bracket arrangement is used to enable the prosthesis to follow the residual limb movement. The proposed design of the ankle joint would enable the mechanical type ankle joint to overcome the limitation of stability, flexion and extension within an affordable price. This would enhance the range of motion of the mechanical type prosthesis without incorporating any expensive electronic devices into the ankle joint. Unlike the typical mechanical prosthesis, the new design would allow the prosthesis to bend forward and backward to any desired angle with enough stability. The pattern of the prosthetic gait cycle shows that the spring based ankle joint could imitate the movement of the prosthesis closely to the biological limb. The motion analysis and finite-element analysis (*FEA*) of knee joint and ankle joints components were carried out to assess the feasibility of the design. The *FEA* results were then compared with the real data obtained from the healthy subject. Stability analysis under disturbance and gait analysis during walking with the prosthesis was carried out to test

the performance of the prosthesis. According to the simulation results, the patterns of kinematic and kinetic parameters profiles have shown a great resemblance with that of the gait cycle of a healthy biological limb. The factor of safety obtained from the stress analysis results of *FEA* was 3.5 and 4.9 for knee joint and ankle joint components respectively, which indicated to no possibility of design failure. From the performance analysis results, though the exact shape and amplitude of the motion analysis results were deviated 0.5 to 14 times than the healthy gait cycle data, the trend of the curves were still in good agreement. At dynamic platform setting, the overall postural stability was found to improve by 3.3 to 5 times, and fall risk was observed to increase by 1.2 to 3.3 times while using prosthesis; whereas at static platform setting, the postural stability and fall risk performances were found to decline by 1.3 times and by 1.8 times respectively. Finally, the cost of quasi-active type above knee prosthesis designed for a lower limb amputee was found considerably cheap and thus affordable for mass proportion of amputee.

ABSTRAK

Satu sistem kawalan mekanikal prosthesis telah direka bentuk dan dilaksanakan untuk meningkatkan kawalan prosthesis jenis pasif konvensional dengan harga yang berpatutan. Berbeza dengan prosthesis mekanikal yang umum, reka bentuk baru telah membuat prosthesis untuk mengikuti pergerakan sisa anggota badan tanpa sebarang pergerakan yang rumit. Pengenalan sendi lutut berasaskan gigi roda telah menggerakkan prosthesis berpandukan kepada pergerakan sisa anggota badan. Di samping itu, spring berpangkalan di pergelangan kaki dapat membantu orang kehilangan anggota badan mengatasi kesukaran untuk renggang dan lanjutan pada kaki prosthesis. Ia juga dapat mempercepatkan penyimpanan tenaga dan kualiti pembahagi pergelangan kaki prosthesis. Spring kilasan telah membolehkan sendi pergelangan kaki untuk berputar dengan cara terkawal pada sudut yang dikehendaki tanpa memerlukan persediaan tambahan. Sendi lutut berasaskan gigi roda direka untuk meningkatkan prestasi prosthesis jenis mekanikal di bahagian atas lutut. Set gigi roda dengan pengaman dan aturan pendakap telah diguna pakai untuk membolehkan prosthesis bergerak berdasarkan sisa anggota badan. Reka bentuk pergelangan kaki yang dicadangkan membolehkan pergelangan kaki jenis mekanikal untuk mengatasi kelemahan dari segi kestabilan, renggang dan lanjutan pada kadar berpatutan. Ini dapat meningkatkan pelbagai gerakan prosthesis jenis mekanikal tanpa menggunakan alat-alat peranti elektronik yang mahal di dalam pergelangan kaki. Berlainan dengan prosthesis mekanikal yang umum, reka bentuk baru membolehkan untuk bengkokkan prosthesis ke hadapan dan ke belakang dengan keadaan yang kestabilan yang mencukupi. Corak perjalanan prosthesis menunjukkan bahawa spring berpangkalan di pergelangan kaki hampir menyerupai pergerakan anggota badan yang sebenar. Analisis pergerakan dan analisis "Finite-element" (*FEA*) terhadap komponen sendi lutut dan sendi pergelangan

kaki telah dilaksanakan untuk menilai reka bentuk tersebut. Hasil analisis *FEA* telah dibandingkan dengan data sebenar yang diperolehi dari subjek yang sihat. Ujian kestabilan dalam suasana gangguan dan ujian corak perjalanan dengan prosthesis juga telah dilaksanakan untuk menilai prestasi prosthesis. Menurut hasil kajian simulasi, corak pergerakan kinematik dan kinetik telah menunjukkan persamaan yang tinggi berbanding dengan corak perjalanan seseorang yang mempunyai anggota badan yang sihat. Faktor keselamatan yang diperolehi daripada keputusan analisis *FEA* adalah 3.5 dan 4.9 pada komponen sendi lutut dan sendi pergelangan kaki, dengan itu menunjukkan bahawa tiada kebarangkalian kegagalan pada reka bentuk. Prestasi analisis menunjukkan walaupun bentuk dan amplitud yang tepat, hasil analisis gerakan telah menyimpang 0.5 hingga 14 kali berbanding corak perjalanan sihat. Walaubagaimanapun hasil kajian masih diterima pakai. Pada penetapan platform yang dinamik, kestabilan postur didapati meningkat sebanyak 3.3 hingga 5 kali, dan risiko untuk jatuh telah meningkat sebanyak 1.3 kali; manakala pada platform static, prestasi kestabilan postur dan kebarangkalian untuk jatuh menurun sebanyak 1.3 kali dan 1.8 kali. Kesimpulan, harga reka bentuk prosthesis di bahagian atas lutut bagi orang tanpa anggota badan didapati lebih rendah dan berpatutan untuk posisi orang kurang upaya.

ACKNOWLEDGEMENT

At the very first I would like to thank Almighty Allah for helping me out to successfully finish my work.

This thesis is based on a research work carried out at workshop, body performance lab, and motion analysis lab, University of Malaya, Malaysia, from February 2013 until June 2016, under the supervision of Prof. Dr. Imtiaz Ahmed Choudhury and Dr. Mahidzal Bin Dahari. I greatly appreciate the learning opportunity that they gave me through these years. Besides, I would like express my sincere gratitude to them for their valuable suggestions, advices, criticisms and comments on this research.

Moreover, I would like to thank University of Malaya for providing me financial support with grants UM.C/HIR/MOHE/ENG/28 (D000028-16001) and UMRG (RP010B - 13AET) to carry out this research. I am grateful to Dr. Nukman Bin Yusoff for supporting me with his grant and thus making me complete my research work without any interruption. Furthermore, I would like to express my gratitude to the scientific officers and technicians of different labs I used during my work for assisting me in fabrication and testing the prosthesis.

Finally, I would like to thank my family especially my parents and siblings for their encouragement and support.

TABLE OF CONTENT

ABSTRACT	iii
ABSTRAK	v
ACKNOWLEDGEMENT	vii
TABLE OF CONTENT	viii
LIST OF TABLES	xii
LIST OF FIGURES	xv
LIST OF APPENDICES	xxiv
CHAPTER 1: INTRODUCTION	1
1.1 Background of the study	1
1.2 Aim of study	3
1.3 Objectives	4
1.4 Importance of study and research motivation	4
1.5 Scope of study	6
1.6 Thesis outline	6
CHAPTER 2: LITERATURE REVIEW	8
2.1 Gait cycle movement of human lower limb	9
2.2 Biomechanics of lower limb joints	12
2.3 Mechanically controlled prosthesis and other types	16
2.4 Prosthesis design and development	25
2.4.1 Components of prosthesis	25
2.4.2 Design of an above knee prosthesis	26
2.4.3 Simulation and finite-element analysis	29
2.4.4 Prosthesis construction	32
2.4.5 Performance testing	37

2.4.6. Literature Summary	44
CHAPTER 3: METHODOLOGY	45
3.1 Capturing gait cycle of healthy lower limb	51
3.2 Measuring stability index of healthy individual	54
3.3 Material selection	56
3.4 Designing the prosthetic components.....	57
3.5 Modeling and simulation of prosthetic joints.....	58
3.6 Fabrication of prosthesis	59
3.7 Performance testing.....	60
CHAPTER 4: DESIGN OF PROSTHESIS.....	65
4.1 Design of prosthetic knee joint.....	65
4.2 Design of prosthetic ankle joint.....	77
4.2.1. Compression spring design.....	81
4.2.2. Torsional spring design.....	84
4.3 Design of the above knee prosthesis	89
CHAPTER 5: RESULTS AND DISCUSSIONS	95
5.1 Gait analysis of healthy lower limb.....	95
5.1.1 Kinematic analysis	98
5.1.2 Kinetic analysis	105
5.2 Stability test of healthy individual.....	111
5.2.1 Postural Stability test	111
5.2.2 Fall risk test.....	114
5.3 Finite element analysis of prosthesis components.....	115
5.3.1 Finite element analysis of knee joint components	115
5.3.1.1 Knee joint model	116
5.3.1.2 FEA results of knee joint components.....	122

5.3.2	Finite element analysis of ankle joint components	125
5.3.2.1	Ankle joint model	125
5.3.2.2	FEA results of ankle joint components	130
5.4	Simulation results of the prosthesis joints	136
5.4.1	Results of kinematic analysis	137
5.4.2	Results of kinetic analysis	146
5.5	Gait analysis of lower limb prosthesis	149
5.5.1	Kinematic analysis	151
5.5.2	Kinetic analysis	159
5.6	Stability test of the subject with prosthesis	166
5.6.1	Postural Stability test	166
5.6.2	Fall risk test	168
5.7	Performance analysis of the prosthesis	169
5.7.1	Kinematic performance analysis	169
5.7.2	Kinetic performance analysis	174
5.7.3	Stability performance analysis:	179
5.7.3.1	Postural Stability performance	180
5.7.3.2	Fall risk performance	180
5.8	Cost analysis of the prosthesis development	182
CHAPTER 6: CONCLUSIONS AND RECOMMENDESTIONS		183
6.1	Conclusions	183
6.2	Recommendations	185
REFERENCES		186
LIST OF PUBLICATIONS		194
APPENDICES		195
APPENDIX A: STATISTICAL DATA		195

APPENDIX B: DESIGN CALCULATION	198
APPENDIX B1: GEAR SET DESIGN CALCULATION.....	198
APPENDIX B2: COMPRESSION SPRING DESIGNCALCULATION.....	209
APPENDIX B3: TORSIONAL SPRING DESIGN CALCULATION.....	215
APPENDIX C: MATERIALS.....	221
APPENDIX D: DESIGN MATERIALS.....	222
APPENDIX E: GAIT CYCLE DATA.....	234

University of Malaya

LIST OF TABLES

Table 2.1: The different phases of gait cycle of human lower limb during level ground walking (Rajtůková et al., 2014)	9
Table 2.2: A comparison among different type of prosthesis	22
Table 2.3: Steps of prosthesis construction (Rajtůková, et al. 2014)	35
Table 3.1: Subject characteristics and anthropometrical data	51
Table 3.2: Foot placement of healthy individual on the platform of Biodex Balance machine	55
Table 3.3: Material used for making knee joint components.....	56
Table 3.4: Material used for making ankle joint components.....	56
Table 3.5: Components of prosthesis	57
Table 3.6: Process and machine used in making prosthesis components	59
Table 3.7: Characteristics and anthropometrical variable of subject with prosthesis.....	62
Table 3.8: Foot placement of subject with prosthesis on the platform of Biodex Balance machine.....	63
Table 4.1: Dimensions of different knee joint components	76
Table 4.2: Dimensions of different ankle joint components	88
Table 5.1: Gait analysis data from normal speed walking of healthy individual	96
Table 5.2: Events involved in lower limb gait during normal speed walking	97
Table 5.3: Postural stability analysis of healthy individual	113
Table 5.4: Fall risk test of healthy individual	114
Table 5.5: Key features of finite element modeling of knee joint components	117
Table 5.6: Boundary conditions of knee joint simulation	120

Table 5.7: Key features of finite element modeling of ankle joint components	126
Table 5.8: Boundary conditions of ankle joint simulation.....	129
Table 5.9: Boundary conditions of knee joint simulation.....	137
Table 5.10: Boundary conditions of ankle joint simulation.....	139
Table 5.11: Gait analysis data from normal speed walking of subject with prosthesis.....	150
Table 5.12: Real events involved in prosthesis gait during normal speed walking.....	151
Table 5.13: Postural stability analysis of subject with prosthesis.....	167
Table 5.14: Fall risk test of subject with prosthesis.....	168
Table 5.15: Cost of prototype development.....	182
Table A1: Prices of different type of prosthesis available for amputees (Mc Gimpsey and Brandford, 2010).....	197
Table C1: Properties of Materials	221
Table D1: End-Condition Constants α for Helical Compression Springs*(Source: Table 10-2, Shigly and Mischke, 2001)	227
Table D2: High-Carbon and Alloy Spring Steels Source: From Harold C. R. Carlson, "Selection and Application of Spring Materials," Mechanical Engineering (Source: Table 10-3, Shigly and Mischke, 2001).....	228
Table D3: Constants A and m of $S_{ut} = A/d^m$ for Estimating Minimum Tensile Strength of Common Spring Wires Source: From Design Handbook, Courtesy of Associated Spring (Source: Table 10-4, Shigly and Mischke, 2001)	229
Table D4: Mechanical Properties of Some Spring Wires (Source: Table 10-5, Shigly and Mischke, 2001)	230

Table D5: Maximum Allowable Torsional Stresses for Helical Compression Springs in Static Applications Source: Robert E. Joerres, Standard Handbook of Machine Design (Source: Table 10-6, Shigly and Mischke, 2001)	231
Table D6: Maximum Recommended Bending Stresses (KB Corrected) for Helical Torsion Springs in Cyclic Applications as Percent of Sut Source: Courtesy of Associated Spring (Source: Table 10-10, Shigly and Mischke, 2001)	231
Table D7: PROPERTIES OF COMMON SPRING MATERIALS, ace wire spring & form company, inc. 1105 thompson avenue - mckees rocks	232
Table D8: Empirical Constants A, B, and C, Face Width F in Inches* (Source: Table 14-9, Shigly and Mischke, 2001)	233
Table E1: Kinematic data of left leg gait cycle of healthy subject	234
Table E2: Kinematic data of left leg gait cycle of able-body subject while using prosthesis	234
Table E3: Kinetic data of left leg gait cycle of healthy subject	235
Table E4: Kinetic data of left leg gait cycle of able-body subject while using prosthesis	235

LIST OF FIGURES

Figure 2.1: Normal gait cycle vs. gait cycle with prosthesis (Rajtůková et al., 2014).	11
Figure 2.2: Types of lower limb prosthesis.....	17
Figure 2.3: Examples of mechanically controlled prostheses for a) shoulder disarticulation amputees, and b) above-knee amputees (Schultz and Kuiken 2011).	19
Figure 2.4: Components of a passive type above knee prosthesis.	26
Figure 2.5: Load line: 1) - 2mm posterior from the hip joint, 2) - 15mm anterior from the knee joint and 3) - 60mm anterior from the ankle joint (Rajtůková, et al. 2014).	34
Figure 2.6: Construction line (Rajtůková, et al. 2014).	34
Figure 2.7: Load line in Transfemoral prosthesis (Rajtůková et al. 2014).	36
Figure 3.1: Design and development cycle of a prosthesis.	46
Figure 3.2: Steps of prosthesis design improvement.	47
Figure 3.3: Flow chart of design and development of the lower limb prosthesis.....	50
Figure 3.4: Plug-in-Gait Marker Placement.....	53
Figure 3.5: Marker positions on the lower limb of healthy individual in gait analysis.....	54
Figure 3.6: Foot positions on the platform of the Biodex machine in stability test of healthy individual.....	55
Figure 3.7: Marker positions on the prosthesis in gait analysis.	61
Figure 3.8: Foot positions on the platform of the Biodex machine in stability test.	63

Figure 3.9: Different phases of prosthesis gait cycle.....	64
Figure 4.1: Different view of the gear based knee joint.....	67
Figure 4.2: The exploded view of knee joint showing the different components.....	68
Figure 4.3: Different components of knee joint with parts number.....	69
Figure 4.4: The exploded view of knee joint showing the connections among components.....	70
Figure 4.5: Free body diagram of prosthesis at stance phase.....	72
Figure 4.6: Free body diagram of prosthesis at 150 of rotation at swing phase.....	73
Figure 4.7: Free body diagram of prosthesis at 700 of rotation at swing phase.....	74
Figure 4.8: Isometric view of ankle joint.....	78
Figure 4.9: The exploded view of the different ankle joint components.....	79
Figure 4.10: Different components of ankle joint with parts number.....	80
Figure 4.11: The exploded view of ankle joint showing the connections among components.....	81
Figure 4.12: The load distribution in the prosthetic foot.....	83
Figure 4.13: The angle of rotation produced by the ankle joint.....	85
Figure 4.14: Different view of the mechanically controlled above knee prosthesis.....	90
Figure 4.15: The exploded view of prosthesis showing the different components.....	91
Figure 4.16: Different components of the prosthesis with part number.....	92
Figure 4.17: Connections among different components of the prosthesis.....	93
Figure 5.1: The angular displacement of the lower limb joints.....	99

Figure 5.2: Angular displacement of foot progression.	100
Figure 5.3: Angular velocity of lower limb joints during walking at normal speed.....	101
Figure 5.4: Angular velocity of foot progression during walking at normal speed.....	102
Figure 5.5: Angular acceleration of lower limb joints during walking at normal speed.	103
Figure 5.6: Angular acceleration of foot progression during walking at normal speed.	104
Figure 5.7: Forces in the lower limb joints.	105
Figure 5.8: Ground reaction forces of healthy lower limb foot.	106
Figure 5.9: Joint moments of healthy lower limb	108
Figure 5.10: Ground reaction moment of healthy lower limb foot.....	109
Figure 5.11: Joint power of healthy lower limb.....	110
Figure 5.12: a) Model of gear based knee joint, b) Solid mesh of the model.....	120
Figure 5.13: von Mises stress of knee joint components.	122
Figure 5.14: Strain analysis of knee joint components.	123
Figure 5.15: Displacement analysis of knee joint components.....	124
Figure 5.16: The angle of rotation produced by a) the ankle joint, and b) shank of the prosthetic ankle.....	127
Figure 5.17: a) Model of spring based ankle joint, b) Solid mesh of the model.....	130
Figure 5.18: von Mises stress of different components of ankle joint.....	131
Figure 5.19: Strain analysis of ankle joint components.	133
Figure 5.20: Displacement analysis of ankle joint components.....	135
Figure 5.21: Angular displacement of gears at different phases of gait cycle.	138

Figure 5.22: Angular displacement of shank during flexion of ankle joint.	140
Figure 5.23: Angular displacement of shank during extension of ankle joint.	141
Figure 5.24: Angular displacement, velocity and acceleration of the prosthetic knee and ankle joints.	143
Figure 5.25: Joint force, joint moment and joint power of the prosthetic knee and ankle joints.	147
Figure 5.26: The angular displacement of the prosthetic joints.	152
Figure 5.27: Angular progression of foot.....	153
Figure 5.28: Angular velocity of lower limb joints during walking at normal speed.....	154
Figure 5.29: Angular velocity of foot progression during walking at normal speed.....	155
Figure 5.30: Angular acceleration of lower limb joints during walking at normal speed.	157
Figure 5.31: Angular acceleration of foot progression during walking at normal speed.	158
Figure 5.32: Forces in the lower limb prosthetic joints.	160
Figure 5.33: Ground reaction forces of prosthetic foot.....	161
Figure 5.34: Joint moments of prosthetic lower limb.	163
Figure 5.35: Ground reaction moment of prosthetic foot.	164
Figure 5.36: Joint power of prosthetic lower limb.....	165
Figure A1: Country wise number of amputees (extrapolated data except for USA) (Data Source: 2004 World Development Indicators, Last updated date: 13/08/2015).	195
Figure A2: Country wise expenditure on health sector (Data Source: 2004 World Development Indicators, Last updated date: 13/08/2015).	196

Figure B1: The angle of knee joint gear rotation.....	198
Figure D1: Roadmap of gear bending equations based on AGMA standards (Source: Figure 14-17, Shigly and Mischke, 2001).....	222
Figure D2: Roadmap of gear wear equations based on AGMA standards (Source: Figure 14-18, Shigly and Mischke, 2001).....	223
Figure D3: Allowable bending stress number for through-hardened steels (Source: Figure 14-2, Shigly and Mischke, 2001).....	224
Figure D4: Repeatedly applied bending strength stress-cycle factor YN (Source: Figure 14-14, Shigly and Mischke, 2001).....	224
Figure D5: Pitting resistance stress-cycle factor ZN (Source: Figure 14-15, Shigly and Mischke, 2001).	225
Figure D6: Contact-fatigue strength S_c at 107 cycles and 0.99 reliability for through-hardened (Source: Figure 14-5, Shigly and Mischke, 2001).....	225
Figure D7: Spur-gear geometry factors J. Source: The graph is from AGMA 218.01 (Source: Figure 14-6, Shigly and Mischke, 2001).....	226
Figure D8: Dynamic factor K_v (Source: Figure 14-9, Shigly and Mischke, 2001).	226
Figure D9: Hardness ratio factor C_H (through-hardened steel) (Source: Figure 14-12, Shigly and Mischke, 2001).....	227

LIST OF SYMBOLS AND ABBREVIATIONS

ASIS	: Anterior Superior Iliac Spine
RIAS	: Right Ilium Anterior Superior (Anterior Superior Iliac Spine)
LIAS	: Left Ilium Anterior Superior (Anterior Superior Iliac Spine)
RIPS	: Right Ilium Posterior Superior (Posterior Superior Iliac Spine)
LIPS	: Left Ilium Posterior Superior (Posterior Superior Iliac Spine)
RHJC	: Right Hip joint center
LHJC	: Left Hip joint center
RTHI	: Right Lateral Thigh marker
LTHI	: Left Lateral Thigh marker
RKNE	: Right Lateral Knee marker
LKNE	: Left Lateral Knee marker
RTIB	: Right Lateral Shank marker
LTIB	: Left Lateral Shank marker
RKJC	: Right Knee Joint Center
LKJC	: Left Knee Joint Center
RANK	: Right Lateral Malleolus marker
LANK	: Left Lateral Malleolus marker
RTOE	: Right Second metatarsal head
LTOE	: Left Second metatarsal head
RAJC	: Right Ankle Joint Center
LAJC	: Left Ankle Joint Center
RHEE	: Right Center of Calcaneus
LHEE	: Left Center of Calcaneus

W	: Subject weight	N
W_t	: Tangential transmitted load	N
W_r	: Resultant load	N
b	: Width of the gear face	mm
d_w	: Pitch diameter of the gear	mm
D_1, D_2	: Gear diameter	mm
T_1, T_2	: Number of gear tooth	
n_1, n_2	: Gear revolution per minute	rpm
ω_1, ω_2	: Angular speed	rads ⁻¹
V	: Pitch-line velocity	ms ⁻¹
σ_b	: Bending stress	Nm ⁻² , MPa
$\sigma_{b,all}$: Bending endurance strength	Nm ⁻² , MPa
σ_c	: Contact stress	Nm ⁻² , MPa
$\sigma_{c,all}$: Contact endurance strength	
σ_{HP}	: Allowable contact stress number	
σ_{FP}	: Allowable bending stress number	Nm ⁻² , MPa
Y_N	: Stress cycle factor for bending stress	
Y_θ	: Temperature factor	
Y_Z	: Reliability factor	
S_F	: AGMA factor of safety	
K_o	: Overload factor	
K_s	: Size factor	
K_H	: Load distribution factor	
K_V	: Dynamic factor	
K_B	: Rim-thickness factor	

Y_j	: Geometry factor	
K_f	: Root fillet stress-concentration factor	
Z_E	: Elastic coefficient	
Z_R	: Surface condition factor for pitting resistance	
Z_I	: Geometry factor for pitting resistance	
Z_N	: Cycle life factor	
Z_W	: Hardness ratio factors for pitting resistance	
S_H	: <i>AGMA</i> factor of safety	
N_t	: Number of coils	
N_a	: Number of active coils	
R, k	: Spring rate/ Spring constant	N/mm
E	: Modulus of elasticity	MPa
G	: Modulus of rigidity	MPa
T	: Deflection, number of turns or revolutions of spring	
M	: Moment or torque	Nm, N.mm
D	: Mean coil diameter	mm
$I.D$: Internal diameter of the spring	mm
$O.D$: Outer diameter of the spring	mm
d	: Wire diameter	mm
t	: Rectangular wire thickness	mm
b	: Rectangular wire width	mm
l	: Torque arm length	mm
L_0	: Free length of spring	mm
L_s	: Solid length of spring	mm
L_f	: Spring length at final load	mm

L_1	: Spring length at initial load	mm
F_s	: Load at solid length	N
y_s	: Spring deflection caused by yield stress	mm
f_n	: Critical frequency of the spring	Hz
S_{ut}	: Tensile strength of the spring material	MPa
S_{sy}	: Maximum allowable design stress	MPa
S_{su}	: Allowable strength for infinite life	MPa
τ_a	: Alternating shear stress component	MPa
τ_m	: Midrange shear-stress component	MPa
τ_s	: Shear stress at soliding	MPa

University of Malaya

LIST OF APPENDICES

- APPENDIX A : DESIGN MATERIALS
- APPENDIX B : DESIGN CALCULATION
 - APPENDIX B.1 : GEAR SET DESIGN CALCULATION
 - APPENDIX B.2 : COMPRESSION SPRING DESIGN CALCULATION
 - APPENDIX B.3 : TORSIONAL SPRING DESIGN CALCULATION
- APPENDIX C : DESIGN MATERIALS
- APPENDIX D : DESIGN MATERIALS
- APPENDIX E : GAIT CYCLE DATA

University of Malaya

CHAPTER 1: INTRODUCTION

1.1 Background of the study

The prevalence of limb loss and amputation due to congenital effect, war effect, accident, natural disaster and so on has been increasing steadily around the world. Amputation or limb defect causes difficulties to the subjects in performing different daily activities. It creates the need of getting help from different assistive devices depending on the nature of the disability. The amputees have been aided by walking stick/cane, walking frame, crutch, wheelchair, motor wheelchair, stroller, motor stroller, and more recently artificial prosthetics is being used to rehabilitate them (Gao et al. 2010). The amputee with transfemoral, and knee level amputation generally uses wheelchairs, whereas amputee with lower-level amputations (transtibial and foot amputation) primarily uses artificial prosthesis (Karmarkar et al. 2009). An artificial limb or prosthetic limb is a kind of prosthesis that replaces a missing arm or leg. The extent of an amputation or loss and location of the missing extremity largely determine the type of prosthesis to be used. Recently, the design of artificial limb has been significantly improved by incorporating some extra features as well as introducing new controlling methods.

In newer and more improved designs of artificial limbs, more control is given to the users by employing different control system, muscle of carbon fiber, mechanical linkages, motors, computer microprocessors, and innovative combinations of these technologies mentioned (Wen-Wei Hsu et al. 1999). More importantly, the essential factors like weight-force ratio, strength, durability, adaptability, wear-ability, degree of freedom, resistance to environment, functional capabilities, etc. are being addressed seriously to develop a more efficient artificial limb. The operating power consumed by

the artificial prosthesis is another essential factor to be considered, which varies depending on the prosthesis type. The desired movement of artificial limb is obtained with the help of different types of joints, sensors, controllers and actuators. The application of the artificial intelligence has made the control system more spontaneous with the ability of decision making.

As the main objective of the latest research is to develop a more sophisticated prosthesis, the matter of price of the prosthesis has been overlooked. The price of the prosthesis is a major issue needs to be taken into consideration when to design and develop a prosthesis. This is because the majority of the amputees around the world are from the average or below average economic group. The more advance-controlled prostheses are more expensive, which are unaffordable to the amputees with an average economic status. Therefore, needs to tradeoff between the level of control amputees want in their prostheses and how much they will to pay for it. Based on this answer, type of control system is chosen for the prostheses.

The damage of limb is the most commonly seen defect among the disable people due to diseases, congenital, accidental or war effects, which most often causes amputation (Sagawa Jr et al. 2011). Industrial, vehicular, and war-related accidents are the leading causes of amputations in developing countries, such as large portions of Africa (Burger et al. 2004). In more developed countries like North America and Europe, disease is the primary cause of amputations (Rosenfeld et al. 2000). Cancer, infection and circulatory disease are the leading diseases that may be followed by amputation (Albertini et al. 2000). From the review report of Sagawa Jr, et al. (2011), approximately 1.7 million people experienced limb loss in the United States in 2007, and more than 185,000 new amputations were performed each year in that country. According to a forecast carried out by Ziegler-Graham et al. (2008) that there were close to one million people living with the loss of a limb who were below the age of 65 years and 302,000 people below

the age of 45 years in *USA*. Over the next 45 years, the number of amputee is expected to be more than double from 1.6 million in 2005 to 3.6 million in 2050. These people will need a replacement of missing (amputated) limb to overcome their disabilities in performing different daily activities.

The amputation alters the biomechanics of the amputee body movement. Different study shows, the intact limb of a lower-limb amputee often being stressed or favored more during their everyday activities. This primarily causes osteoarthritis of the knee and/or hip joints of the intact limb, which in the long run causes osteoporosis that limits the sufficient loading of the lower limb through the long bones. The equal distribution of forces across the intact and prosthetic limbs during ambulation is required to ensure minimum effect and the best solution is the proper prosthetic fit development. A poor prosthetic fit and alignment, postural changes, leg-length discrepancy, amputation level, and general deconditioning commonly cause back pain to the lower-limb amputee. The right selection of an artificial prosthesis with appropriate physics would be helpful in this case, which is usually defined by the amputee's body construction and his/her activity (Robinson et al. 2010). The correct choice of a control system complements the other part of artificial prosthesis development, which is usually performed by some external device such as electrical, mechanical and artificial intelligence. The entire difficulties connected with the amputation necessitate the amputee to obtain a tailor made artificial limb with an appropriate control system, which should be capable of balancing the patient's body dynamics and providing desired movement to its user.

1.2 Aim of study

The aim of the study is to develop some prosthesis with a greater efficiency within an affordable price to mass proportion of amputee. As the majority of amputees are from

below average economic group, development of some prosthesis with a comparative cheaper price is worthy.

1.3 Objectives

The research has been embarked to design and develop a more efficient above knee (AK) prosthesis with an affordable price for the amputee with lower economic status.

- To identify a suitable type of above knee prostheses (based on controlling method used) for the mass proportion of amputees in Malaysia and some developing countries where amputation is prevalent.
- To design, model and simulate the movements of the prosthesis under different conditions, in particular during standing and level ground walking.
- To fabricate the designed prosthesis and test the performance of the prosthesis during standing and walking.

1.4 Importance of study and research motivation

Having a look into the statistics of amputee in different countries around the world make one perceived the necessity of prosthesis development. According to a statistics of amputee in USA, 2004, the prevalence of amputation is 7 per 1000 (NHIS95: excludes toes/fingers only) people in the USA are living with limb loss (estimated data). The extrapolated data based on the statistical report has shown that the number of amputee in Malaysia was 164,657 (Figure A1). According to Resnik et al. (2012), there are approximately 1 in 200 persons having limb loss in USA, 80% of whom have lower limb loss caused by dysvascular disease. From another study carried out by Watve et al. (2011), the ratio of arm to leg amputations was estimated to be 1:3. Development of artificial limb is necessary to ensure high-quality, active, and productive lives for these

amputees. Further, the lower limb prosthesis demands more to be reconstructed to rehabilitate mass proportion of the amputee.

Costs of prosthesis depend on the type of leg and the level of amputation. According to Mc Gimpsey and Brandford (2010), the price of a basic below knee prosthetic leg that allows an amputee to walk on the flat ground is \$5,000 to \$7,000. The price of an above knee prosthesis is \$37,000 to \$45,563. The price of a C-leg, a more advanced computerized or microprocessor controlled prosthetic leg is \$50,000 to \$70,000 (Table A1). This type of prosthesis can follow the muscle movement more precisely. On contrary, the per-capita spending on health in Malaysia is \$676, which is much lower than the price of the basic type prosthesis. Per-capita spending in other least-developed countries like Afghanistan, Pakistan, Bangladesh, India, Senegal, etc. is much lower than the price of a basic prosthetic leg. According to the statistical data reported in different articles, the rate of limb loss is more prevalent in the least developed and third-world countries, where the majority of the population lives below an average economic status. The costly sophisticated prosthesis would always remain beyond reach to them. In this case, a cheap passive type prosthesis becomes quite appealing to them. They could afford it and at the same time they could overcome the difficulties caused by their missing limb. Instead of concentrating on development of a more high-tech prosthesis, focusing on improvement of existing passive type prosthesis would be more justified. Hence, development of a quasi-active type mechanically controlled prosthesis could assist much proportion of people by enabling them obtaining a more efficient prosthesis with reasonably cheap price.

1.5 Scope of study

The major drawback of the available passive type mechanically controlled prosthesis is low efficiency; whereas for electrically controlled prosthesis, source of power supply for controlling/regulating the artificial limb is a big setback. Other microprocessors and micro-controller based prostheses are quite expensive, which are unaffordable to the amputee from lower economic group.

- An improvement in the mechanically controlled passive type prosthesis, upgrading it to a semi-active/quasi-active level would help to overcome the above-mentioned setbacks.
- A gear based knee joint, and a spring based ankle joint in the prosthesis arrangement would rather help to follow the residual limb movements without any external devices and any external power supply. Therefore, price of the prosthesis will still be cheap and affordable to majority proportion of people.

1.6 Thesis outline

Chapter 1 describes introduction, research background, aim, objectives, importance and motivation of research, and scope of the study.

The literature review on gait cycle of human lower limb, biomechanics of lower limb, different type of prosthesis based on nature and control system, components of prosthesis, standard procedure of prosthesis development including modeling and simulation, finite element analysis and prosthesis construction and performance testing are presented in Chapter 2. Finally a summary of literature review is also presented at the end of this chapter.

Chapter 3 presents the methodology of research. The procedure of gait cycle data recording and analysis, the process of stability data recording and analysis, the process

of modeling and simulation of different prosthetic components, fabrication and performance testing procedure of prosthesis are described in this chapter.

The detail design of prosthesis and its components are presented in Chapter 4. The gear set design, the compression and torsional spring design are thoroughly described in this chapter.

The gait analysis, finite element analysis, stability test, and performance test results are discussed in Chapter 5. A cost analysis is also presented in this chapter.

Chapter 6 presents the conclusions of this work and recommendation for future work.

University of Malaysia

CHAPTER 2: LITERATURE REVIEW

Prosthesis is a device designed to replace a missing biological body part or to improve the functionality of existing impaired body parts. Diseased or missing eyes, arms, hands, legs, or joints are commonly replaced by prosthetic devices. Prosthetic limb is an arrangement replacing a missing biological limb, which assist users in performing similar activities like that of a healthy limb. The prosthesis is to replicate a biological limb structure and its movements with a set of linkage, joints and accessories. There are four major types of prostheses are available in the market. They are Above Knee (*AK*) prosthesis, Below Knee (*BK*) prosthesis, Above Elbow (*AE*) prosthesis, and Below Elbow (*BE*) prosthesis. The above knee (*AK*) prosthesis is to replace the lower limb missing from above the knee and to reproduce its movements with the prosthetic arrangement. The below knee (*BK*) prosthesis is to replace the lower limb missing from below the knee and to reproduce its movements with the prosthetic arrangement. The above elbow (*AE*) prosthesis is to replace the upper limb missing from above the elbow and to reproduce its movements with the prosthesis arrangement. The below elbow (*BE*) prosthesis is to replace the upper limb missing from below the elbow and to reproduce its movements with the prosthesis arrangement. Rather than the above, some prostheses replacing other body parts are also available depending on the need, e.g. nose prosthesis, eye prosthesis, finger prosthesis and so on.

An above knee (*AK*) prosthesis has to replicate the structure and construction of a healthy biological lower limb. In addition to this, it is required to reproduce similar gait cycle movement like that of a healthy biological leg. A closer replication of the limb construction as well as its gait cycle movements would come up with a more efficient prosthesis. The knee and the ankle joints essentially play the major rule in operating the lower limb, and thus producing movement in the prosthetic limb arrangement. To

develop a knee and ankle joint for prosthesis that capable of replicating the gait cycle movements of a biological knee and ankle joint, the joints are required to imitate the biomechanics of the healthy natural limb joints.

2.1 Gait cycle movement of human lower limb

A thorough study on gait cycle movement of human leg is obligatory before designing a knee or ankle joint for a prosthesis. This is to incorporate maximum possible features into the prosthetic knee or ankle joint to make it imitating the gait cycle movements of the healthy biological leg. The gait cycle of natural level-ground walking comprises of five distinct stages (Martinez-Villalpando et al. 2008). The different phases of gait cycle of human lower limb during level ground walking are shown in following Table 2.1.

Table 2.1: The different phases of gait cycle of human lower limb during level ground walking (Rajtůková et al., 2014)

GAIT CYCLE	
Phases	Description
Support phase	
Initial contact [0%]	At initial contact phase, the heel touches the ground; the knee joint undergoes extension, and the hip joint experiences flexion. Then the ankle joint shifts from the dorsal flexion to a neutral position. During this time, the other leg completes the support phase. In this phase, m. gluteus maximus, medius and m. peroneus are identified as the most activated muscles.
Loading response [0-10%]	Loading response is basically a double support phase. In this phase, one-foot touches the ground and remains touched until the other foot is lifted for a step. Then the whole body weight is carried by the support leg. The shock absorption, body weight transfer and forward movements are essentially executed in this phase. At the same time, supporting the body weight and providing stability to the body are performed with one leg. The quadriceps femoris and m. tibialis anterior are activated in this phase. However, then there is no extension in the knee joint.

Table 2.1: Continued

Phases	Description
Swing phase	
Midstance [10-30%]	Midstance phase starts with elevation of the other leg and continues until the whole body weight is transferred to the support limb. Both the hip and the knee joint of the support leg go under extension. There is dorsal flexion of the leg occurred. The primarily the posterior calf muscles are activated.
Terminal stance [30-50%]	The support limb heel begins to move away from the ground until the other limb heel touches the ground. There is an increase of extension at the hip joint of support leg; therefore, the body weight is transferred onward beyond the vertical axis of the body.
Preparation for a step [50-60%]	This phase is the second double support phase. At the end of this phase, the toe rolled away from the ground. There is an increase in the plantar flexion of the ankle and knee joint and a decrease in hip extension when the other foot touches the ground. The body weight is transferred to the other leg becomes the support limb. The activation of m. sartorius, m. rectus femoris and m. psoas major/ minor and m. iliacus causes a reduction in the hip extension and increase in the knee flexion. The m. flexor halucis longus ensures the toe takes off from the ground.
Initial swing [60-70%]	Initial swing phase starts with the elevation of feet from the ground and continues until the swing leg is inverse the support leg. There is partial dorsal flexion in the ankle joint, and some increase of flexion in the hip and knee joints. In this phase, the flexion becomes most evident. The other leg reaches at the centre of the support.
Mid-swing [70-85%]	In mid-swing phase, the step continues until the swing leg reach in front of the body and the fibula reach at vertical position. There is some hip flexion and knee extension in reaction to the gravitation force. It lasts from the dorsal flexion to the neutral position.
Step termination [85-100%]	This phase starts with the fibula at the vertical position and continues until the foot touches the ground. There is some knee extension facilitated by m. quadriceps femoris and hip flexion produced by lateral group of adductors. From the dorsal flexion to the neutral position, the ankle remains in the transition.

All these phases of a gait cycle are illustrated in following Figure 2.1 to make the whole cycle comprehensive.

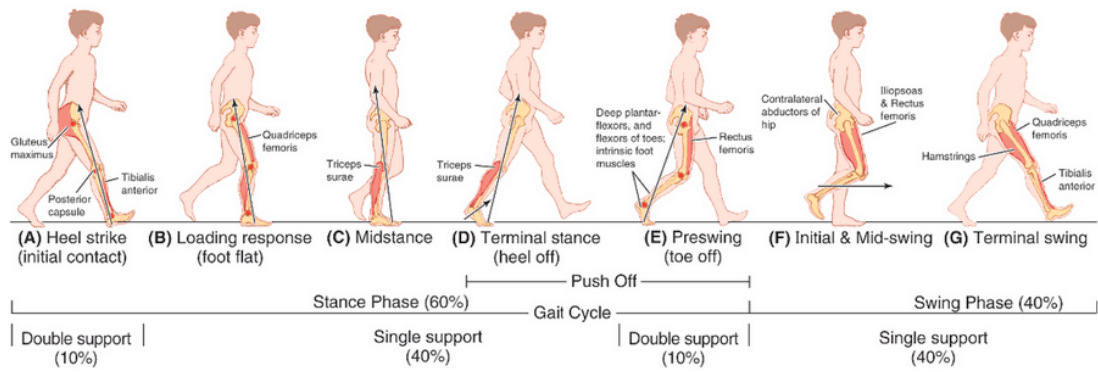


Figure 2.1: Normal gait cycle vs. gait cycle with prosthesis (Rajčúková et al., 2014).

Performing different types of daily activities require the lower limb to obtain various gait cycle movements. The gait cycle movement for walking on the plane field is not similar to that for ascending or descending activities. Gait cycle movement during walking varies from that during running or leaping. Walking or running on a free ground and doing same things on a field with obstacles is also different. All these factors are to be studied thoroughly to take into account when to design a knee joint or a complete prosthesis. From an investigation carried out by van Keeken et al. (2012), some factors are found contributing significantly to obtain a successful clearance when avoiding obstacle by Transfemoral (*TF*) amputee subjects. They used a knee flexion strategy to identify the significant contributing factor. The factors are a) maintaining a sufficient distance between the foot and the obstacle at the start of the swing phase, b) producing sufficient hip torques, and c) making use of the static ground friction on the prosthetic foot.

In case of normal level ground walking, the muscle forces, ground reaction forces, and joint motions are identified as important factors for lower limb. Two factors control the force distribution between the medial and lateral compartments: the moment of external varus or valgus about the knee joint, and the contribution of the muscles and ligaments in sharing the moment. During walking, the leg bends inward due to the moment acting in the frontal plane (the adduction moment), then most of the tibiofemoral joint load is

transmitted by the medial compartment. Morrison and Harrington (1970) have predicted the location of the resultant tibiofemoral force in normal walking for the first time. Then Schipplein and Andriacchi (1991) have shown that besides shifting the tibiofemoral load to the medial side, the lateral opening of the joint is also performed by the adduction moment. They came up with the conclusions that a combination of muscle and ligament forces is necessary to control the external adduction moment and prevent lateral joint opening when someone walks at normal speeds (Shelburne, et al. 2006). All these factors are to be optimized to ensure an ease walking.

2.2 Biomechanics of lower limb joints

The lower-limb structure incorporates two joints – knee joint and ankle joint. The biomechanics of these two joints plays the most important role in performing different movement by the lower limb during various daily activities. Both the kinematic and the kinetics of the joints have to be studied to investigate the biomechanics of the lower limb. The study of body movement in the space without considering the forces that cause the movement is called kinematics. The study of body movement and also the forces involved in producing that movement is called kinetics. The gait analysis shows that the knee kinematics of different individuals is different. Based on normal gait analysis, Barton et al. (2011) have reported that there are large variations in the kinematics of the foot and ankle. The kinetics of the knee and ankle joints is also found to vary from individual to individual and also depending on the walking speeds.

The performance of the knee joint in above knee (AK) prosthesis is typically assessed by the kinematic and kinetic analyses of the joint. The joint angular movement (kinematics), ground reaction forces and internal joint moment (kinetics), and joint power (energetics) were measured by Okita et al. (2013) to evaluate the quantitative performance of a knee joint. The study of joint kinetics is essential for interpretation of

gait mechanics and compensatory strategies used in above-knee (AK) prosthesis. The joint reaction forces, moments and powers, are often used to calculate segment anthropometrics. Regression equations from cadaver studies are used for calculating the anthropometric variables like mass, center of gravity (CG) and moment of inertia (MI). In several studies, the calculation of anthropometrics has been performed by direct measurements of the residual limb and prosthesis (Goldberger et al. 2008). To calculate the joint actuation torque, Wu et al. (2011) have developed an 'active-reactive' control algorithm by linearizing the muscle-tendon actuation mechanism. An 'active' actuation torque and a 'reactive' torque (as the response to the joint motion) were combined together to make it happen.

To explore the physiological functional stiffness of the knee joint is essential for upgrading the design of the prosthesis that intends to imitate normal gait cycle. The stiffness of the knee joint differs from activity to activity in our daily life. The magnitude of the knee stiffness during performing different movements indicates the level of energy storage element adequacy in terms of harvesting/returning energy (Bayram, et al. 2014). The socket alignment in a prosthetic arrangement is also necessary to measure. There are some constant effects on the socket reaction moment for changing the alignment in transtibial prostheses (Boone et al., 2012; Kobayashi et al., 2013). During walking, these effects become prevalent, act about the center of the socket and transmitted to its distal end through the prosthesis (Kobayashi et al., 2012; Kobayashi et al. 2013; Short et al. 1999). In a particular investigation, Kaufman et al. (2012) have investigated the influences of kinematic and kinetic characteristics of the prosthesis due to the prosthetic knee joint components while walking on flat level ground.

During level ground walking, the ankle motion is quasi-periodic, which is mainly comprised of two phases: stance phase and swing phase. An ideal gait cycle begins with

the heel of one foot strike on the ground and ends at the next strike of the same heel on the ground surface. The stance phase starts with the heel strike on the floor and continues until the toe of the same foot off from the ground. The period of the gait cycle when the foot is off the ground is called the swing phase. The stance phase is comprised of three sub-phases: controlled plantar flexion, controlled dorsiflexion and powered plantar flexion (Palmer, 2002). The controlled plantar flexion initiates with the heel strike and remains until the foot becomes flat. The controlled dorsiflexion starts from the foot flat and ends when the dorsiflexion reaches a peak point. The powered plantar flexion begins next and continues until the foot leaves the floor. Some additional energy is required for switching the walking speed from moderate to fast, which is generally supplied from the energy stored in the previous sub-phase. During swing, the position of ankle is controlled until the rotation angle becomes enough for heel to strike the ground. The duration and shape of the gait cycle changes from one step to another step, the gait speed, subject weight, subject morphology, and terrain conditions largely determine the pattern of a gait cycle (Jiménez-Fabián & Verlinden, 2012).

To mimic unimpaired ankle joint function during gait, prosthetic devices for individuals with transtibial amputation (*TTA*) must approximate unimpaired ankle range of motion (*ROM*), torque, and power with similar synchrony and magnitude. During the gait cycle, the unimpaired ankle serves 4 distinct functions: 1) controlled plantarflexion—during loading response, dorsiflexors eccentrically control plantarflexion until foot flat; 2) controlled dorsiflexion— during mid and terminal stance, plantarflexors eccentrically control the forward rotation of the tibia over the foot; 3) powered plantarflexion—during preswing, plantarflexors concentrically produce ankle power, propelling the body forward; 4) powered dorsiflexion—during swing, dorsiflexion of the foot occurs, aiding toe clearance (Ferris et al. 2012). According to Schache et al. (2014), the ankle plantar flexors play a very important role to support body and achieve fast walking

speed. For individual with gait abnormalities, the poor plantar flexor function of ankle was identified as one of the strongest predictors of lower limb poor mobility.

The amputation of lower limb causes the amputee to lose functionality of the ankle plantar flexors, which consequently affect the process of supporting and forward propulsion of the body, and also the initiation of leg swing during walking (Ventura et al. 2011). The amputation causes a kinematic difference between the intact leg and the residual leg, particularly during late stance and the early swing phase of the gait cycle. With the increase of mechanical loading on the intact limb, the push-off power and ground reaction force of the prosthesis are decreased (Winter and Sienko 1988). During changing the limb position from one stance to the next, both velocity of the body center and the mass change from a forward-and-down direction to a forward-and-up direction. This change in the direction is because of the ground reaction impulse (the integral of ground reaction forces) during transition of step from step, which represents the double support phase (Robertson and Winter 1980). From the investigation, the increase in the foot-ankle push-off work was caused by the decrease in the first external adduction moment (*EAM*) of the intact knee. The largest magnitude of push-off work, the Controlled energy storage and return (*CESR*), were attributed to the lowest first peak knee *EAM* of the intact knee (Morgenroth et al., 2011).

Vrieling et al. (2008) have found the lower-limb amputees to have poorer balance compare to able-bodied subjects. With the cycle of time, the experienced amputees are found using a decreased hip reliance strategy and increased ankle utilization strategy during dynamic balancing (Vanicek et al. 2009). It is also suggested using more rigid ankle mechanism in prosthesis when to control balance task of the lower limb (Barnett et al. 2013).

To improve the design of prosthesis and the rehabilitation process, a thorough knowledge on dynamics of balance control is indispensable. Curtze et al. (2012) have

investigated the role of the prosthetic and healthy limb/joints in balance control by making them disentangled. Under the application of mild perturbation, the subject was found capable of withstanding without stepping. The perturbations in the sagittal plane led to an increase in the ankle moment of the sound leg comparing to the prosthetic leg. There were no differences between the contributions of the prosthetic and sound leg in the frontal plane due to perturbations. The muscle empowered load–unload strategy used in the hip joints of transtibial amputees has made it act like that in able-bodied controls. However, instead of increasing the contribution of the sound limb, the stiffness of the prosthetic ankle of the lower-limb amputee has found to contribute to balance control in response to the platform perturbations.

2.3 Mechanically controlled prosthesis and other types

The lower-limb prostheses are developed to serve one purpose of assisting users and thus enabling them to overcome the difficulties in performing different daily activities due to amputation. However, the prostheses are categorized into different types based on their nature and controlling method they used. The different types of prostheses are shown in following Figure 2.2.

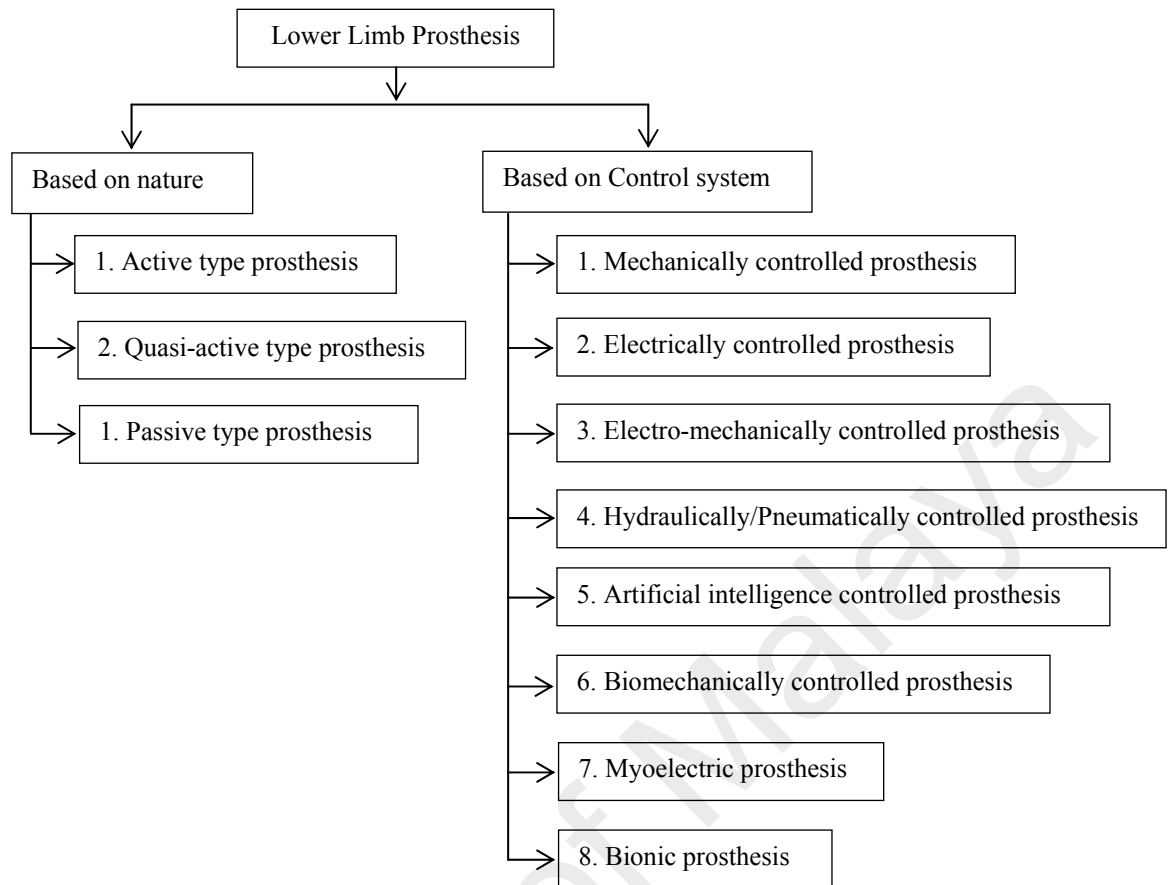


Figure 2.2: Types of lower limb prosthesis.

The prostheses are basically two types based on the nature of the prosthesis, i.e. passive type prosthesis and active type prosthesis. The passive type prosthetic limbs are used to replace the missing limb structure, which are unable to follow the movement of the residual limb and unable to produce any movement to the prosthesis like a natural limb. Passive type prostheses are usually very cheap. Most of the early age prostheses were the passive type. With the replacement of the missing limb structure, the active type prostheses are capable of following the residual limb movement and thus producing different movement into the prosthesis similar/closer to the natural gait of a corresponding unimpaired limb. This is done with help of some sensor, motor, microprocessor, microcontroller, interfacing unit and so on. The active type prostheses are expensive, and the price of which vary depending on how much control is given to

its users. Another type of prosthesis is called semi active/ quasi-active prosthesis, which can follow the movement of the residual limb and can partially imitate the movement of a corresponding natural limb. These types of prostheses normally utilize the material properties that used for different component in reproducing movement in the prosthesis. These types of prostheses are moderate in terms of price.

According to the control system applied to the prosthesis, the prostheses are again divided into few categories. Prostheses are defined based on the nature of the control system used for controlling their movements. Some are mechanically controlled prostheses, some are electrically controlled prostheses, some are electromechanically controlled and so on.

The modern concept of prosthesis index finger to the functional prostheses, which are categorized into three major groups, i.e. 1) body-powered (mechanical or cable operated), 2) myoelectric, and 3) hybrid. Body-powered prostheses are largely mechanical devices. To control a body powered upper limb prosthesis, amputees use remaining shoulder movements to pull on a cable and sequentially operate prosthetic functions such as the elbow, wrist, and terminal device. Myoelectric prostheses are motorized and are controlled via surface electromyogram (*EMG*) signals from residual muscles sites. Control of myoelectric prostheses is generally achieved by recording from two independent muscles or by differentiating weak and strong contractions of one muscle. Currently, it is a common practice to combine myoelectric control and body-powered operation in hybrid prosthesis, such as a body-powered elbow combined with a myoelectric terminal device (Schultz and Kuiken 2011). Mechanical and electromechanical switches, locks, and joints, electric motor, transducer, myoelectric sensor, biosensor, etc. are accessory components of an active type/functional prosthesis.

The mechanically controlled prosthesis is tersely discussed in the following paragraphs. The mechanically controlled prostheses have an arrangement of some mechanical components meant to receive input from amputee and thus follow his/her intention to produce desired movement to the artificial limb. The mechanically controlled prostheses are mostly body-powered type prosthesis. To control a mechanically controlled prosthesis, amputees use remaining shoulder movements to pull on a cable [Bowden cable] and sequentially operate prosthetic functions such as the elbow, wrist, and terminal device. To switch between functions, users must lock the joints they wish to remain stationary by pressing a switch or using body movements to pull a locking cable (Schultz and Kuiken 2011). Mechanically controlled lower limb prostheses are usually controlled with a cam shaped linkage and residual limb movement. Different types of mechanically controlled prosthesis are shown in Figure 2.3.



a)

b)

Figure 2.3: Examples of mechanically controlled prostheses for a) shoulder disarticulation amputees, and b) above-knee amputees (Schultz and Kuiken 2011).

Though the mechanically controlled prostheses are cheap, however, these are no longer being admired due to the poor accuracy. Rusaw and Ramstrand (2010) have developed a

mechanical type prosthesis where operating the ankle-foot joint was the main focus, and the other intact limb was used as a control. The sagittal position of the functional joint center was determined by the three-dimensional kinematics of feet investigated. The motion of the prosthetic feet tested appeared to be unlike than that of an intact ankle. As the constraint for kinematic of prosthetic ankle based on intact ankle, some systematic error pertinent to this would impede to replicate the real motion of the prosthetic foot. The interaction of the foot with the ground during bipedal walking is unavoidable, which is the major cause of the energy loss. A reduction in this friction would minimize an appreciable amount of energy loss during walking; however, development of a prosthesis with such a controlling method is really challenging.

Ghorbani and Wu (2009) developed a mechanically controlled prosthesis using the adjustable stiffness elastic elements in artificial lower limb's structure. They believed that a control strategy by adjusting elasticity could significantly reduce the energy loss during the collision phase and thus improve the energetics of locomotion in bipedal walking robots. They approached two conceptual designs and elaborated them with mathematical model. Each conceptual design of adjustable stiffness artificial tendons (ASAT) was applied to the ankle joint of a bipedal walking robot model. To implement the dynamic modelling of the bipedal walking robot during the collision phase, the Lagrangian equations and impulsive constraints have been used. They were able to reduce the kinetic energy loss up to 20% by using their proposed technique for controlling the limb. However, the accuracy of different movement by the mechanically controlled prosthesis was not that impressive.

The electrical, electromechanical, myoelectric, artificial intelligence aided controlled and many more types of prostheses have been introduced to obtain more natural biomechanics in the prosthesis arrangement. The ultimate goal is to achieve a "Biomechatronic design" where the mechatronic system of the prosthetic leg is inspired

and works like the living limb. To achieve this goal, integration of the prostheses with the central nervous system is necessary so that the replacement moves and is perceived as if it were the natural hand without the requirement for any training or adaptation. The use of intraneural electrodes is perhaps the most promising technology that may hold the key to successful integration of bionic limbs into the biological system. Intraneural electrodes interface directly into the nerves in the limb stump and have the ability to carry a bidirectional flow of information between the bionic prosthesis and patient. There are still many obstacles to overcome before this technology is commercially available, but it is hoped that eventually it will be advanced enough to allow limb amputees to have the bionic prosthesis that act and feel like the innate limb. The salient features of the various prostheses based on the controlling method are presented in Table 2.2.

Table 2.2: A comparison among different type of prosthesis

Type of Prosthesis	Significant characteristics	Advantages	Disadvantages
Mechanically controlled prosthesis	<ul style="list-style-type: none"> • Required to have an appreciable residual limb to be used for controlling the prosthesis. • Controllability of the prosthesis is influenced by the material properties used for operating the prosthesis arrangement. 	<ul style="list-style-type: none"> • Cheap and affordable for average classes of people • Robust in design 	<ul style="list-style-type: none"> • Unable to reproduce the real motion of a biological prosthesis • Poor accuracy (comparatively)
Electrically controlled prosthesis	<ul style="list-style-type: none"> • Prosthesis is controlled by stimulating the respective biological controlling organ. • Preferable for the patient with the difficulty in operating limb. • Not commonly used controlling technique for prosthesis. 	<ul style="list-style-type: none"> • Highly regarded in treating the stroke patient. 	<ul style="list-style-type: none"> • Damages the muscle in the long run • Obtained some minimal delay in transferring electrical signals from skin to the muscle. • Maximum force of prostheses cannot be achieved due to its limitation to stimulate the whole limb.
Electro-mechanically controlled prosthesis	<ul style="list-style-type: none"> • Both electrical and mechanical sensors are used to assess the change in the system. • The electrical and mechanical elements are used together to control the prosthesis. 	<ul style="list-style-type: none"> • Prostheses are good for the amputees having difficulties in controlling locomotion. 	<ul style="list-style-type: none"> • Not accurate enough. • Application is limited to some amputees having particular types and frequency of feedback signal.

Table 2.2 continued

Type of Prosthesis	Significant characteristics	Advantages	Disadvantages
Hydraulically/pneumatically controlled prosthesis	<ul style="list-style-type: none"> • The control of the prosthesis is usually performed based on the force controlling unlike to the electrical and electromechanical methods, which are used position controlling technique. 	<ul style="list-style-type: none"> • Heavily devoted for the people with sports injury. • Used to assist people moving in hilly place. • Useful in military application 	<ul style="list-style-type: none"> • The fluid reservoir is considered to be a burden to its user.
Artificial intelligence controlled prosthesis	<ul style="list-style-type: none"> • Inherent correlations between intrinsic impaired neuromuscular activities are identified using artificial neural network. • Inverse kinematics of the prosthesis is controlled by training up the artificial neural network with variety of input data. 	<ul style="list-style-type: none"> • About 80% more predictive control than other prosthesis can be made. • Able to successfully control the tremor and inverse kinematics of prosthesis. 	<ul style="list-style-type: none"> • Required large database and numerous trials to train the controller before applying to the prosthesis
Biomechanically controlled prosthesis	<ul style="list-style-type: none"> • Prosthesis is controlled by switching the controller feedback by actuating the musculotendon 	<ul style="list-style-type: none"> • Can be used successfully for a patient with stability problem in knee-flexion extension. 	<ul style="list-style-type: none"> • Limited application due to limitation in controlling method based on only use of mass position and mass velocity • Inadequate efficiency

Table 2.2 continued

Type of Prosthesis	Significant characteristics	Advantages	Disadvantages
Myoelectric prosthesis	<ul style="list-style-type: none"> • Prosthesis is controlled using the neural information from muscle contraction, i.e. EMG signal. • EMG signal is usually captured from the residual limb. • Required substantial analysis of signal to extract the important information out. 	<ul style="list-style-type: none"> • Preferable because of its non-invasive type controlling characteristics 	<ul style="list-style-type: none"> • Prosthesis control is inefficient for the patient with poor/weak EMG signal production capacity.
Myoelectric prosthesis	<ul style="list-style-type: none"> • Prosthesis is controlled using the neural information from muscle contraction, i.e. EMG signal. • EMG signal is usually captured from the residual limb. • Required substantial analysis of signal to extract the important information out 	<ul style="list-style-type: none"> • Preferable because of its non-invasive type controlling characteristics 	<ul style="list-style-type: none"> • Prosthesis control is inefficient for the patient with poor/weak EMG signal production capacity.
Bionic prosthesis	<ul style="list-style-type: none"> • Prosthesis control is performed by stimulating the brain signal • EMG signal and invasive electrode implantation are used to innervate muscle and enhance the prosthesis control. 	<ul style="list-style-type: none"> • Capable of significantly improve the controllability of the prosthesis. 	<ul style="list-style-type: none"> • Extensive training with occupational therapy input is required. • Intraneural electrode causes infection to the patient body.

2.4 Prosthesis design and development

Prosthesis design and development process follow a particular method. The anthropometric variable measurement, designing and simulating the components under possible loading condition, fabrication of components followed by assembling, and testing the performance in real application.

2.4.1 Components of prosthesis

Based on the type, the prostheses are comprised with different types of mechanical, electrical and electronic components. Passive type prostheses are generally constructed with different mechanical components only. A typical passive type above knee prosthesis contains six major components, i.e. socket, knee joint, shank, ankle joint, foot and cosmetic cover.

- **Socket:** Socket of a prosthesis is an interfacing unit used to connect the prosthesis with the residual limb of the amputee.
- **Knee joint:** Knee joint in a prosthesis is an arrangement to imitate the movement of a healthy biological knee.
- **Shank:** Shank is the middle section of a prosthesis, which replace the section from knee to ankle of the biological lower limb.
- **Ankle joint:** Ankle joint in a prosthesis is an arrangement to imitate the movement of a healthy biological ankle.
- **Foot:** Foot of a prosthesis replaces the biological foot and provides ground contact, shock absorption and stability during stance phase.

- **Cosmetic Cover:** Cosmetic cover is to disguise injuries and disfigurements of the prosthetic arrangement.

Different components of a passive type mechanically controlled *AK* prosthesis are shown in the following Figure 2.4.

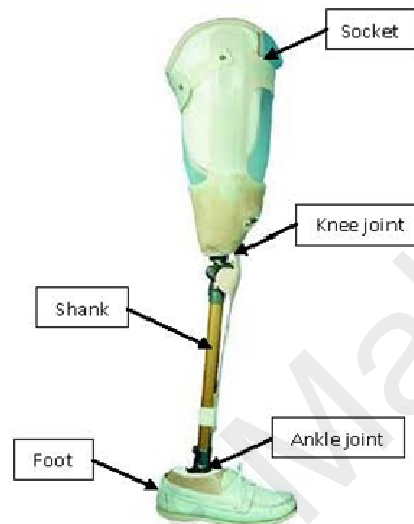


Figure 2.4: Components of a passive type above knee prosthesis.

Active type prosthesis incorporates different types of sensors, controller, actuator and interfacing unit into the mechanical structure of the prosthesis to convert the prosthesis from passive to active (Klute et al. 2009). A more effective combination of different elements mentioned would develop a more efficient prosthesis.

2.4.2 Design of an above knee prosthesis

The design of an above knee prosthesis is carried out with an objective of replicating the structure of the missing limb and reproducing the functions of the amputated limb. Prosthesis with similar features like that of a healthy biological lower limb would be more natural and effective. For the transtibial amputees

(TTA), the prosthetic limbs should ideally substitute the anatomical functions of the lost limb. The knee and ankle-foot system play the most significant roles in reproducing desired gait cycle in the prosthesis.

The natural knee joints carry load and transfer motion from thigh to shank of the lower limb. The most complicated and biggest joint of a human body is the knee joint, which has to bear massive load during production of flexible movement. During walking, the knees support 1.5 times of human body weight; during climbing stairs and squatting, about 3-4 times and 8 times of human body weight respectively. The knee is a synovial hinge joint, which acts to enable the lower limb to flex and extend relative to the thigh. The bones and ligaments' anatomy limits the range of knee movements; however, it can flex around 120 degrees. The function of the knee joint is very complex; it should be flexible enough during walking and bending and, at the same time, it must be capable of offering quite stability to human while standing up. The characteristics of permitting a little degree of medial and lateral rotation during moderate flexion make the knee joint to stand out. The features of load carrying, providing stability and imitating movement have been obtained using cam shaped joint, rope – pulley system, springs, electronic motor, microprocessor, artificial intelligence, etc. at different phases of development of a prosthetic knee joint. The knee joints consist with motor, actuator, microprocessor, etc. are called active type prostheses, which are usually more effective than those comprised with cam, spring, rope-pulley arrangements.

The natural ankle-foot system (NAFS) also acts to provide required flexion and extension to the prosthesis. The normal gait of the prosthesis is preserved by restoring the mechanical energy profile by the NAFS. For ages, the design of the prosthesis has been influenced by the knowledge of natural knee joint mechanics

and *NAFS* mechanics. The role of the knee joint and ankle joint musculatures primarily define the design approach.

In case of plane field normal walking, energy is stored/ absorbed by the natural ankle joint early to midstance phase, and the energy is generated in the late stance phase. During energy absorption and generation, negative and positive works are done by the eccentric and concentric muscle activities respectively. With an aim to imitate this function, the energy storing and returning (*ESR*) prostheses were introduced in early 1980s for the first time (Segal et al. 2012). The passive-dynamic characteristics of elastic carbon fiber materials have been used to develop these devices where energy was stored as the material deformed and returned when they recoiled. Though a quite number of *ESR* designs have been developed since introduced, none of these are capable of returning more energy than stored. This is the primary limitation of all passive-type dynamic systems.

In normal gait, energy generated/positive work by the ankle joint musculature is greater than the energy absorption/ negative work amount of positive work (DeVita et al. 2007). However, for *ESR* prosthesis, the inability of doing net positive work is considered affecting the gait of *TTA* and essentially characterized by lower self-selected walking velocity (Hsu et al. 2006), greater expenditure of metabolic energy, and larger inter-limb asymmetry (Silverman et al. 2008). Active prostheses comprised of motors or actuators have been developed to overcome this limitation. It has been reported in several studies that using the active prosthesis, the *TTA* amputees are able to reproduce natural ankle joint mechanics (Eilenberg et al. 2010) by spending less metabolic energy than that with the passive-dynamic prostheses (Herr and Grabowski 2012; Takahashi and Stanhope 2013). However, these active types of prostheses are

expensive and not affordable to the majority proportion of amputees with average economic status.

2.4.3 Simulation and finite-element analysis

Motion analysis (kinetic and kinematic) of the prosthesis arrangement and finite-element analysis of various components have to be carried out prior to prosthesis fabrication. This is to check the feasibility of the design by correlating the motion analysis results with the gait cycle of the healthy biological limb, and the *FEA* results with the properties of the material used for making different parts of the prosthesis.

To model and analyze the knee joint has a great long history. Due to complexity of the knee joint, the majority of the models are developed based on the simplified formula. Using mathematical model, better understanding on multifaceted mechanical behavior of substructures has been obtained. The substructures included the human musculoskeletal system with the knee joint in the model. Ribeiro et al. (2011) have developed a computational multibody model capable of capturing some of the basic properties of the knee joint and simulating human gait during the stance phase, including the kinetics of the real knee. A biomechanical multibody system knee model was developed, where two rigid bodies – tibia and femur were taken into consideration. They have carried out the modeling to obtain an understanding of the kinematics of the knee components.

The mechanics of movement of a normal and pathological human can be understood from the motion analysis of the knee joint (Rowe et al., 2000). During design phase, the computer model of the human knee can effectively evaluate the characteristic of the knee joint and thus can predict the possible

clinical performance of the knee (Bei and Fregly, 2004; Halloran et al., 2005). The knee joint kinematics and pressure data have been obtained from the simulation of different functional activities like, full gait cycle and one-legged forward hopping (Godest et al., 2002, Beillas et al., 2004). The quality of experimental data (e.g. loads) used for deriving the model has substantially influenced the accuracy of the prediction process (Beillas et al., 2004). BožidarPotočnik et al. (2008) have modeled and simulate a knee joint of a patient to see the kinematics for a flexion of 0° to around 40° of the femur with respect to the tibia. They have used the *MRI* data captured from the patient to do the simulation.

The entire types of available prosthetic feet are designed with an aim to imitate the anatomy and motion of foot and ankle (Hofstad et al., 2009). The desired movements in the prosthesis can obtain with some mechanical joints incorporated in the design or using material (e.g. carbon laminate components or foam/rubber materials) with good elasticity of spring-back qualities (Rusaw and Ramstrand, 2010). The inverse dynamic model is used to determine ankle kinetics and thus to evaluate the functional performance of a prosthetic feet respect to others. However, this approach got some limitation where the foot is considered as a rigid segment with definable axes of the ankle joint (Winter, 2009). Majority of prostheses with energy storing and return (*ESR*) quality have no component with articulated construction. All those prosthesis are found to produce dorsi-flexion and plantar-flexion movements about some undefined axis instead of undergoing deformation during foot's flexible keels. In case of using some device with articulated connection, these types of deformations are also taken place. The interpretation of 'ankle' kinetics, therefore, can be somewhat

problematic and sometimes misleading also (Geil et al. 2000; Miller and Childress 2005).

Hansen et al. (2000) have proposed some other type of interpretation method based on the center of pressure (*CoP*) trajectory to overcome the mentioned limitations. This has been done by transforming the *CoP* from a global coordinate system (laboratory-based) to the local coordinate system of the shank. The entire arrangement was to determine the effective shape of a 'rocker' to be used in a certain prosthetic foot. The proposed method has eliminated the necessity of modeling the ankle joint as segment and joint.

In addition, the global function of the prosthetic ankle-foot system was assessed by determining the radius and shape of this rocker. Though the approach was widely regarded by prosthetists (Curtze et al. 2009; Major et al. 2011), it has obtained some error due to using a limited number of *CoP* displacement samples in determining the radius of the best-fit curve. This method of roll-over shape characterization has overlooked the disruptions for short duration in progression of *CoP*. Therefore, the different characteristics of prosthetic components have remained uncounted due to ignorance of such disruption magnitudes (De Asha et al. 2013).

Zach et al. (2014) have evaluated the von Mises stress, plastic stability of material, and also the distribution of contact pressure on the surface of *PEEK* hinged bushing pin when the knee was bended within the range of 15.4–69.4° hip joint flexion. From the finite element (*FE*) analysis, the ankle flexion angle was obtained to be 32.7°, while the real value of that angle was measured to be 28.41° for the corresponding maximal flexion angle of hip joint of 69.40. The maximal difference between the data from experiment and *FE* analysis was 4.3°. The variations of the von Mises stress distributions in bipolar hemi-knee

prosthesis and unipolar prosthesis were observed by Lian et al. (2014) when the prosthesis was moved at different gait cycle under static upright posture. Maximum stress values were determined based on the dynamic analysis of the unipolar and bipolar joint prostheses. Though, the simulation and *FE* analysis result have some deviation from the real test result, at least it can provide some idea about the potentiality of the design before fabrication.

2.4.4 Prosthesis construction

The body weight in most of the healthy individuals is shared equally by the both legs. An ideal symmetric loading of the lower limb joint is developed by the weight distribution in 50:50 ratios. This type of symmetric distribution helps to maintain the balance of the body requires no extra energy consumption and no making of pointless compensation movements in the ankle and foot area. The amputation changes the biomechanics of the subject body and affects the normal gait cycle movement of the amputee. In amputee, the path of load transmission is changed due to shifting of center of gravity in the frontal plane. The center of gravity is moved to healthy limb side.

An appropriate construction and a proper selection of components for transfemoral (*TF*) prosthesis can ensure transfer of subject body weight up to 40%.

The amputation height or the residual muscle defines the stability of the prosthesis and the stabilization activity of the limb. Under amputation, the extent of muscular function (flexors/extensors, abductors/adductors) reduction is determined by the transaction height of the damaged muscle.

Development of a prosthesis functioning properly includes some important factors:

- The user physical and mental condition, the type of activity to be performed using the prosthesis and the methods of use essentially define the components to be used for the prosthesis. The patient weight and physical activity are the primary concern for selecting components for some prosthesis. The materials for prosthesis components are chosen according to the user weight to ensure a safe operation of the prosthesis under an average weight of the transtibial prosthesis.
- The height, shape and condition of residual limb, the scar and dieses due to amputation are also to be taken into consideration while construction a prosthesis.
- The prosthesis construction is accomplished with the following steps: basic construction, static and dynamic correction.

The load line plays a very significant role in proper distribution of subject's body weight. To identify the course of the line is essentially important for the prosthesis construction. The load line in healthy individual is considered as a vertical line, which in the sagittal plane passes through the center of gravity, 2 mm posterior from the hip, 15 mm anterior from the knee, and 60 mm anterior from the ankle joints (Figure 2.5). The load line goes through the body center when is looked from the frontal plane. During prosthesis construction, the load line should run through the centers of the mentioned limb joints. In stable stance, the foot stabilizes the prosthesis by shifting the center of gravity in the name of compensation of the horizontal movements. The center of gravity is moved by shifting weight left and right, forward and backward (Walsh 2006).

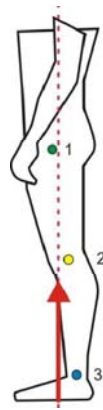


Figure 2.5: Load line: 1) - 2mm posterior from the hip joint, 2) - 15mm anterior from the knee joint and 3) - 60mm anterior from the ankle joint (Rajčúková, et al. 2014).

The prosthesis construction is an empirical process, the performance of which is defined by the skill of orthopaedic technician and feedback from the patient. A good construction of a lower limb prosthesis can provide adequate stability, balance, certainty and comfort to the users throughout the gait cycle. It can also reduce the energy consumption and gait asymmetry. Determining the construction line is critically important for prosthesis development. It is an arbitrary vertical line shown in Figure 2.6.

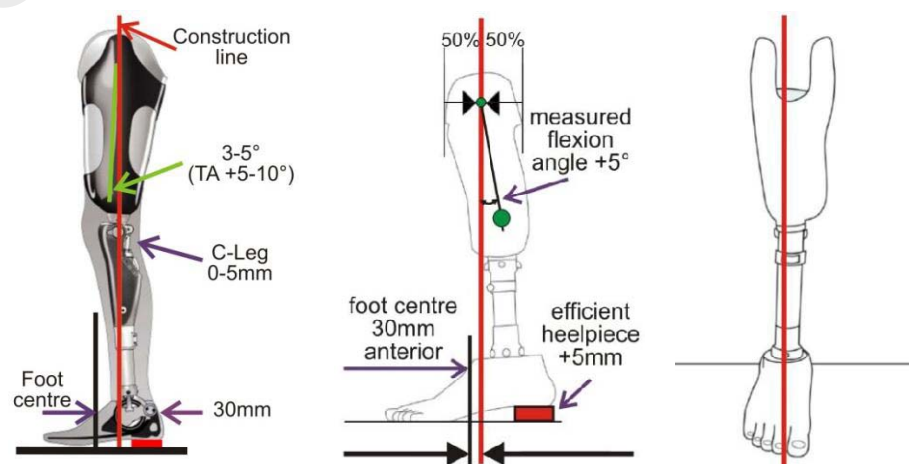


Figure 2.6: Construction line (Rajčúková, et al. 2014).

Usually, the components of the prosthesis are positioned toward the construction line based on some particular rule presented in Table 2.3.

The entire process of prosthesis construction is performed into the following three steps shown in Table 2.3.

Table 2.3: Steps of prosthesis construction (Rajčúková, et al. 2014)

	Construction	TT	TF	
Basic construction	foot	Sagittal plane (AP)	Heelpiece height – efficient heelpiece + 5 mm Foot centre moved forward before the construction line in 30 mm	
		Transverse plane	External rotation 5-7°	
	socket	Sagittal plane	Flexion–measured value of the flexion angle + 5°	Flexion–measured value of the flexion angle + 5° to 10°
		Frontal plane		Adduction angle, depending on the residual limb length 3, 7, 12°.
Knee joint	Sagittal plane (AP)	-	Position according to the construction Rotation centre 20 mm above the MPT of the second limb	
Static correction	Frontal plane	Prosthesis length M – L foot position Pronation/supination	Prosthesis length M – L knee and foot position Pronation/supination	
	Sagittal plane (AP)	Plantar flexion A-P foot position	Plantar flexion A-P knee and foot position	
	Transverse plane	Foot shift	Foot shift	
Dynamic correction	Frontal plane	Knee joint movement control in the support phase, minimum M-L forces		
	Sagittal plane (AP)	Knee joint movement control in the support phase, natural flexion and extension when loaded		
	Gait test in various environments			

The static adjustment is the second step of prosthesis development, which is performed with the patient. During prosthesis construction, the components are required to turn, shift and adjust to obtaining stability in stance. To adjust the correct length to the prosthesis is very important for static adjustment. It is performed to ensure both limb are evenly loaded, and the pelvises of the legs are at the same level. The stance of a prosthesis is influenced by the shift of the load

line while moving the foot forward (by the movement of plantar flexion). The load-line in an above knee prosthesis is shown in Figure 2.7.

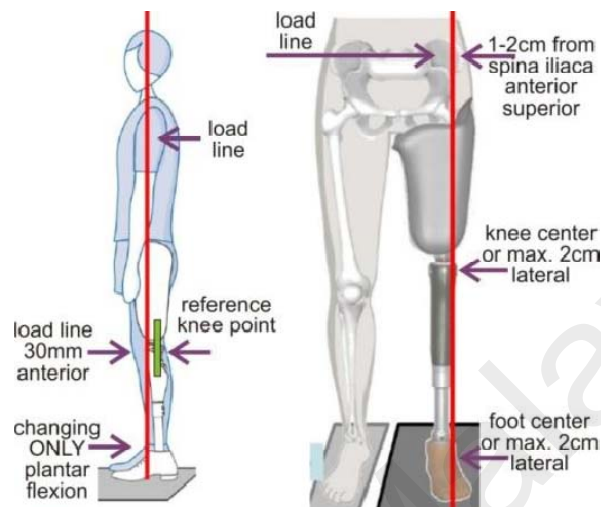


Figure 2.7: Load line in Transfemoral prosthesis (Rajtůková et al. 2014).

In dynamic adjustment of the prosthesis, the deviations of gait from the normal step cycle are assessed in both the frontal and sagittal planes. The incorrect constructions of prosthesis, physical and mental conditions of the subject are the main reasons for the gait deviations. The first contact between the foot and ground and the load transfer to the foot are essentially important for prosthesis gait. For more natural walking, the foot contact is started with the heel and followed by the entire sole and then the load is transmitted to the foot. After that the foot rolls away from the ground, and the toe pushes off when additional energy supply is necessary for the swing phase.

In the swing phase, the correct selection of foot and proper placement of the knee joint is very important. The components as well as their arrangement influence the performance of the prosthesis and thus affect the individual's activity. The knee function plays a significant role in swing phase; the movement from flexion to extension (extension moment of the knee) has to

perform to facilitate the transition of foot from plantar flexion to the dorsal flexion. This is required to ensure toe elevation in order to avoid stumbling and subsequent falling of the subject (Bowker and Michael, 1992).

2.4.5 Performance testing

The performance testing is the final step of prosthesis development. It is performed to assess the mechanical, biomechanical properties of the prosthesis and also to check the compatibility with the user. The performance test helps to identify the defects and limitation of the prosthesis and thus to fix the problems belong to the prosthesis arrangement. The difficulties, the user experience/might experience due to the defects of the prosthesis construction are also figured out with the performance test and analysis. For instance, Major et al. (2013) have identified that during terminal stance, a bilateral transtibial amputee (*BTA*) has difficulty in producing plantarflexion motion in the ankle joint. Limited power generation for rolling the limb forward is another constraint caused by the nature of the passive transtibial prostheses. The performance test and analysis also help to correct and improve the design of the prosthesis and thus to protect user from any sufferings caused from the pertinent defects and to make the prosthesis comfortable to the users.

The performance of the prosthesis is analyzed based on some parameters like spatial-temporal variables, kinematics and kinetics of the prosthesis. The spatial-temporal variables deal with stride length, stride duration, single support, double support, swing duration, and period (Kirtley, 1998). Prior to testing, it is required to decide which variable to be investigated during the evaluation. The performance evaluation of the above knee prosthesis includes both the kinematic and the kinetic analyses.

The kinematic of the prosthesis is evaluated by measuring the angular displacement, angular velocity of the joints and linkages. Toe clearance and anterior – posterior heel contact velocity ($A - P HCV$) are influenced by the velocities of the joint, angular displacements, and shank of the leg. Toe clearance is essentially susceptible to the angles at the ankle, knee and hip joints of the swing leg, whereas $A - P HCV$ is principally determined by the angular velocities of the shank and thigh of the swing leg (Winter, 1992). The similar factors and variables have to be investigated to evaluate the performance of the prosthesis. The movement information is obtained from the kinematic analysis; however, the forces involved in that movement are not reflected in the results of the analysis (Winter, 2009). On the other hand, the forces, moments, and powers associated with the movements are studied in the kinetic analysis.

The gait aspects can be thoroughly assessed by the kinetic measures, particularly the factors which are not readily evident in the kinematic analysis data. In stance phase, a net extensor moment is produced by the ankle, knee and hip joints to avoid limb collapse (Winter, 1991). On the other hand, some forces are exerted by the body to resist the pull of gravity and advancing the body forward during swing phase, which is equal and opposite to the reaction forces by the ground, and is therefore called the Ground Reaction Force. Both the magnitude and the direction of the ground reaction force vector determine the moments in the ankle, knee and hip joints at different phases of gait. The joint moments either create or oppose rotation during the gait cycle. The amount of mass, the position of the center of mass, and the mass distribution in different limb segments is essentially important for calculating the accurate moment. The calculation of all these data is a prerequisite for interpreting and analyzing the joint moment data.

Leading-log approximation (*LLA*) is a widely used method for calculating all these variables (Arampatzis et al., 2005).

The Joint Power represents significant information about the muscle contributions to the rolling forward of the limb. This can be obtained from the moment and angular velocity of the joint. However, interpretation of prosthesis movements sometimes becomes difficult while doing powerful calculation using this method. The assumptions and the limitations of this model are the main causes of this difficulty. For instance, the event of energy storage and return at the ankle push-off in late stance phase is simulated as power absorption and generation by foot/ankle mechanism, which is unreal for the passive type prosthesis (Arampatzis et al., 2005). A proper investigation and analysis of all these parameters would make the performance analysis of the prosthesis effective.

Different prosthetists choose different parameters based on the type of the developed prosthesis and requirements of the subject to do the performance test. Rusaw and Rmastrand (2010) have identified the functional joint center (*FJC*) of a commonly used prosthetic foot as a mean of kinematic analysis of the prosthetic feet. Analysis was carried out to assess the difference between the *FJCs* of the prosthetic feet and intact control foot. This study also carried out a comparative study between the commonly used methods, and the *FJC* method based on the intact side (anatomical method) in estimating joint parameters. Their study has described the clinical usefulness of the *FJC* method and also indicated the errors belong to the traditional joint marker methods used for gait analysis. To analyze the relationships between the ankle dorsiflexion, leg loading, and energy storage and return is essentially required prior to design

components for prosthesis. An effective design of a prosthesis can improve the loading symmetry in gait of amputee.

Ventura et al. (2011) have identified the effect of ankle dorsiflexion and ESR at loading phase of the prosthetic leg. They have also studied the intersegmental moments and powers, and GRFs in steady-state walking. A vertical load with variable magnitudes of 50N to 1230N was applied at a rate of 20 mm/min to test the level of stiffness of the C-shaped articulated ankle joint. The stiffness of the stiff ankle and the compliant ankle were measured to be 783 ± 9 N/mm and 388 ± 14 N/mm respectively. Five different foot conditions were compared with a solid ankle (SA) condition. The solid ankle (SA) genuinely had no ankle and was recognized as a Seattle Lightfoot2. The five-foot conditions under which the ankle was tested were SA, compliant FA, stiff FA, stiff RA and compliant reverse-facing ankles (RA). Their investigation showed that the amputee gait mechanics was largely defined by the magnitude of stiffness and energy storing and returning capacity of the prosthetic ankle.

In another controlled investigation, Major et al. (2013) have studied the connections between the rotation stiffness of articulated Custom-built Foot-Ankle Mechanism (CFAM) and users gait performance while performing different daily ambulation (i.e., level, uphill, and downhill) in various walking conditions. The CFAM was used to facilitate the systematic testing under at different ankle stiffness without affecting the other properties. As the alteration of prosthetic components and alignment causes the mechanical properties of the prosthesis to change in a complex and interactive manner, the CFAM was used to avoid these influences. According to Russell et al. (2014), with the increase of walking speed, the peak vertical forces, external flexor moment and the loading rate were decreased in powered prosthesis; however, the peak adduction moment

or its impulse remained unaffected. In addition, the loading rate was found to decrease from the control by the powered prosthesis. No significant greater risk in the sound limb than the intact limb due to knee osteoarthritis was observed.

The performance test is performed through a number of mechanical and biomechanical tests. Testing the gait deviation is very important for prosthesis development. Undesired deviation is seen in the gait cycle when the prosthesis alignment is not properly achieved. Among numerous effects, excess energy consumption, uneven loading and overloading of a particular group of muscles and damage of joint structure and skins are the most common aspects occurred from the gait deviation. The gait aesthetic discomfort (step cycle asymmetry, body inclination, etc.) is another factor caused from the deviation in physiological gait (Sanders et al. 1998). The following factors are mostly tested during the construction of a transfemoral prostheses:

1. Vaulting

- features – the amputee "steps up" to the prosthesis to accomplish the stride,
- reasons – the length of the prosthesis is too long or the resistance of the knee is excessive.

2. Medial / Lateral Whip

- features – at toe off, the prosthesis heel is tracked to be nearing/ going away from the midline of the body,
- reasons – extra rotation (external or internal) of the prosthetic knee axis.

3. Circumduction

- features – the outward swing of the foot follows an exaggerated curved track in swing,

- reasons – excessively large resistance to the prosthetic knee flexion, limited knee flexion, development of an avoidance mechanism in the event of pain caused by socket medial brim and extra length of the prosthesis.

4. Lateral Trunk Bending

- features – the gait of the patient is leaned, the shoulder of the users is tilted toward the affected side,
- reasons – the foot of the prosthesis is outset more than 25 mm, the length of the prosthesis is inappropriate, the adduction of the socket is inadequate or lack of amputee sensitivity.

5. Excessive Heel Rise

- features – the prosthetic heel travel up quite far and very fast,
- reasons – inadequacy in the prosthetic knee flexion resistance.

6. Drop Off

- features – there is excessive abrupt knee flexion in the late stance,
- reasons – extra softness of the keel, shortness of the toe lever, excessive heel height of the prosthetic foot.

7. Foot Slap

- features – there is a quick and uncosmetic plantarflexion moves right after heel contact,
- reasons – inadequate plantarflexion resistance and too soft bumper in the prosthetic foot.

8. Hyperextension of the knee on the affected side

- features – there is hyperextension in the knee of the amputated leg in midstance,

- reasons – typically appears as the prosthesis design switch from a joint and thigh lacer type to a patella tendon bearing type, excessive softness of the heel, extra-long or extra-firm toe lever arm, slackness of posterior knee capsule or hamstrings' tendons.

9. Pistoning

- features – there are some vertical movements in the residual limb when the load-bearing alternates,
- reasons – extra-large socket size and insufficient suspension in the prosthesis.

The natural walking stereotype of the amputee largely influences the prosthesis adjustment. The prosthesis function and stump pressure significantly determine the energy consumption and comfort in using the prosthesis. User would experience pain in performing different daily activities if the prosthetic fitting is wrong. Lateral asymmetry in the body due to inappropriate prosthesis length and wrong component selection is manifested as pain. There are chances of force discrepancy, muscle overloading, tripping risk and damage of soft tissue in stump when the prosthesis is wrongly constructed (Rajčúková et al., 2014).

The event of performance testing of a prosthesis also includes some dynamic tests. The strength and vibration frequency of loading of different prosthetic components and the prosthesis itself are measured to make sure the structure of the prosthesis is safe to bear the amputee body weight and the applied load. The stability of the prosthesis has to be tested to ensure a stable operation of the prosthesis, both at the stance and swing phases.

2.4.6. Literature Summery

There are numerous types of prostheses available for amputees which all developed aiming to imitate the biomechanics of the healthy biological limb as closely as possible. Using these prostheses, some extents of success at overcoming some particular difficulty with the amputees have been achieved. However, these prostheses are still having some limitation in terms of features or in terms of prices. Though there are some limitations in mechanical type of prosthesis, this type of prosthesis is identified as the most suitable type for the mass proportion of amputee who are our target users. The prosthesis design and construction required to follow some particular procedure and to conform to some important design factors to make it properly made and to ensure a better performance. To evaluate the performance of a prosthesis, some parameters have to be measured and checked by comparing with that of the healthy biological limb. Usually, different mechanical tests are performed on various components of a prosthesis at the first place, and then biomechanical tests are carried out on the prosthesis to evaluate the feasibility of the design of the prosthesis. Particularly, kinematic and kinetic test and stability test results are important to assess the performance of a prosthesis. The efficiency of a prosthesis or its joints is evaluated by comparing the gait cycle movement of the prosthesis/ prosthetic joints to that of the corresponding healthy biological limb.

CHAPTER 3: METHODOLOGY

A thorough study on prosthesis has been carried out; their types based on nature, controlling method used has been studied meticulously; the efficiency, limitation, development cost of these prostheses have been analyzed to identify the best suitable type for mass proportion of amputees from developing and least developed countries. The selection process has taken some factors into consideration while to choose one particular type of prosthesis for the target group of amputees, e.g. the functionality, difficulties in performing different daily activities, and most importantly the prices of the prosthesis have been evaluated the most to select the suitable type of prosthesis for the target group of amputee. Due to the cheap prices, the mechanical type prosthesis was identified as the best suitable type of prosthesis for the amputees with below average economic status. There were also some difficulties pointed out in the existing mechanical type prosthesis which have been tried to eliminate by introducing some new mechanism and joints in the prosthesis arrangements. The entire procedure of design and development of the proposed mechanical type prosthesis has been described in the following sections and subsections.

Some systematic procedure has been followed to design and development of the above knee prosthesis. The design process has been accomplished by few steps, starting with identifying the subject's need, followed by researching the problem, developing the possible solutions, selecting the most promising solution, constructing a prosthesis prototype, testing and evaluating the prototype, and redesigning the prosthesis. After repeating the whole process couple of times, the final version of the design has been obtained. Modeling and simulation of each design have been carried out on Solidworks

platform to see the feasibility of the design. The design and development cycle of the prosthesis is shown in the Figure 3.1.

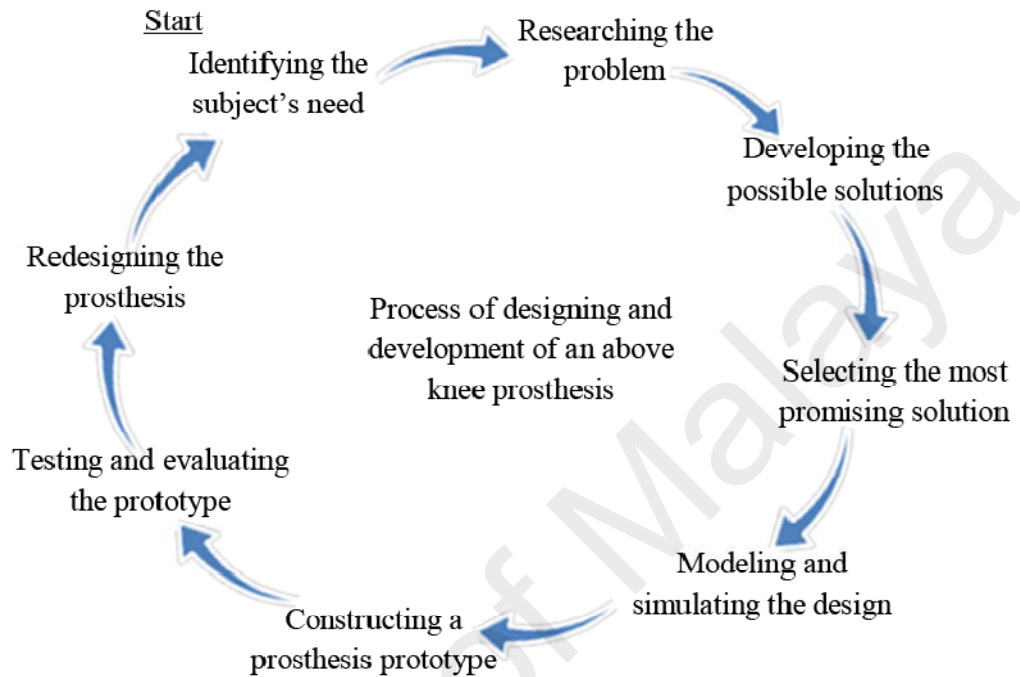


Figure 3.1: Design and development cycle of a prosthesis.

The final design of prosthesis and its components has been accomplished into different stages of improvement. The following Figure 3.2 is showing the different steps of design improvement to obtain the optimum design of the prosthesis.

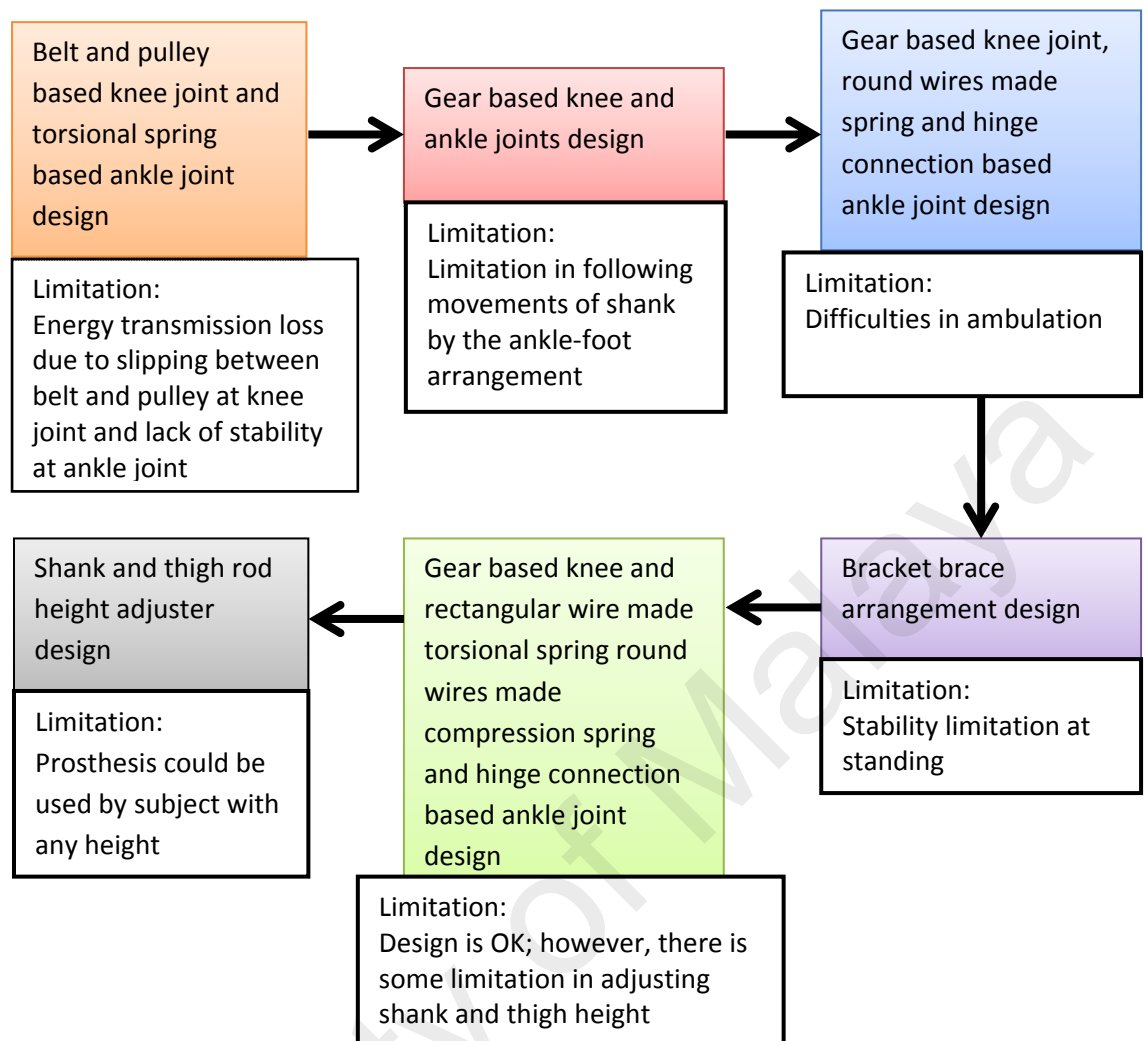


Figure 3.2: Steps of prosthesis design improvement.

At the first place, pulley and belt were chosen to operate the knee joint of the prosthesis according to the residual limb; a set of torsional springs were used as ankle-foot arrangement in the design. However, the static and dynamic analysis results of simulation showed that the design could not provide enough stability to the prosthesis. There were also some limitations in creating desired angle and proving adequate stiffness to the prosthesis.

The second design was purely based on gear mechanism. A set of external spur gears were used at the knee joint whereas a set of sun and planet gear mechanism was used at the ankle joint to operate the prosthesis. The static and dynamic analysis results of

simulation showed that the purely gear based prosthesis had some difficulties in following the movement of the residual limb, particularly in ambulation of the ankle as per the demand of the shank rotation.

The third version of the design is a combination of the both designs, where the gear mechanism is still used in the knee joint. However, a hinge joint type connection with help of some compression and torsional springs were introduced at the ankle joint to overcome the difficulties with the previous designs. The static and dynamic analysis results of simulation showed that the gear based knee joint was having some difficulties in producing the desired movement into the prosthesis, the shank of the prosthesis could not follow the movement of the thigh or residual movement properly. The analysis showed that, some support was required for the prosthesis to make the shank moving corresponding to the residual limb movements, which was missing in that design.

In the fourth version of the prosthesis, a bracket and bracing arrangement has been introduced into the design. The bracket –bracing system has been designed and incorporated into the prosthesis to overcome that difficulty. The static and dynamic analysis results of simulation showed that the gear based knee joint with help of the bracket – bracing arrangement was capable of producing the desired movement into the prosthesis, however the stability of the prosthesis was yet to improve. The investigation showed that the torsional spring of the ankle joint was not stiff enough to provide adequate stability to the prosthesis. The torsional spring has been redesigned to provide ample stability to the prosthesis. A special shaped spring has been designed, which will behave like a torsional spring and at the same time act like a rigid support for the shank.

The fifth version of prosthesis comprised of the gear based ankle joint, some bracing and bracket arrangement, and spring based ankle joint which in combination were capable of producing the desired movement into the prosthesis without compromising

with the stability and stiffness of the prosthesis. In addition to this, this design offered some extra advantage by providing a great range of flexion and compression ability to the ankle joint when required for performing different daily activities. There were still some difficulties in fitting the prosthesis to different subjects due to the variation in the shank and thigh lengths. Therefore, some height adjustment systems were introduced into the shank and thigh rods to make the prosthesis universal and adjustable for subjects with different heights. The final version of the prosthesis was suitable for a wide range of subjects of different heights.

The newly designed prosthesis will add a new dimension in the mechanical type prosthesis. This will enhance the controllability of the mechanical type prosthesis within an affordable price. Unlike the typical mechanical prosthesis, the new design will make the prosthesis to follow the residual limb movements without having any additional guidance arrangement. A gear based knee joint will make the prosthesis to move according to the residual limb movement. A spring based ankle joint, on the other hand, will help the amputee to overcome the difficulties in producing required angle of rotation in their prosthetic feet. A torsion spring will enable the ankle joint to rotate in a controlled way to any desired angle without demanding any additional setup.

The following Figure 3.3 shows the steps used for development of the prosthesis.

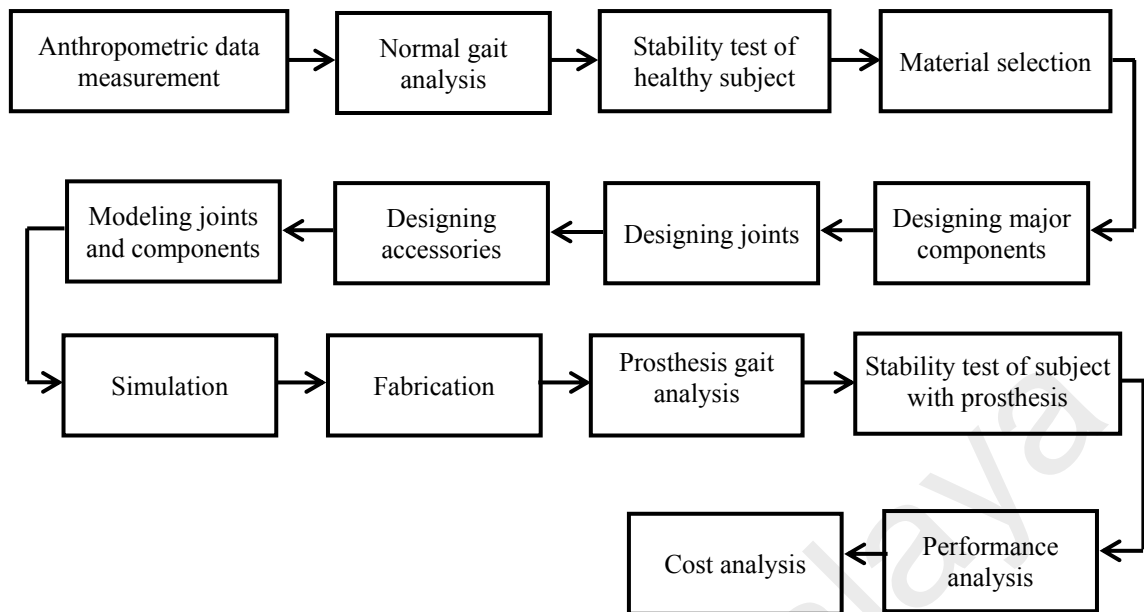


Figure 3.3: Flow chart of design and development of the lower limb prosthesis.

The normal gait cycle data, stability and fall risk index values of the healthy individual were recorded prior to the design of a prosthesis. The anthropometric variable of the subjects were also measured before designing the lower limb prosthesis. Then the prosthesis structure was sketched based on the anthropometric data aiming to replicate the normal gait cycle and obtain similar stability index with the prosthesis. After that, suitable material was chosen for the prosthesis and its components. The major components of the prosthesis were designed first, which followed by designing the main joints, and the accessories. The model of the joints and different components were developed and then simulated under different possible conditions. The designed prosthetic components were fabricated and assembled to develop the prosthesis. The gait cycle data and the stability test index of the subject with the prosthesis were captured and analyzed. Finally, comparative studies were carried out between the natural gait cycle and prosthesis gait cycle. The stability index values from healthy subject and those from the subject with prosthesis were also compared. The

performance of the designed prosthesis was then evaluated based on the results obtained from the available mechanical type prosthesis.

3.1 Capturing gait cycle of healthy lower limb

The anthropometric variables were measured before capturing the natural gait cycle of the healthy lower limb. Roller, weighing machine and calipers were used to measure height and weight of the subject, and to measure the length and diameters/dimensions of different lower limb extremities. The anthropometric data measured from the subject were used to design and develop the prosthesis. Three trials were given to measure the mean value of anthropometric variables. Different anthropometric data of the subject are shown in the following Table 3.1.

Table 3.1: Subject characteristics and anthropometrical data

Variable	Mean value
Subject height (who the prosthesis is designed for)(cm)	166.5± 0.13
Mass (Kg)	69± 0.29
Left leg length (cm)	92.5 ² 0.13
Left thigh length (cm)	51.5 ² 0.11
Left shank length (cm)	41.0 ² 0.13
Left knee width (cm)	10.8 ² 0.03
Left ankle width (cm)	6.9 ² 0.02
Left ankle-heel distance (cm)	8.6 ² 0.01
Right leg length (cm)	92.0± 0.13
Right thigh length (cm)	50.0 ² 0.11
Right shank length (cm)	42.0 ² 0.12
Right knee width (cm)	10.9 ² 0.02
Right ankle width (cm)	7.1± 0.01
Right ankle-heel distance (cm)	8.6 ² 0.01

Gait cycle of healthy lower limb was recorded prior to model and simulate a prosthesis design. The natural gait analysis was performed to extract required information for designing a prosthesis. The design was optimized based on these gait analysis data

before fabrication. Those data were also used as reference during the performance test of the prosthesis. The measurement of the anthropometric variables is a prerequisite to calculate the boundary conditions calculations for motion analysis.

The gait analysis of the subject required the subject to be equipped with some reflective markers and produce movements within a defined area, which is encompassed by an arrangement of some near infrared (*NIR*) cameras and a data recording system. Sixteen reflective markers were placed at different location of the joints and segments of the lower limb. A set of markers was placed at left and right feet (*LTOE* and *RTOE*). The exact position of the marker was at the second metatarsal head, on the mid-foot side of the equinus break between fore-foot and mid-foot. Then, another set of markers were placed at the calcaneus of each heel (*LHEE* and *RHEE*) at the same height above the plantar surface. At the ankle joint, markers were placed on the lateral malleolus (*LANK*, and *RANK*) along an imaginary line that passes through the transmalleolar axis. The tibial markers (*LTIB* and *RTIB*) were placed over the lower 1/3 of the shank to determine the alignment of the ankle flexion axis. The tibial markers were positioned such a way that they lied in a plane that contains the knee and ankle joint centers and the ankle flexion/extension axis. Similarly, the thigh marker (*LTHI* and *RTHI*) were placed over the lower lateral 1/3 surface of the thigh, just below the swing of the hand, although the height is not critical. The thigh markers were used to calculate the knee flexion axis location and orientation. The knee markers (*LKNE* and *RKNE*) were placed on the lateral epicondyle of the knees. The pelvis markers (*LASI* and *RASI*) were placed directly over the left and right anterior superior iliac spine. These were positioned medially to the Anterior Superior Iliac Spines (*ASIS*) at slight bony prominences to get the marker to the correct position due to the curvature of the abdomen. These markers have defined the pelvic axes. After placing all sixteen reflective markers at the technically correct positions, gait cycle data have been captured and stored with five *MX*

cameras and the *VICON* system. The near infrared (*NIR*) ray imping on the reflective markers have identified the movement of the lower limb when the ray reflected back to the camera. Since the ray was *NIR*, it was not disturbed by any possible obstacles coming to its way. Two force plates were used to capture the ground reaction forces during the experiment. The data captured from the subject were further analyzed with *VICON NEXUS 1.8.5* system and Microsoft excels to obtain the required information. The following Figure 3.4 shows the marker position used for capturing the gait cycle.

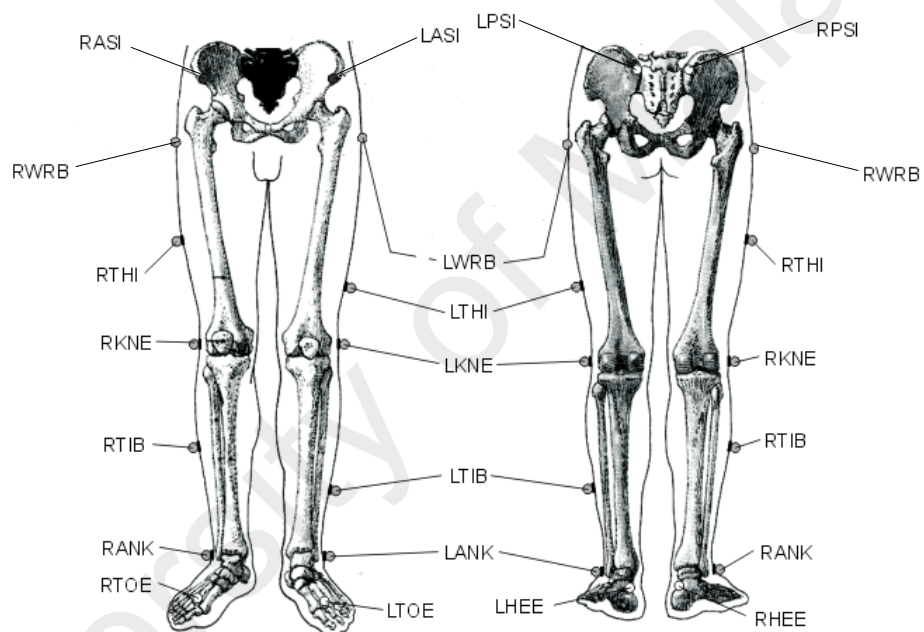


Figure 3.4: Plug-in-Gait Marker Placement.

The arrangement for capturing the normal gait of the healthy individual is illustrated in the following Figure 3.5.

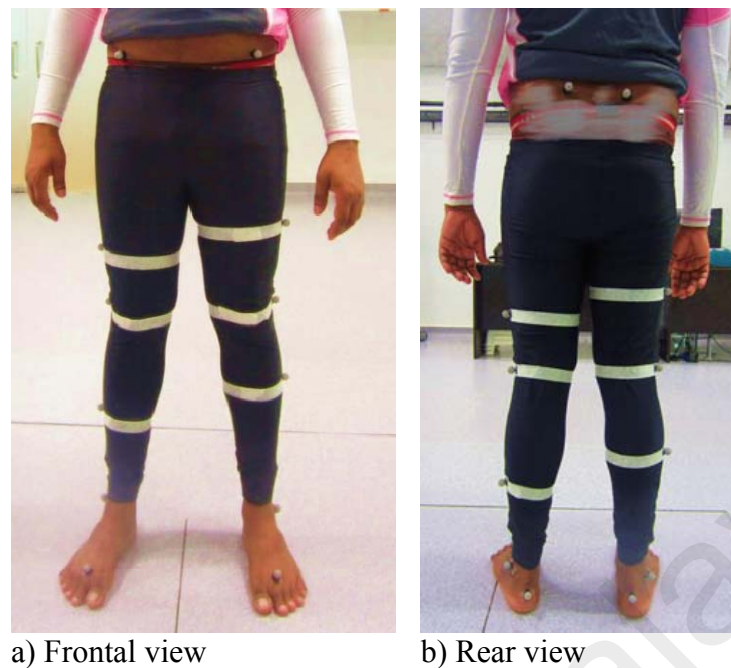


Figure 3.5: Marker positions on the lower limb of healthy individual in gait analysis.

3.2 Measuring stability index of healthy individual

The stability index of the subject was measured using a balance system named ‘Biodex Balance System SD’ and the data was processed using a software called ‘Biodex Medical System, Inc., version 1.3.5. The subject climbed and stood on the platform of the Biodex machine at some comfortable foot position where the center of body mass remained at the center of the platform. In postural stability test, the left and right feet were placed at an angle of 20° each, and then the respective heel positions were at E6 and E16 lines of platform scale. During the fall risk test, the left and right feet of the subject were placed on the platform at an angle of 25° and 20° respectively, and then the corresponding heel were positioned at E6 and E16 lines of platform scale. The feet positions during the postural stability and fall risk tests of the healthy individual are shown in the following Table 3.2.

Table 3.2: Foot placement of healthy individual on the platform of Biodex Balance machine

Foot placement		
Foot position on machine platform	Left	Right
In postural stability test		
Foot angle (degree)	5	20
Heel position (line number platform scale)	F11	F15
In fall risk test		
Foot angle (angle)	25	20
Heel position (line number on platform scale)	E6	E16

Both the static and dynamic tests were conducted to collect data and thus to evaluate the stability of the subject. Two levels of stability and fall risk were tested: first by setting the platform of the machine at level 8, which is comparatively easier, and then by setting the platform at level 2 which is much tougher to maintain the balance. Three readings were recorded in each test. Each trial duration was 20 seconds and the rest between the trials was 5 seconds. The setup used for recording the balance data from the healthy subject is shown in the Figure 3.6.

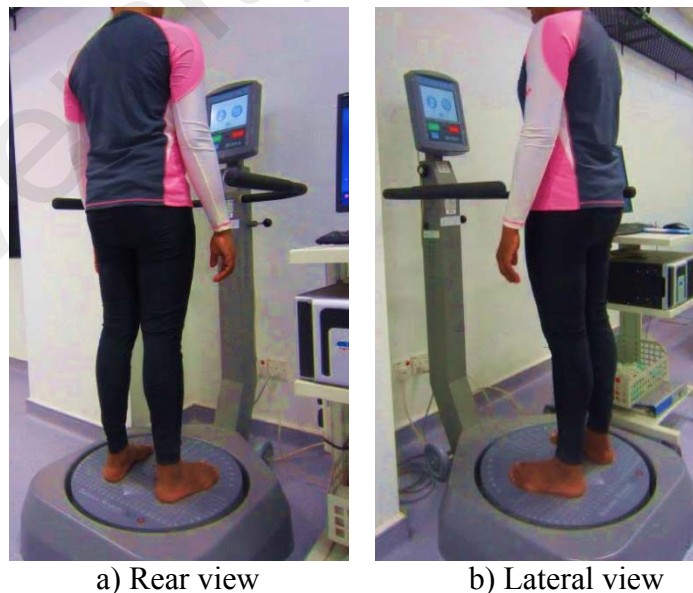


Figure 3.6: Foot positions on the platform of the Biodex machine in stability test of healthy individual.

3.3 Material selection

The material selection was a very important issue to be solved properly to accomplish the design process effectively. Materials for each component have been chosen based on the application and purpose of the component. Both the static and dynamic properties of the materials were studied before selecting the material for the components. Following Table 3.3 shows the materials for the knee joint components.

Table 3.3: Material used for making knee joint components

SN	Component	Material used
1	Gear	Aluminium alloy – <i>AISI 1060-H12</i>
2	Gear stopper	Aluminium alloy – <i>AISI 1060-H12</i>
3	Bracing plates	Aluminium alloy – <i>AISI 1060-H12</i>
4	Ball bearing	Chrome steel – <i>SAE 52100</i>
5	Bushing pin	Steel alloy – <i>AISI 4140</i>
6	Thigh rod	Aluminium alloy – <i>AISI 1060-H12</i>
7	Thigh rod height adjuster	Aluminium alloy – <i>AISI 1060-H12</i>
8	Shank rod	Aluminium alloy – <i>AISI 1060-H12</i>
9	Shank rod height adjuster	Aluminium alloy – <i>AISI 1060-H12</i>
10	Bracket arm (guiding plate)	Aluminium alloy – <i>AISI 1060-H12</i>
11	Bracket hook	Aluminium alloy – <i>AISI 1060-H12</i>
12	Bracket-belt interfacing plate	Aluminium alloy – <i>AISI 1060-H12</i>

Table 3.4 shows the materials chosen for the ankle joint components.

Table 3.4: Material used for making ankle joint components

SN	Component	Material used
1	Shank	Aluminium alloy – <i>AISI 1060-H12</i>
2	Shank rod height adjuster	Aluminium alloy – <i>AISI 1060-H12</i>
3	Knuckle frame	Aluminium alloy – <i>AISI 1060-H12</i>
4	Bushing pin	Steel alloy – <i>AISI 4140</i>
5	Ball bearing	Chrome steel – <i>SAE 52100</i>
6	Sleeve bearing	Cast copper alloy – <i>A1063</i>
7	Torsional spring	Music wire
8	Torsional spring guide 1	Aluminium alloy – <i>AISI 1060-H12</i>
9	Torsional spring guide 2	Aluminium alloy – <i>AISI 1060-H12</i>
10	Upper foot plate	Aluminium alloy – <i>AISI 1060-H12</i>
11	Lower foot plate	Aluminium alloy – <i>AISI 1060-H12</i>
12	Compression spring	Music wire
13	Compression spring holder	Aluminium alloy – <i>AISI 1060-H12</i>
14	Compression spring guide	Aluminium alloy – <i>AISI 1060-H12</i>

The suitability of the materials chosen for different prosthesis components were evaluated with finite element analysis. A proper selection of material is essentially important for making some component and fabrication of prosthesis.

3.4 Designing the prosthetic components

The prosthesis was designed based on the anthropometrics of the subject, focusing on the limitations the subject have during performing different daily activities and creating natural gait cycle movements. The basic structure of the prosthesis was designed at the first place, then assisting components were designed to enable it to imitate the natural gait cycle of the prosthesis, and to improve its performance. The components of the prosthesis are shown in the following Table 3.5.

Table 3.5: Components of prosthesis

Major Components	Auxiliary Components
Socket	Gear
Thigh rod	Bracing plates
Knee joint	Ball bearing
Shank rod	Bushing pin
Ankle joint	Thigh rod height adjuster
Foot	Shank rod height adjuster
	Bracket
	Belt
	Compression spring
	Torsional spring
	Compression spring holder
	Compression spring guide
	Knuckle frame
	Upper Foot plate
	Lower foot plate

The thigh rod, shank rod and foot plates were able to replace the structure of missing lower limb extremity. The height adjusters were introduced into the shank and thigh rod to change the length of the rods according to the subject anthropometrics. However,

these basic structures could not make the prosthesis move following the residual limb movement. The gear based knee joint was incorporated into the prosthesis arrangement to make it possible. The basic structure of the prosthesis was unable to produce any flexion and extension at ankle joint in the prosthesis, which was indispensable to perform different daily activities and producing movement in the prosthesis. The torsional spring based ankle joint was introduced into the prosthesis to make it happened. Besides, these major components, the bracing plates, brackets, bushing pin, sleeve bearing, compression and torsional springs, spring holders and guiding components etc. were designed to make the prosthesis function more like a natural leg. The designing software SolidWorks 2013 have been used to design the prosthesis and its components.

3.5 Modeling and simulation of prosthetic joints

Modeling and simulation of the prosthesis, prosthetic joints, and its components were carried out before fabrication. The finite element models of each component were developed at the first place. Then the simulation was carried out under different possible loading conditions to test the mechanical strength of the components and thus the feasibility of the design. The motion analysis of knee and ankle joints was also performed to see the biomechanics of the prosthesis arrangement. The kinematic and kinetic analyses of the prosthesis helped to assess the performance of the prosthesis in imitating the natural gait cycle of lower limb. A comparative study between the natural gait cycle and that from the simulation results was conducted to get some picture on the possible performance of the prosthesis. SolidWorks 2013 platform was used to model and simulate the prosthetic joints and its components.

3.6 Fabrication of prosthesis

Once the results obtained from the finite element analysis were found to remain within the allowable limits of the prosthetic components (based on factor of safety), and the motion analysis results of the prosthetic joints were seen to resemble the natural gait cycle of the lower limb, the process of fabrication was started. The process and machine used for making different components of the prosthesis are tabulated in following Table 3.6.

Table 3.6: Process and machine used in making prosthesis components

SN	Component	Process used	Machine used
1	Thigh rod	Cutting, turning, drilling, boring, face milling, thread cutting, filing	Powered hacksaw, lathe machine, drilling machine, CNC milling machine, face milling machine, file
2	Shank rod	Cutting, turning, drilling, boring, face milling, thread cutting, filing	Powered hacksaw, lathe machine, drilling machine, CNC milling machine, face milling machine, file
3	Thigh rod height adjuster	Cutting, turning, drilling, boring, thread cutting, filing	Powered hacksaw, lathe machine, drilling machine, file
4	Shank rod height adjuster	Cutting, turning, drilling, boring, thread cutting, filing	Powered hacksaw, lathe machine, drilling machine, file
5	Gear	Cutting, turning, milling, drilling, boring, thread cutting, filing	Powered hacksaw, lathe machine, CNC milling machine, drilling machine, file
6	Bracing plates	Cutting, face milling, drilling, boring, filing	Powered hacksaw, face milling machine, drilling machine, file
7	Bracket arm	Cutting, face milling, drilling, bending, filing	Powered hacksaw, face milling machine, drilling machine, hydraulic bending machine, file
8	Bracket hook	Cutting, bending, drilling, filing	Powered hacksaw, hydraulic bending machine, drilling machine, file
9	Bracket-belt interfacing	Cutting, bending, milling, drilling, filing	Powered hacksaw, hydraulic machine, CNC milling machine, drilling machine, file
10	Compression spring	Cutting, coil making, heating, cooling	Hacksaw, lathe machine, furnace, cooling system

Table 3.6 continued

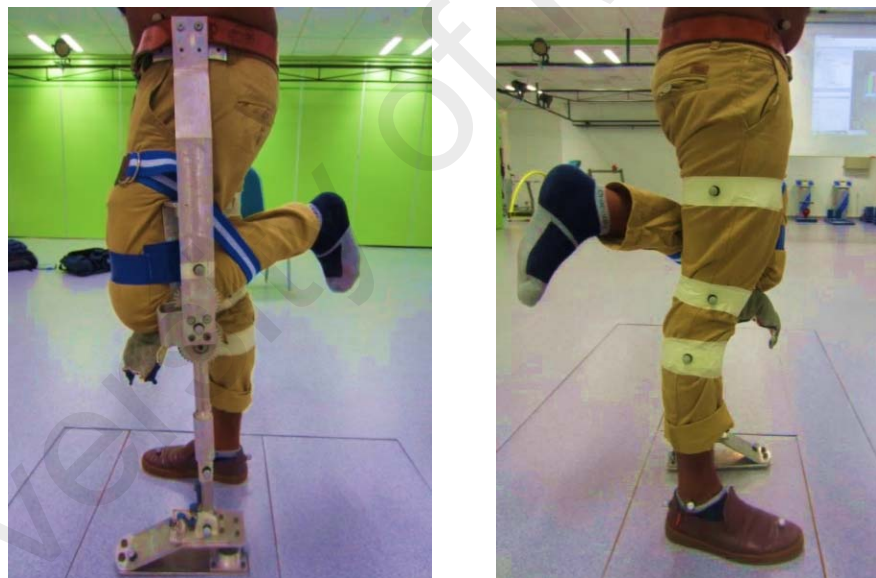
SN	Component	Process used	Machine used
11	Torsional spring	Cutting, coil making, heating, cooling	Hacksaw, lathe machine, furnace, cooling system
12	Compression spring holder	Cutting, milling, drilling, boring, face milling, filing	Powered hacksaw, CNC milling machine, drilling machine, face milling machine, file
13	Compression spring guide	Cutting, turning, milling, drilling, face milling, filing	Powered hacksaw, lathe machine, CNC milling machine, drilling machine, face milling machine, file
14	Knuckle frame	Cutting, milling, drilling, boring, face milling, filing	Powered hacksaw, CNC milling machine, drilling machine, face milling machine, file
15	Upper Foot plate	Cutting, bending, drilling, filing	Powered hacksaw, hydraulic bending machine, drilling machine, file
16	Lower foot plate	Cutting, bending, drilling, filing	Powered hacksaw, hydraulic bending machine, drilling machine, file
17	Sleeve bearing	Cutting, turning, drilling, boring, filing	Powered hacksaw, lathe machine, drilling machine, file
18	Ball bearing	Procured from the market	
19	Bushing pin	Procured from the market	
20	Belt	Procured from the market	
21	Socket	Procured from the prosthesis lab	

The spring making was the toughest part where certain processing conditions had to maintain to obtain the required properties in the springs.

3.7 Performance testing

Due to unavailability of a transfemoral amputee, an able-bodied subject has been obtained to validate the results and thus to test the performance of the prosthesis. The subject has given his written consent prior to participate the experiment. A similar work was carried out by Frank Sup (2009) to test the performance of the prosthesis he developed during his PhD study. The performance testing of the prosthesis was carried

out to evaluate the effectiveness of the prosthesis in overcoming the difficulties the subject experienced due to the amputation. The performance analysis has two types of tests: gait analysis and stability analysis. During performance test, the gait cycle data, the static and dynamic postural stability, and fall risk data were captured from the subject using the prosthesis. Similar procedures that used for recording the natural gait cycle was repeated to capture the prosthesis gait cycle. The marker positions on the prosthesis were little different from that on the healthy limb, however these were managed to locate at approximately same locations on the prosthesis. The marker positions on the prosthesis during the prosthesis gait cycle are shown in Figure 3.7 below.



a) Marker position on left prosthesis

b) Marker position on right leg

Figure 3.7: Marker positions on the prosthesis in gait analysis.

The anthropometric data of the subject with the prosthesis were measured again before capturing the prosthesis gait cycle. The anthropometric variables measured are tabulated in following Table 3.7.

Table 3.7: Characteristics and anthropometrical variable of subject with prosthesis

Variable	Mean value
Subject height (who the prosthesis is designed for)(cm)	166.5 ² 0.14
Mass with prosthesis (Kg)	73.5 ² 0.27
Left leg length (cm)	93.0 ² 0.13
Left thigh length (cm)	51 ² 0.12
Left shank length (cm)	42.0 ² 0.11
Left ankle-heel distance of prosthesis (cm)	9.9 ² 0.01
Left knee width (cm)	6.6 ² 0.02
Left ankle width (cm)	5.1 ² 0.01
Right leg length with shoes (cm)	92.5 ² 0.13
Right thigh length (cm)	50.0 ² 0.11
Right shank length with shoe (cm)	42.5 ² 0.12
Right knee width (cm)	10.9 ² 0.03
Right ankle width (cm)	7.1 ² 0.01
Right ankle-heel distance with shoe (cm)	9.1 ² 0.02

A similar procedure was followed to measure and record the postural stability index and fall risk data from the subject with prosthesis. The similar tests were repeated for same number of trials and equivalent time frames during the prosthesis balance test. In the test of postural stability, the positions of left and right feet of the subject were at an angle of 0° each, and then the corresponding heel were positioned at E2 and D17 lines of the machine platform scale. During the fall risk test, the left foot of the subject was placed on the platform at an angle of 0° when the corresponding heel position was at E5 line of the machine platform scale. The right foot of the subject was placed on the platform at an angle of 10°, and then the corresponding heel was positioned at D17 line of platform scale.

The feet positions during the postural stability and fall risk tests of the subject using the prosthesis are shown in following Table 3.8.

Table 3.8: Foot placement of subject with prosthesis on the platform of Biodex Balance machine

Foot placement		
Foot position on machine platform	Left	Right
In postural stability test		
Foot angle (degree)	0	0
Heel position (line number on platform scale)	E2	D17
In fall risk test		
Foot angle (degree)	0	10
Heel position (line number on platform scale)	E5	D17

The following Figure 3.8 represents the position and posture of the subject with prosthesis during the stability test.

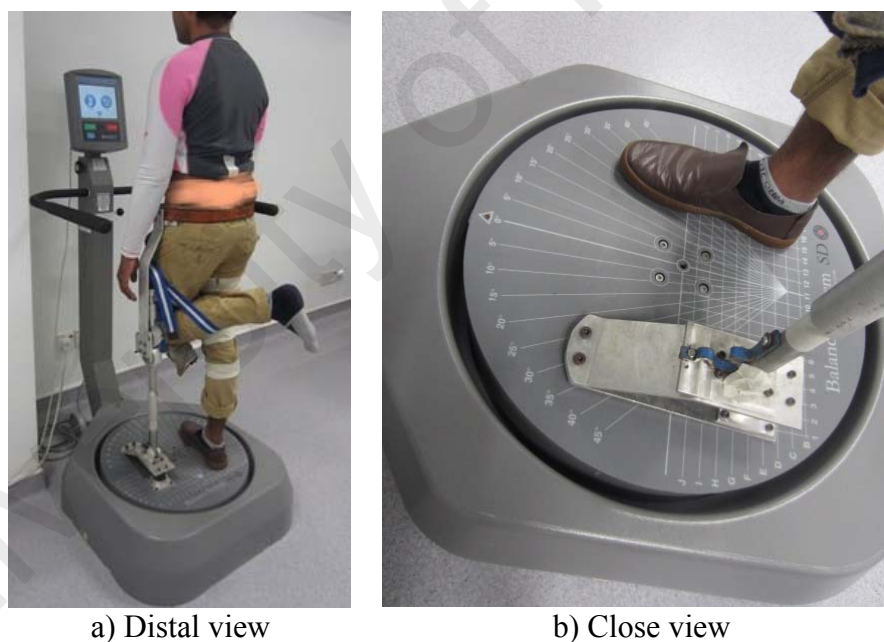


Figure 3.8: Foot positions on the platform of the Biodex machine in stability test.

The gait cycle data from the subject with the prosthesis was recorded to see the pattern of the prosthesis gait. The following Figure 3.9 illustrates different phases of prosthesis gait cycle during data recording.



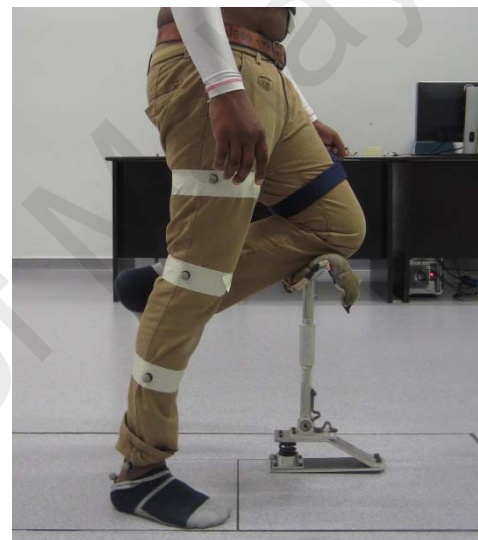
a) Left foot toe off



b) Right foot loading



c) Left heel strike



d) Left foot loading

Figure 3.9: Different phases of prosthesis gait cycle.

The prosthetic gait analysis was conducted to assess the effectiveness of the prosthesis. The data recorded from the healthy individual was compared with the data from the subject with the prosthesis. A comparative study between the gait cycles captured from the healthy subject and that obtained from the simulation results was performed to predict the performance of the designed prosthesis. A comparative study between the natural gait cycle and prosthetic gait cycle was carried out to evaluate the performance of the developed prosthesis.

CHAPTER 4: DESIGN OF PROSTHESIS

A prosthesis has been designed according to the anthropometric data of the subject. The components were designed based on the measurement of anthropometric variables, kinematic and kinetics of the subject. A thorough study has been carried out on the subject to measure his anthropometric variables like body weight and height, thigh length, shank length, etc. The study also investigated the gait cycle, biomechanics of the lower limb, and shape of the residual limb. Then the structure of the prosthesis replacing the missing limb has been designed when the main focus was on the function of the knee and ankle joints.

The knee joint was designed in such a way that it could make the lower limb to follow the residual limb movement. A set of gear was used to make it possible. On the other hand, a torsional and a compression spring were used in the ankle joint to give the ankle enough stiffness as well as range of rotation during walking. The springs acted as an energy storage and return (*ESR*) unit for the prosthesis, and thus to make the gait cycle similar to a natural gait cycle. The socket, thigh rod, shank rod, adjusters, and foot plates were designed based on the measurement of the prosthesis to imitate the structure. The springs, bracing plates were designed according to the subjected load. The bracket and belt were designed based on the measurement of the subject. The bearing and the bushing pins were chosen as per the design requirements.

4.1 Design of prosthetic knee joint

The prosthetic knee joint was developed to replace the biological knee joint and thus to assist the lower limb in creating flexion and extension in the prosthesis. The typical mechanical knee joints are hinge type joint, whereas the newly designed knee joint is

comprised of two spur gears, two bushing pin and two bracing plates. The gears are mounted on the busing pins without having locked to the pins. However, these are not free to rotate about the busing pins because of their connection with the socket and shank rods. One of the two gears is connected with the lower ends of the socket, and another is integrated to the upper end of the shank. They are kept engaged using a set of braces. Each busing pin, on the other hand, is mounted on two ball bearings from two ends, which are themselves mounted on the bracing plates. The lower end of a bracket is bolted with the braces of the gear set whereas the upper end of the bracket is connected to a waist belt. A plano-concave shaped piece of material is used at the joint in between the bracket and waist belt to keep the bracket firm and not moving during flexion and extension of the knee. The mating gears with the help of braces, bracket and the waist belt will make the knee to move following the residual limb movement and thus enable the prosthesis to move according to the user's intention. A set of stopper is attached to the faces of each gear with screw. These are incorporated into the design to prevent the further movement of the gears when the users are at standing position and thus to help them to stay upright. Different views of the newly designed gear based knee joint are shown in the Figure 4.1.

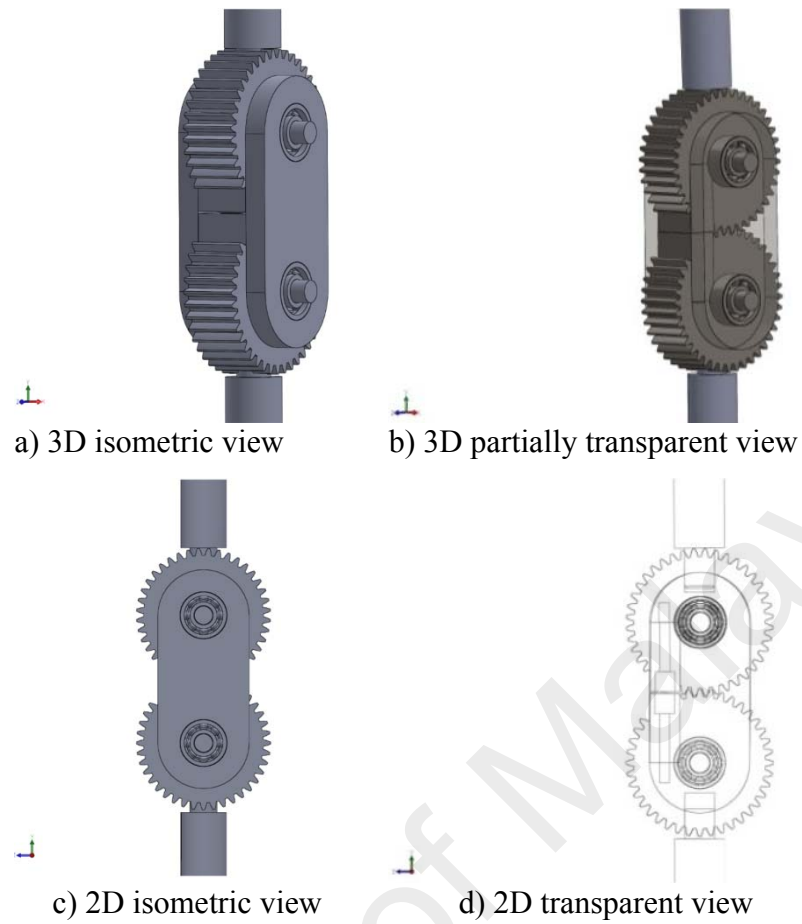


Figure 4.1: Different view of the gear based knee joint.

The whole gear assembly is attached to a waist belt by a bracket and a bracing arrangement to make the knee joint working properly. The additional bracket-bracing arrangement is not shown in the figure. The different components of the gear based knee joints, including the knee guiding arrangement are shown in the following Figure 4.2 and Figure 4.3. The components are numbered and named using Bill of Material (*BOM*) option in Solidworks platform.

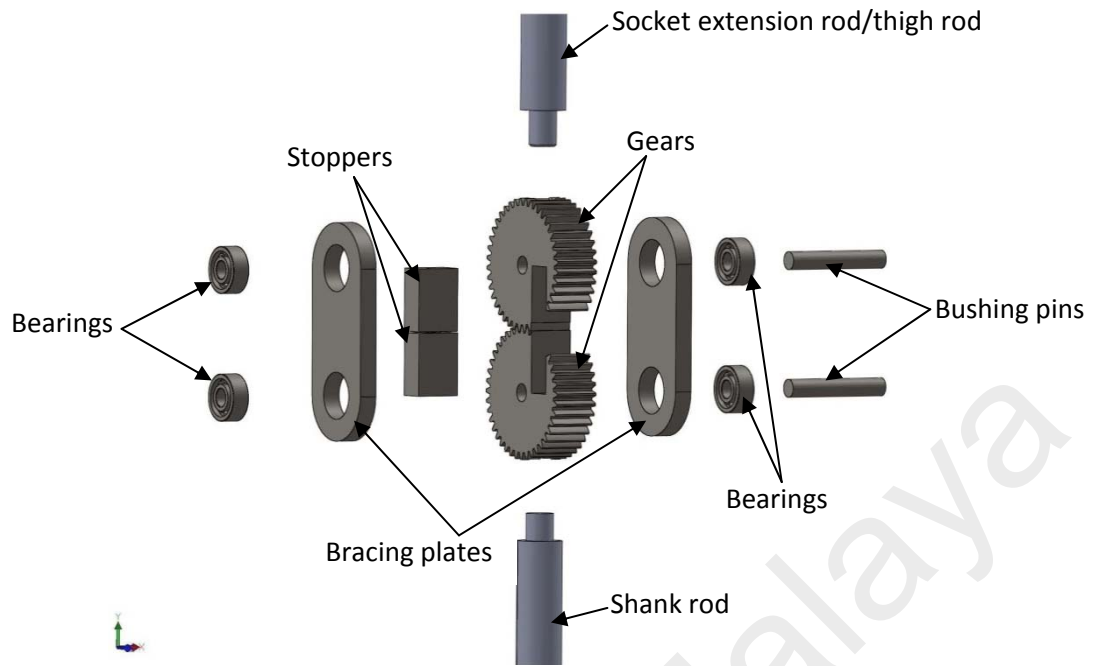
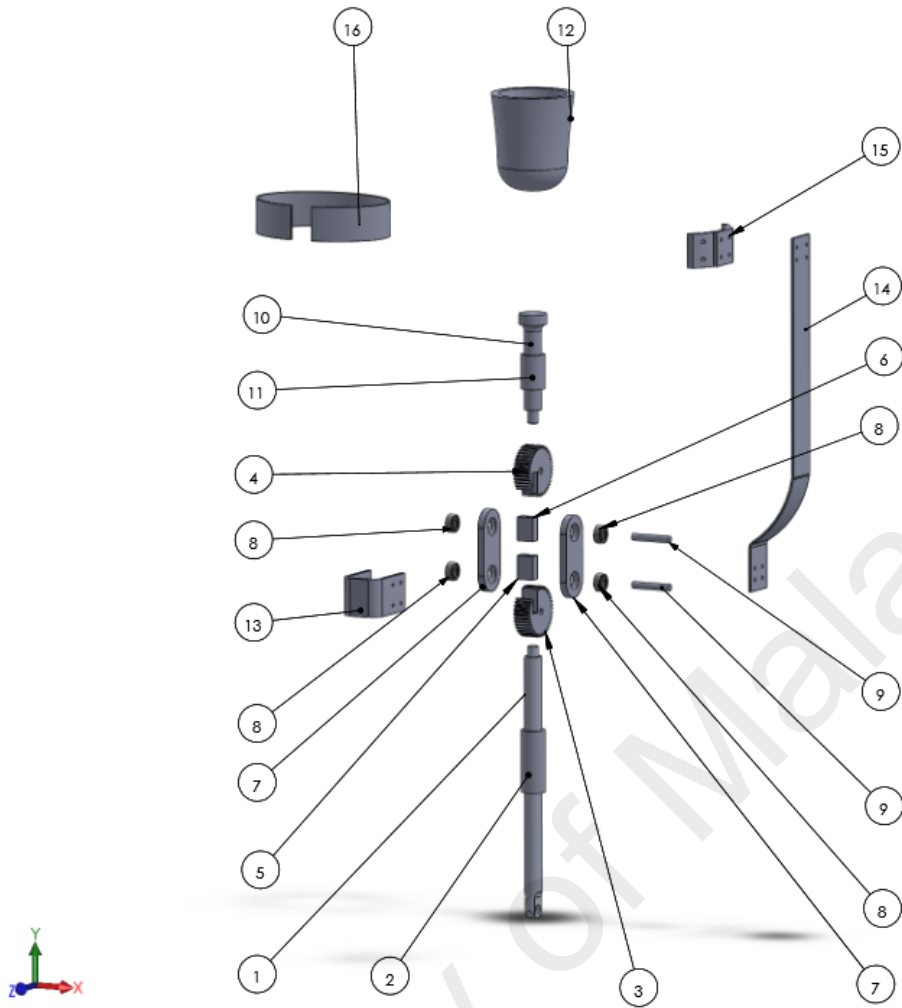


Figure 4.2: The exploded view of knee joint showing the different components.

University of Malaysia



ITEM NO.	PART NUMBER	DESCRIPTION	QTY.
1	SR001	SHANK ROD	1
2	SHA001	SHANK HEIGHT ADJUSTER	1
3	KG001	KNEE GEAR 1	1
4	KG001	KNEE GEAR 2	1
5	GS001	GEAR STOPPER 1	1
6	GS002	GEAR STOPPER 2	1
7	BP001	BRACING PLATE	2
8	BB001	BALL BEARING	4
9	BP001	BUSHING PIN	2
10	TR001	THIGH ROD	1
11	THA001	THIGH HEIGHT ADJUSTER	1
12	SK001	SOCKET	1
13	GH001	GUIDE HOOK	1
14	GA001	GUIDE ARM	1
15	BI001	BELF INTERFACING	1
16	WB001	WEIST BELT	1

Figure 4.3: Different components of knee joint with parts number.

The connections among different knee joint components are illustrated in the following

Figure 4.4.



Figure 4.4: The exploded view of knee joint showing the connections among components.

The knee joint assembly was designed to reproduce similar movement like a healthy biological limb in the above knee prosthesis. The gear sets with help of the bracket, and braces would make the shank to follow the movement of the residual limb rather than just allowing shank to bend. The spur gears of the knee joint served two main functions. First, the gear assembly managed the shank to follow the movement of the residual limb during both the stance and swing phase. Second, the difficulties of shank in following the movement of the residual limb due to inertia of the prosthesis were overcome with

the spur gears arrangement. The user of the prosthesis obtained control over the passive knee during ambulation of the prosthetic foot both in the stance and swing phases. This phenomenon will make the knee joint behaving like an active knee joint. When using the stoppers, the prosthetic knee was stopped in full extension when standing. Though the gear-based knee joint is technically a passive joint, due to its behavior like an active joint, it is named as a quasi-active knee joint.

Unlike the joints of other available prosthesis, gear based joints have been proposed, designed and implemented in this study to overcome the existing setbacks and thus to improve the performance of the joints. The uniqueness of the prosthesis comprised with the gear based joints is that it will not require any additional control system to regulate the prosthesis; the joints will rather act to control the movements of the prosthesis.

To design the prosthesis, the movements of the biological limb were taken as references. The free body diagrams at different phase of gait are shown in the following Figure 4.5 to Figure 4.7.

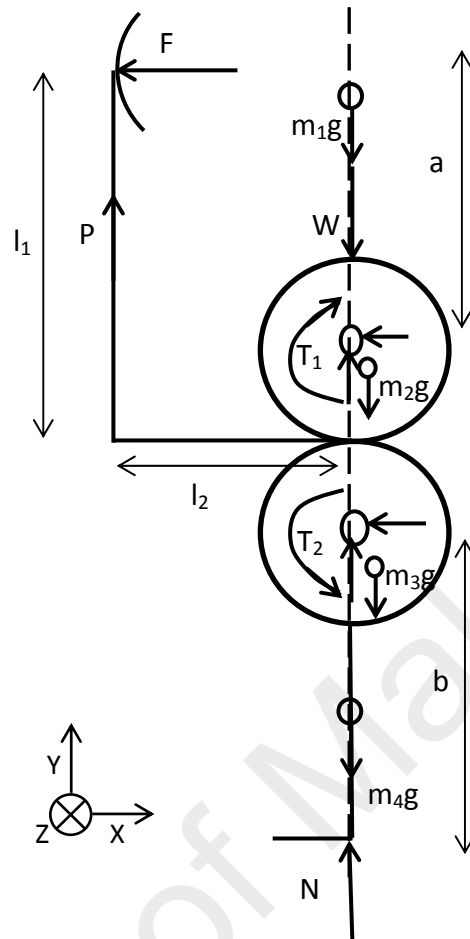


Figure 4.5: Free body diagram of prosthesis at stance phase.

The equilibrium equation of knee joint when standing upright

1) Force equilibrium ($\sum F_x = 0, \sum F_y = 0$)

$$W + (m_1 + m_2 + m_3 + m_4)g + P = 0 \quad (4.1)$$

2) Moment equilibrium ($\sum M_x = 0, \sum M_y = 0$)

$$Fl_1 - T_1 + T_2 - Pl_2 = 0 \quad (4.2)$$

$$T_1 = 0 \quad (4.3)$$

$$T_2 = 0 \quad (4.4)$$

$$P = 0 \quad (4.5)$$

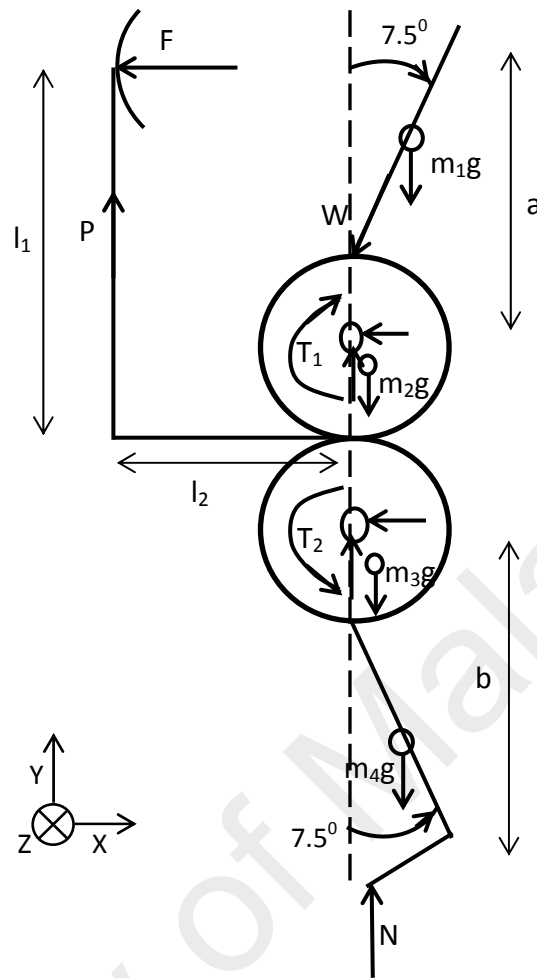


Figure 4.6: Free body diagram of prosthesis at 15° of rotation at swing phase.

The equilibrium equation of knee joint when bending at 15° during swing

1) Force equilibrium

$$W \cos 7.5 + (m_1 + m_2)g - N \cos 7.5 + (m_3 + m_4)g - P = 0 \quad (4.6)$$

2) Moment equilibrium

$$Fl_1 - T_1 + T_2 - Pl_2 = 0 \quad (4.7)$$

$$T_1 = W \sin 7.5 * a \quad (4.8)$$

$$T_2 = N \cos 7.5 * b \quad (4.9)$$

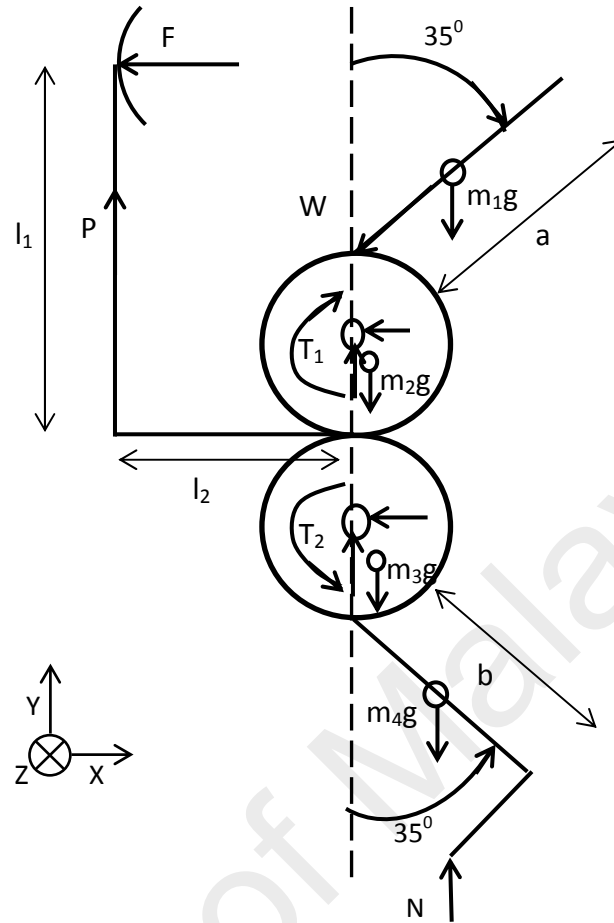


Figure 4.7: Free body diagram of prosthesis at 70° of rotation at swing phase.

The equilibrium equation of knee joint when bending at 70° during swing

1) Force equilibrium

$$W \cos 35 + (m_1 + m_2)g - N \cos 35 + (m_3 + m_4)g - P = 0 \quad (4.10)$$

2) Moment equilibrium

$$Fl_1 - T_1 + T_2 - Pl_2 = 0 \quad (4.11)$$

$$T_1 = W \sin 35 * a \quad (4.12)$$

$$T_2 = N \cos 35 * b \quad (4.13)$$

$$N = 0 \quad (4.14)$$

The movements recorded from the gait analysis of healthy individual are as following:

Angular speed of hip, $\omega_{hip} = 1.34$ rad/s; Angular speed of knee, $\omega_{knee} = 1.71$ rad/s;

Angular speed of ankle, $\omega_{ankle} = 1.93$ rad/s; Angle of knee rotation, $\theta_{knee} = 0^\circ \sim 70^\circ$;

Angle of ankle rotation, $\theta_{ankle} = -15^0 \sim 34^0$; Moment of hip, $M_{hip} = 0.63 \text{ Nm/Kg}$;

Moment of knee, $M_{knee} = 0.26 \text{ Nm/Kg}$; Moment of ankle, $M_{ankle} = 0.25 \text{ Nm/Kg}$

The body weight will be transmitted from one limb to another through the gears of the joints. Since, the gears are integrated to the linking rod by some fixed joint, the total body weight acts radially to the gears at static condition; however during movement, almost entire loads are transmitted to the mating gear. Unlike the conventional gear mounting mechanism, these gears are mounted on the linking rod rather than mounting on the bearing shaft. Hence, the transmitted load is not the tangential load components; it is rather the radial load component. The transmitted load is considered to be the total weight of the body mass and the weight of the prosthesis arrangement.

These speeds are required to incorporate into the gears of the knee and ankle joints and thus to transmit to the connected limb of the prosthesis. Therefore, the *RPMs* of the gears corresponding to the angular speed of the hip, knee and ankle joints are to be calculated from the respective angular velocities.

$$\text{Hip rotation per minutes, } RPM_{hip} = \frac{\omega_1 \times 60}{2\pi} = \frac{1.34 \times 60}{2\pi} = 13 \text{ rpm}$$

$$\text{Knee rotation per minutes, } RPM_{knee} = \frac{\omega_2 \times 60}{2\pi} = \frac{1.71 \times 60}{2\pi} = 16 \text{ rpm}$$

$$\text{Ankle rotation per minutes, } RPM_{ankle} = \frac{\omega_3 \times 60}{2\pi} = \frac{1.93 \times 60}{2\pi} = 16 \text{ rpm}$$

The knee joint of the prosthesis is reproduced with two external gear set, whereas the ankle joint is recreated with a combination of an external and an internal gear set.

The design constraints and the variables are as following:

Pitch diameter of gear installed in stump = D_1

Pitch diameter of gear installed in shank = D_2

The through design calculation of the gear set has been presented in Appendix B1.

The other knee joint components have been designed to make the gear set working properly in creating different movements to the shank according to the residual limb movements. The bracing plates positioned at the two opposite sides of the gear set were

designed to keep the gears in contact. There were two holes made in each plate to contain two ball bearings. Since, the different components of knee joints (e.g. the bracing plates, guiding plates) neither carrying any significant load (dead load) nor subjected to any appreciable external load, no thorough calculation was performed during designing them. The plates were rather designed to simply fulfill the dimensional requirements of the components. Four ball bearings of same size were chosen from the available size in the market. However, stress, strain and plastic deformation analysis were carried out on each component using finite element analysis to see the feasibility of the design. Table 4.1 shows the different dimensions of the knee joint components.

Table 4.1: Dimensions of different knee joint components

SN	Component	Dimensions	Number of item
1	Gear	Diameter = 60 mm Number of teeth = 50 Width = 25 mm Pitch = 2mm	2
2	Gear stopper	Length = 35 mm Width = 25 mm Thickness = 15 mm	2
3	Bracing plates	Length = 120 mm Width = 50 mm Thickness = 10 mm Hole diameter = 26 Distance between the centers of the holes = 60 mm	4
4	Ball bearing	Inner diameter = 10 mm Outer diameter = 26 mm	5
5	Bushing pin	Length = 60 mm Diameter = 10 mm	2
6	Thigh rod	Length = 125 mm Diameter = 25 mm	1
7	Thigh rod height adjuster	Length = 50 mm Inner diameter = 25 mm Outer diameter = 35 mm	1

Table 4.1 Continued

SN	Component	Dimensions	Number of item
8	Shank rod	Length = 369 mm Diameter = 25 mm	1
9	Shank rod height adjuster	Length = 90 mm Inner diameter = 25 mm Outer diameter = 35 mm	1
10	Bracket arm (guiding plate)	Length = 470 mm Width = 50 mm Thickness = 5 mm	1
11	Bracket hook	Length = 85 mm Width = 55 mm Thickness = 5 mm Gap between the hook ends = 60 mm	1
12	Bracket-belt interfacing plate	Length = 108 mm Radius of curvature = 75 mm Width = 50 mm Thickness = 5 mm	1

4.2 Design of prosthetic ankle joint

The design of the spring based ankle joint is unlike any other ankle joint available for prosthetic leg. The typical mechanical ankle joints for normal walking are hinge type of fixed type joint, whereas the ankle joints for running and sprinting are single piece solid plate type. The newly designed ankle joint is comprised of number of components – one shank rod, one hinge knuckle, one bushing pin, two ball bearing, one sleeve bearing, one upper foot plate, one lower foot plate, one torsional spring, two torsional spring holder, one compression spring, one compression spring holder, one compression spring guide and some bolts and nuts. The lower foot plate and upper foot plate are bolted together at frontal end and there is a compression spring positioned between two plates at the posterior end. The compression spring is mounted on a spring holder attached to the lower foot plate and held by a spring guide attached to the upper foot plate from the top. Due to the shape of the upper foot plate, it acts as a leaf spring. The foot plates and the compression spring assembly jointly behave as a shock absorber. At the same time,

this assembly acts as an energy storing and returning (*ESR*) system for the ankle joint. The hinge knuckle is mounted on the top of the upper foot plate where the shank rod is connected with a busing pin and two ball bearings from two opposite sides. A sleeve bearing is placed in between the busing pin and shank rod connector hole. This has been done to protect the busing pin from early damage by heavy load due to weight of amputee. The torsional spring is placed at the hinge joint of shank rod and knuckle with the help of two spring holders from two ends. The torsional spring provides enough stiffness to the ankle joint during rotation and also can store and return energy during compression and expansion respectively.

To replicate the functions of muscles and tendons in storing and returning energy, ankle joints are developed by utilizing the elasticity and stiffness characteristics of spring material, where energy is stored when the material deforms, and energy is returned when the material returns to its initial shape. Different views of the newly designed spring based ankle joint are shown in the Figure 4.8.

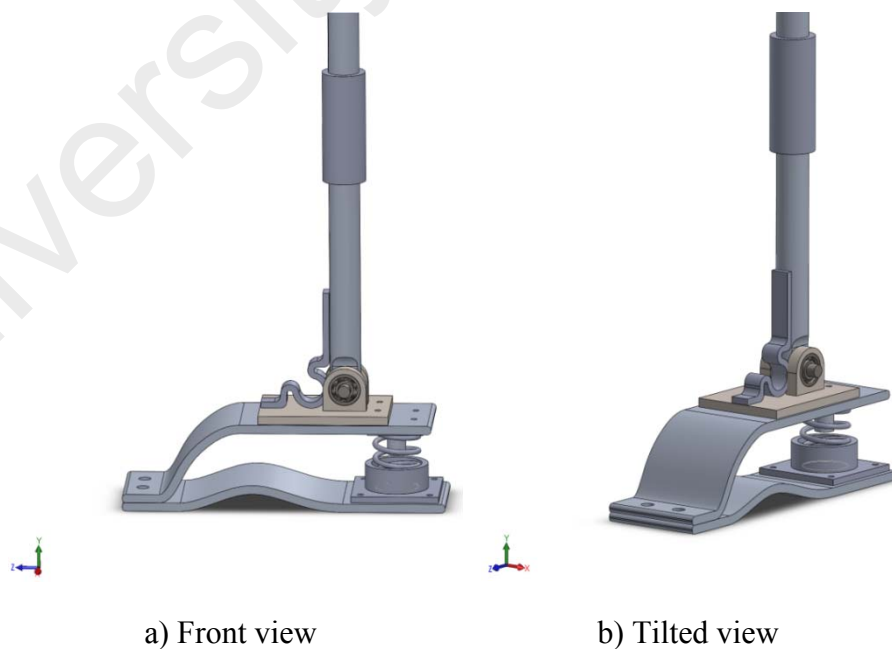


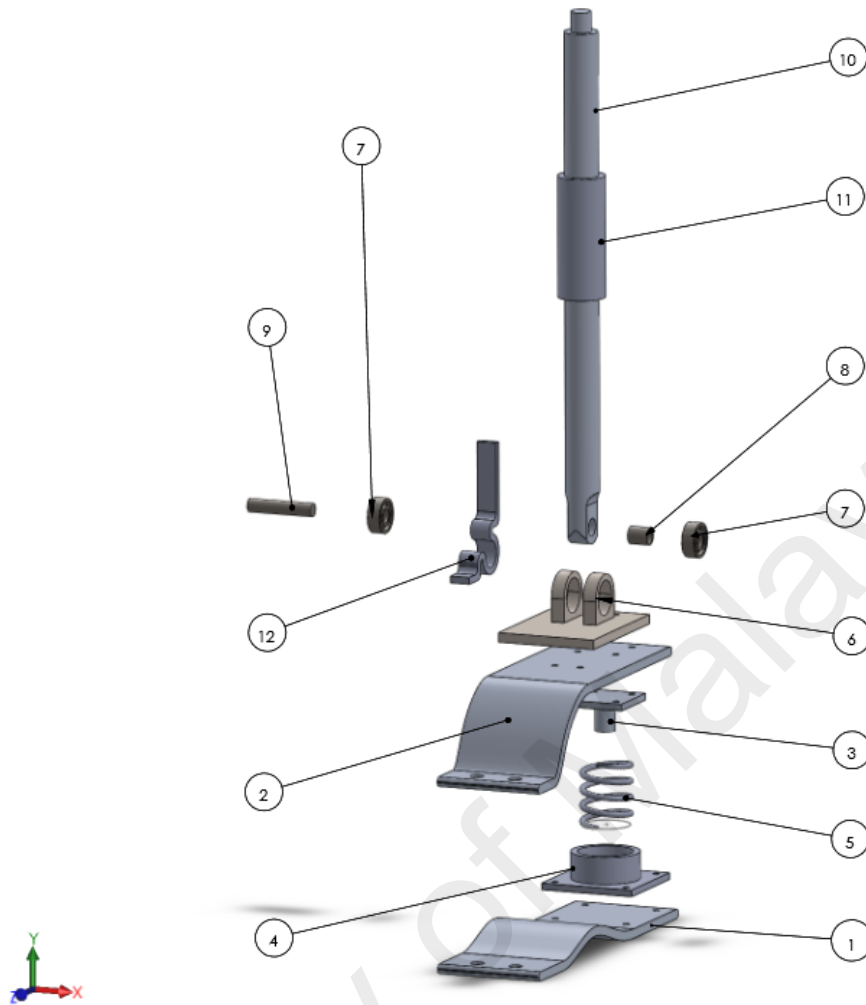
Figure 4.8: Isometric view of ankle joint.

The prosthetic ankle-foot system of the prosthetic leg is enabled to produce flexion at the ankle joint by introducing the torsional spring at the joint. The torsional spring generates a moment between 45 and 0 degrees of flexion. The moment generated is inversely related to the magnitude of flexion, which increases to 12.4 Nm at a 45 degree flexion. The spring moment decreases to 0 Nm in full extension. The compression spring installed at the bottom of the foot plate helps to absorb shocks and store energy during stance phase and return during swing phase. The mass of the knee-ankle-foot system is 3.5 kg. The heel-toe length was 0.3 m.

The different components of the spring based ankle joint, including the energy storing and returning arrangement are shown in the following Figure 4.9 and Figure 4.10.



Figure 4.9: The exploded view of the different ankle joint components.



ITEM NO.	PART NUMBER	DESCRIPTION	QTY.
1	LFP001	LOWER FOOT PLATE	1
2	UFP001	UPPER FOOT PLATE	1
3	SG001	SPRING GUIDE	1
4	SH001	SPRING HOLDER	1
5	CS001	COMPRESSION SPRING	1
6	KF001	KNUCKLE FRAME	1
7	BB001	BALL BEARING	2
8	SB001	SLEEVE BEARING	1
9	BP001	BUSHING PIN	1
10	SR001	SHANK ROD	1
11	SHA001	SHANK HEIGHT ADJUSTER	1
12	TS001	TORSIONAL SPRING	1

Figure 4.10: Different components of ankle joint with parts number.

The connections among different ankle joint components are illustrated in the following Figure 4.11.



Figure 4.11: The exploded view of ankle joint showing the connections among components.

The detail design of the torsional and compression spring used in the prosthetic ankle joint is thoroughly described in the following subsections.

4.2.1. Compression spring design

The compression spring is located between the upper foot plate and the lower foot plate, therefore, the initial applied load is the holding force used by these foot plates. The final applied load to the compression spring is the load due to

the amputee body weight. The weight of the prosthesis is considered to be balanced by the weight of the amputated limb.

To design a compression spring for the prosthesis, the weight of average weight leg prosthesis available is considered to use for calculation.

Assume, the weight of the above knee (AK) prosthesis = 3.5 Kg.

The weight of the above knee prosthesis up to ankle joint = 2.5 Kg.

The weight of the amputee was 69 Kg.

The purpose of the compression spring is to absorb load during stance phase and return it during swing phase. Therefore, the moments, force and torque were to be calculated for the cumulative weight of the subject and the prosthesis up to ankle joint.

Therefore, the resultant load due to the weight of amputee and the prosthesis up to ankle joint was, $W = (69 + 2.5) * 9.81 = 701.4 \text{ N}$

Though, the total weight is shared by both legs, the weight should be divided by two. However, keeping in mind the event of balance loosing, the weight was not divided by two for the reason of design safety.

According to the position of the foot plate and the compression spring in the ankle-foot arrangement, the force/load distribution in the foot plates and the compression spring should be as following shown in Figure 4.12.

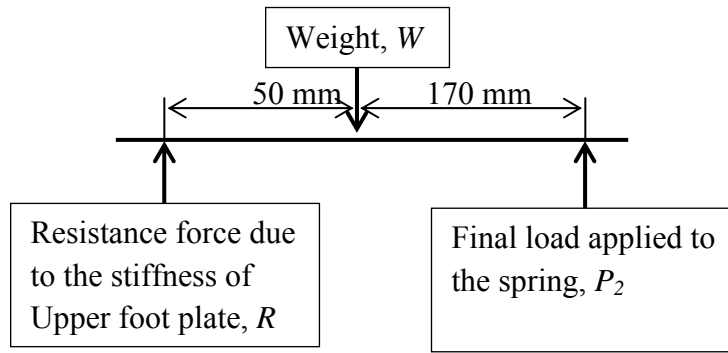


Figure 4.12: The load distribution in the prosthetic foot.

Therefore,

$$\frac{P_2}{W} = \frac{50}{220}$$

$$P_2 = \frac{50}{220} \times W = \frac{50}{220} \times 701.4 = 159.4 \text{ N}$$

Final load, P_2 = load due to the weight proportion shared by the compression spring = 159.4 N

Spring rate, $R = \frac{P_2}{y_2 - y_1} = \frac{159.4}{20} = 7.97 \text{ N/mm}$, which is spring rate of k

Initial load, P_1 = load that causes the spring to deform 5 mm from the free load condition = $R \times (L_f - L_1) = 7.97 \times 5 = 39.9 \text{ N}$

Therefore,

$$F_a = \frac{F_{max} - F_{min}}{2} = \frac{159.4 - 39.9}{2} = 59.8 \text{ N}$$

$$F_m = \frac{F_{max} + F_{min}}{2} = \frac{159.4 + 39.9}{2} = 99.7 \text{ N}$$

Where, $F_{max} = P_2$, and $F_{min} = P_1$,

$y_{max} = 20 \text{ mm}$, and $y_{min} = 5 \text{ mm}$

The detail design calculation of the compression spring has been presented in the Appendix B2.

4.2.2. Torsional spring design

The torsional spring of the ankle joint is incorporated in the design of ankle joint to extend the flexion and extension ability of the joint under different circumstances in a controlled way. The torsional spring is designed to carry partial load of the user during swing phase of walking and when to produce bending movement in the ankle joint.

The load applies to the torsional spring = the proportion of amputee weight shared by the torsional spring during swing phase and flexion and extension movements.

During swing phase of a biological lower limb, the finger joints help to produce desired rotation in the foot. However, there is no finger joint incorporated in the proposed design, the ankle joint has to yield that movement in the foot arrangement.

The rotation angle varies depending on the mode and speed of walking and also on the type of activities performed. The maximum possible angles of rotation are considered as design parameter for the torsional spring design. Therefore, the forces applied on the spring at those particular angles are casual and cannot consider as dynamic load, and thus should not apply dynamic loading condition during the spring design. The maximum angle of rotation produced by the ankle joint is shown in the Figure 4.13.

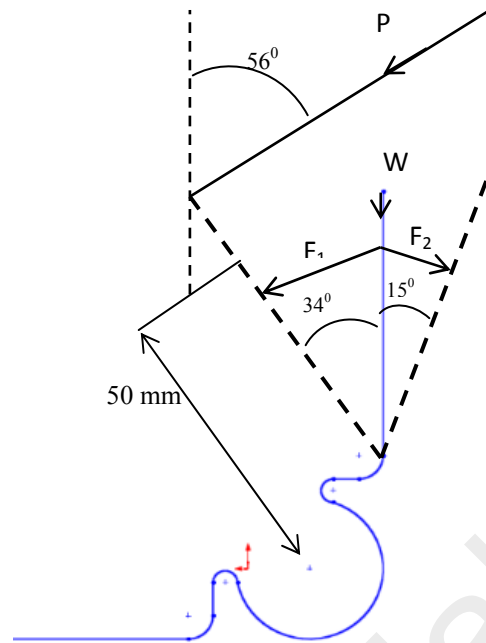


Figure 4.13: The angle of rotation produced by the ankle joint.

Assumed, Length of torque arm, $l = 50\text{ mm}$

During standing, no rotation is occurred at the ankle joint. However, during walking on the plane ground, the ankle rotates from 34° to -15° . Moreover, the range of rotation during performing different daily activities is quite large when both the feet are usually in touch with the ground.

The load applied to the torsional spring at maximum flexion should be the half of the resultant weight of the amputee and the prosthesis component up to the ankle joint. However, during the event of balance loosing, the weight becomes 1 times to 4 times of the body weight. Keeping in mind this event and thus to ensure safety, the resultant weight is not divided by two.

Therefore, the resultant load applied on the torsional spring, $W_r = (\text{amputee weight} + \text{weight of prosthesis components up to ankle joint}) = (69 + 2.5) \times 9.81 = 701.4\text{ N}$.

When the shank produces 34° of rotation angle at the ankle joint, a corresponding angle of 56° is produced at the knee joint.

Therefore, the weight component transmitted to the shank from the hip is

$$P = W \cos 56 = 701.4 * \cos 56 = 392.2 \text{ N}$$

The applied load on the spring arm at 34° clockwise rotation is

$$F_1 = P \sin 34 = 392.2 * \sin 34 = 219.3 \text{ N}$$

The applied load on the spring arm at 15° anti-clockwise rotation is

$$F_2 = P \sin(-15) = 392.2 * \sin(-15) = -101.5 \text{ N}$$

The torque at counterclockwise direction, $M_{max} = M_1 = F_1 \times l = 219.3 \times 50 = 10965 \text{ N.mm}$ (*anticlockwise*)

The torque at counterclockwise direction, $M_{min} = M_2 = F_2 \times l = -101.5 \times 50 = -5075 \text{ N.mm}$, (*or 5075 N.mm, clockwise*)

Total angle of rotation, $\theta = (\theta_1 - \theta_2) = 34^{\circ} - (-15^{\circ}) = 49^{\circ}$

The comprehensive design calculation of the torsional spring has been presented in the Appendix B3.

The other ankle joint components have been designed to enable the ankle joint to produce required angle of rotation with adequate stiffness during the gait cycle.

A knuckle frame of the joint is designed to make a hinge joint between the shank and the foot arrangement. A bushing pin is incorporated in the design to assist development of the hinge joint. This bushing pin is placed at the interlink point of the knuckle and shank as a connector. The lower foot plate and the upper foot plate are bolted together from the front end of the plates. The lower foot plate is intended to replicate the structure of the natural foot sole and thus to provide stability to the prosthesis when standing. The upper foot plate is to provide shock absorbing capacity to the prosthesis. One of the two spring holders are bolted on the platform of the knuckle frame and another on the shank rod. Both

of them are located at the two ends of the torsional spring. The spring holders for torsional spring are to hold and guide the spring when rotating in different angles. The spring holder for compression spring is attached on the top surface of the lower foot plate, and the spring guide for the compression spring is bolted on the bottom surface of the upper foot plate. Both of them are positioned at the back portion of the foot at the heel area. The spring holder for the compression spring is to position the spring at a fixed point and thus to prevent sliding when subjected to any external load. A ball bearing and a sleeve bearing are placed at the interface of the shank and bushing pin at the connecting point. The sleeve bearing is used to protect the shank slot from early damage, whereas the ball bearing is to reduce friction between the shank rod and the bushing pin when rotating.

Since, the different components of ankle joints except the springs (e.g. the knuckle, foot plates, bushing pin, spring holder and guides, etc.) are simple in design and shape, no complex calculation was carried out to design those components. The other components are rather designed to simply fulfill the dimensional requirements of the components. A ball bearings and a sleeve bearing are chosen from the available size in the market. However, there is stress, strain and plastic deformation analysis were carried out on each components using finite element analysis to see the feasibility of the design.

Table 4.2 shows the different dimensions of the ankle joint components.

Table 4.2: Dimensions of different ankle joint components

SN	Component	Dimensions	Number of item
1	Shank	Length = 369 mm Diameter = 25 mm	1
2	Shank rod height adjuster	Length = 90 mm Inner diameter = 25 mm Outer diameter = 35 mm	1
2	Knuckle frame	Length = 105 mm Width = 65 mm Thickness = 7 mm Hole diameter = 26 mm Spacing between the arms of the knuckle = 55mm	1
3	Bushing pin	Length = 60 mm Diameter = 10 mm	1
4	Ball bearing	Inner diameter = 10 mm Outer diameter = 26 mm	2
5	Sleeve bearing	Length = 15 mm Inner diameter = 10 mm Outer diameter = 13 mm	1
6	Torsional spring	Spring rate per turn (k) = 73.85 N.mm/turn Number of active turn = 2.7 Spring free length = 42.4 mm	1
7	Upper foot plate	Length = 265 mm Width = 80 mm Thickness = 5 mm	1
8	Lower foot plate	Length = 260 mm Width = 80 mm Thickness = 5 mm	1
11	Compression spring	Spring constant (k) = 7.7 N/mm Number of active turn = 2.54 Spring free length = 35.36 mm	1
12	Compression spring holder	Base L×W×H = 70×70×3 mm Spring holding cylinder inner diameter = 41 mm Outer diameter = 44 mm Height = 20 mm	1
13	Compression spring guide	Base L×W×H = 45×45×3 mm Guiding rod diameter = 15 mm Guiding rod height = 25 mm	1

4.3 Design of the above knee prosthesis

The newly designed prosthesis is constructed based on the gear based knee joint and the spring based ankle joint. In addition to these joints, the shank rod, thigh rod, foot plates, socket, bracket, braces and waist belt are incorporated in the design to make the prosthesis imitating the structure and the movements of the missing biological limb.

The lower end of the thigh rod and the upper end of the shank rod are connected to the gears from the top and bottom of the prosthetic knee joint respectively. Thread joint are used to connect the thigh rod and the shank rod to the gear assembly. A socket is bolted at the top of the thigh rod, which is to be worn on the residual limb of the amputee. The knee joint is encased with a brace like hook, which is attached with a long bracket. The bracket is connected to the knee hook from the lower end and to a waist belt from the upper end. A concave shaped interfacing piece of material is put between the bracket and the waist belt to make the bracket the holding the knee joint stationary and thus help shank rod to follow the thigh rod with the help of the engaged gear set.

The lower end of the shank rod and the top surface of the upper foot plate are connected to the hinge knuckle. A bushing pin is used to connect the shank rod and the knuckle whereas the bolt joint is used to connect the upper foot plate of the foot assembly to the hinge knuckle. Different views of the newly designed mechanically controlled above knee prosthesis are shown in the Figure 4.14.



Figure 4.14: Different view of the mechanically controlled above knee prosthesis.

The different components of the prosthesis, including the knee and ankle joints are shown in the following Figure 4.15 and Figure 4.16.

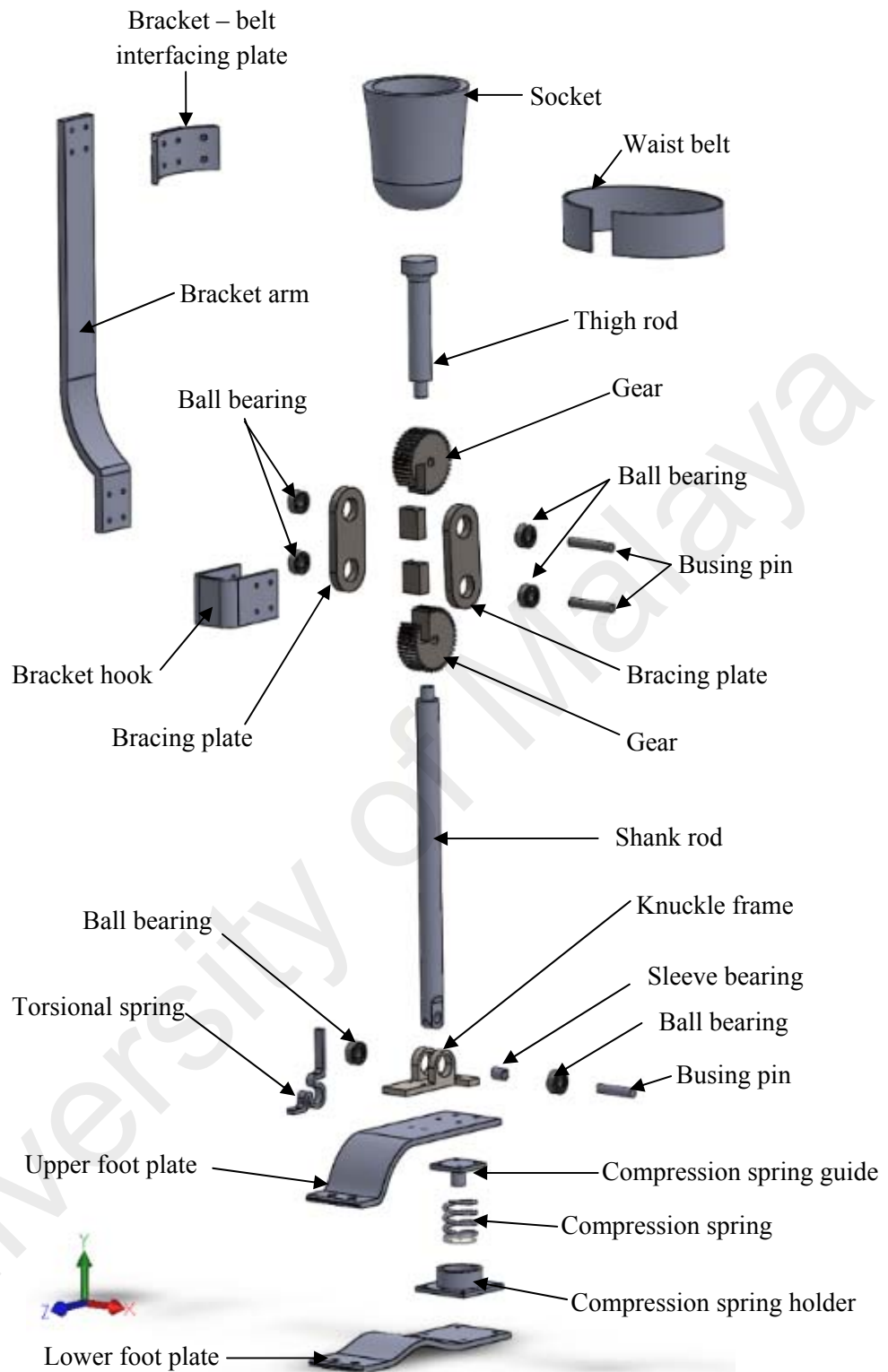
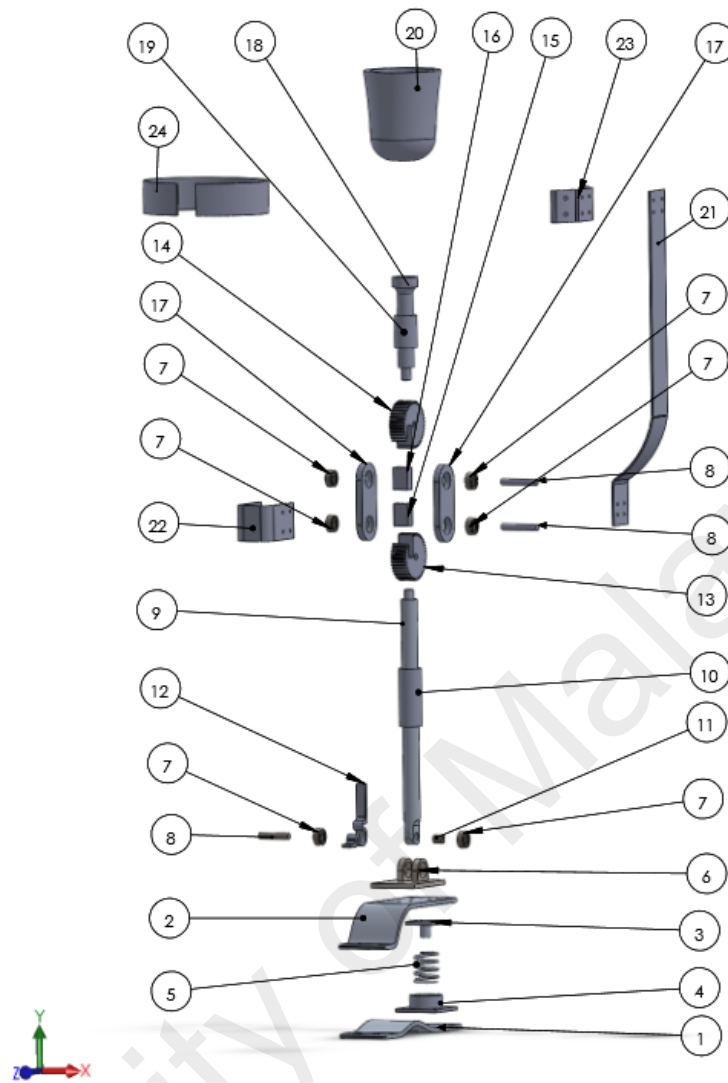


Figure 4.15: The exploded view of prosthesis showing the different components.



ITEM NO.	PART NUMBER	DESCRIPTION	QTY.
1	LFP001	LOWER FOOT PLATE	1
2	UFP001	UPPER FOOT PLATE	1
3	SG001	SPRING GUIDE	1
4	SH001	SPRING HOLDER	1
5	CS001	COMPRESSION SPRING	1
6	KF001	KNUCKLE FRAME	1
7	BB001	BALL BEARING	6
8	BP001	BUSHING PIN	3
9	SR001	SHANK ROD	1
10	SHA001	SHANK HEIGHT ADJUSTER	1
11	SB001	SLEEVE BEARING	1
12	TS001	TORSIONAL SPRING	1
13	KG001	KNEE GEAR 1	1
14	KG001	KNEE GEAR 2	1
15	GS001	GEAR STOPPER 1	1
16	GS002	GEAR STOPPER 2	1
17	BP001	BRACING PLATE	2
18	TR001	THIGH ROD	1
19	THA001	THIGH HEIGHT ADJUSTER	1
20	SK001	SOCKET	1
21	GA001	GUIDE ARM	1
22	GH001	GUIDE HOOK	1
22	GA001	GUIDE ARM	1
23	BI001	BELF INTERFACING	1
24	WB001	WEIST BELT	1

Figure 4.16: Different components of the prosthesis with part number.

The connections among the prosthesis components are illustrated in the following Figure 4.17.



Figure 4.17: Connections among different components of the prosthesis.

One end of the prosthesis is attached to the residual stump by a socket arrangement and the other end maintained a contact with the ground during stance phase and a certain period of time of swing phase. The residual stump/thigh can rotate about the hip joint whereas the foot can rotate about the ankle joint and the finger joint. In prosthesis arrangement, the finger joint has been avoided to simplify the design; therefore, the foot rotation about the ankle can only be taken into consideration, not the rotation about the finger joint. Since the force and moments are transmitted from residual limb to the foot through the shank, therefore the shank follows the residual limb movement and the ankle follows the shank movement. The body load is transmitted to foot through a knee and a hinge joint, a leaf spring like foot plate and a compression and torsional spring arrangement. The mechanics of the knee and ankle joints would define the dynamics of the prosthesis. Due to limitation of manufacturing facility, no rocker is incorporated in the heel design.

CHAPTER 5: RESULTS AND DISCUSSIONS

The entire process of prosthesis design and development includes three types of data – i) motion analysis data from simulation, ii) motion analysis data from healthy subject, and iii) motion analysis data from subjects with prosthesis. The data from the natural gait cycle movement of healthy lower limb has been captured at the first place. Then the motion analysis data of the prosthetic arrangement for the same anthropometric variables have been obtained from the simulation result. Finally, the data from the gait cycle movements of the lower limb with prosthesis have been recorded from the subject. The natural gait cycle data from the healthy subject have been recorded to compare with the simulation data and also with the data from the subject with prosthesis. The comparative study would help to assess the performance of the newly developed prosthesis. A closer replication of the natural gait cycle by the prosthesis leads to obtain a more efficient prosthesis.

5.1 Gait analysis of healthy lower limb

The gait analysis of lower limb of the healthy subject was carried out before analyzing the prosthetic gait cycle. The performance test was carried out by making a comparison between the gait cycles data captured from healthy limb and that from the prosthetic limb. The data recorded during the gait analysis of the healthy lower limb are presented in the following Table 5.1.

Table 5.1: Gait analysis data from normal speed walking of healthy individual

ANALYSIS				
Subject	Context	Name	Value	Units
Barefoot	Left	Cadence	84.507	steps/min
Barefoot	Left	Walking Speed	0.825115	m/s
Barefoot	Left	Stride Time	1.42	s
Barefoot	Left	Step Time	0.71	s
Barefoot	Left	Opposite Foot Contact	50	%
Barefoot	Left	Foot Off	58.45071	%
Barefoot	Left	Stride Length	1.171663	m
Barefoot	Left	Step Length	0.607675	m
Barefoot	Left	Opposite Foot Off	8.450705	%
Barefoot	Left	Single Support	0.59	s
Barefoot	Left	Double Support	0.24	s
Barefoot	Right	Cadence	90.90909	steps/min
Barefoot	Right	Walking Speed	0.890234	m/s
Barefoot	Right	Stride Time	1.32	s
Barefoot	Right	Step Time	0.66	s
Barefoot	Right	Opposite Foot Off	9.090909	%
Barefoot	Right	Opposite Foot Contact	50	%
Barefoot	Right	Foot Off	58.33333	%
Barefoot	Right	Single Support	0.54	s
Barefoot	Right	Double Support	0.23	s
Barefoot	Right	Stride Length	1.175109	m
Barefoot	Right	Step Length	0.594199	m

The cadence, walking speed, stride time, step time, opposite foot contact, foot off, stride length, step length, opposite foot off, single support, double support etc. for both the left and right lower limbs are tabulated in Table 5.1. From the data, there are some differences between the data obtained from left and right limbs. From the data, the cadence of left leg is lower than that of right leg; however, the opposite scenario is observed for the walking speed. The stride and step times for left leg is found to be greater than that of right leg. Though, the percentage of opposite foot contact was same for both the feet, opposite foot off for left lower limb was less than the right foot off. The proportion of left foot off is observed to be little more than the right foot off. The stride and step lengths for left leg is seen to be slightly longer than that of right leg. The

single support and double support sub-phases of left lower limb are observed to last little longer than that of right lower limb. Table 5.2 represents the different events in lower limb gait cycle while walking at normal speed.

Table 5.2: Events involved in lower limb gait during normal speed walking

EVENTS				
Subject	Context	Name	Time (s)	Description
Barefoot	Left	Heel Strike	1.31	The instant the heel strikes the ground
Barefoot	Left	Toe Off	2.07	The instant the toe leaves the ground
Barefoot	Right	Heel Strike	1.97	The instant the heel strikes the ground
Barefoot	Right	Toe Off	1.42	The instant the toe leaves the ground

The time elapsed for the events of foot strike and foot off by both the right and left feet during normal speed walking are shown in the Table 5.2. From the data, the lengths of time for these events are not identical for both limbs. A mixed nature is observed in the elapsed time length for different events performed by left and right legs while walking.

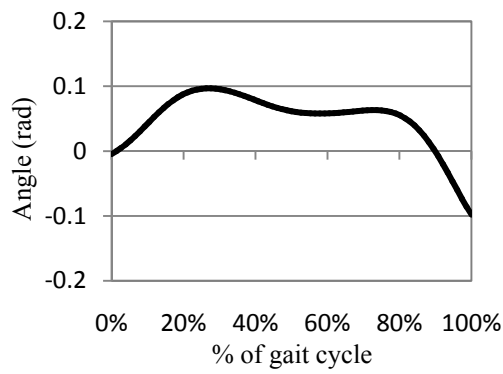
The angular displacement, the forces, moments and power of the limb joints and segments are also recorded to analyze the gait cycle of the healthy lower limb. Two types of data were obtained from the motion analysis of the healthy lower limb. One type data described the angular displacement, velocity and acceleration of the lower limb joints and segments whereas the other type of data illustrated the force, moment and power of the same entities. All these data fall under the categories of kinematic and kinetic data.

According to the coordinate system of the force plates, the significant changes in angular position of different segments of the lower limb, and variation in ground reaction force during ambulation is mainly at Z direction, therefore the Z components of data illustrate the most significant changes in the lower limb kinematics and kinetics, and the X components and Y components of the data characterize the trivial changes in the lower limb biomechanics during normal speed walking. Therefore, only the Z-

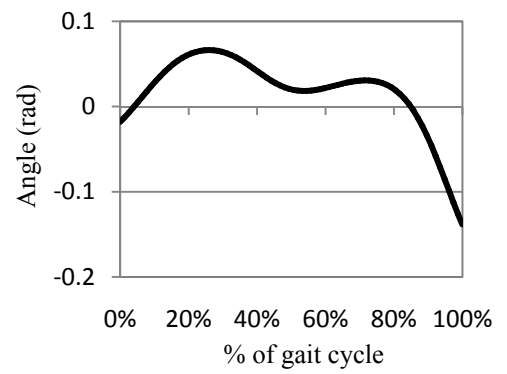
components of the gait cycle data are plotted to carry out the motion analysis of the lower limb. Some three trials were carried out, and the average values have been used to plot the gait cycle. Some of these mean data, including their standard deviation are tabulated in the Appendix E.

5.1.1 Kinematic analysis

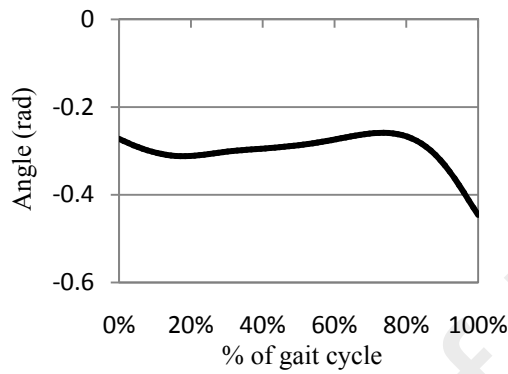
The kinematic analysis includes information about the displacement, velocity and acceleration of the prosthesis joints and components during the gait cycle. The kinematics of the lower limb can be obtained from the plug-gait data. Though the plug-gait data were recorded for entire prescribed locations, the graphs are plotted only for the data from the hip, knee and ankle joints, and foot progression. The following figures represent the kinematic of the lower limb joints and segments.



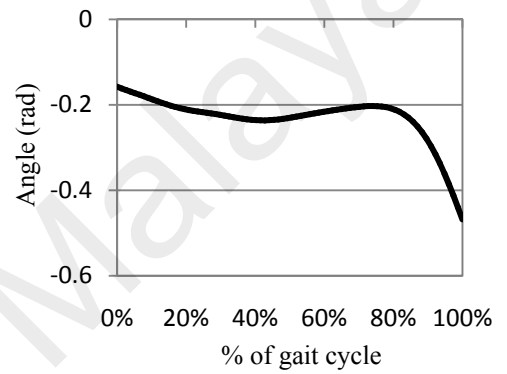
a) Angular displacement of Left Hip



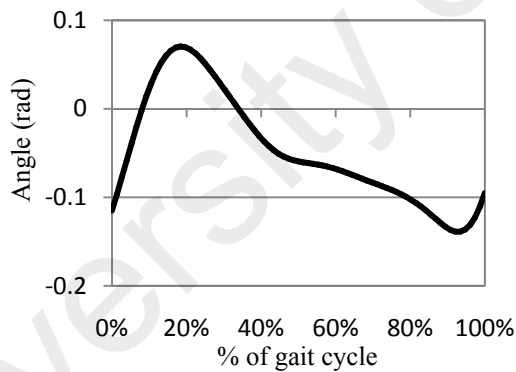
b) Angular displacement of Right Hip



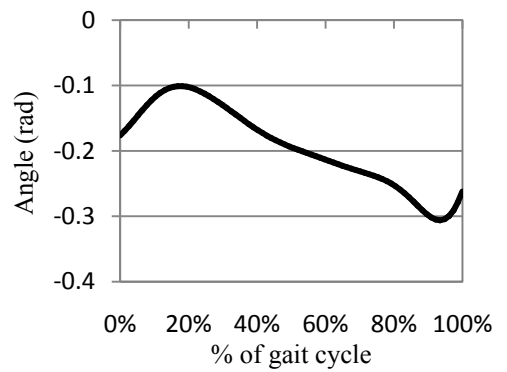
c) Angular displacement of Left Knee



d) Angular displacement of Right Knee



e) Angular displacement of Left Ankle



f) Angular displacement of Right Ankle

Figure 5.1: The angular displacement of the lower limb joints.

Figure 5.1 shows the angular displacement of the hip, knee and ankle joints while walking at normal speed on a level ground. Figure 5.1a), 5.1c) and 5.1e) represents the angular displacement of left hip, knee and ankle joints whereas Figure 5.1b), 5.1d) and 5.1f) illustrate the same parameters for the right hip,

knee and ankle respectively. From the figures, though there are some differences between the magnitudes of the angular displacement of left and right leg joints, the pattern is still the same for the respective joints of the both lower limb. Due to variation in biomechanics of the left and right leg, the pattern of left and right leg cycle is different. The shape of the angular displacement graphs obtained from the gait analysis is quite similar to that reported in majority of previous investigations (Mills and Barrett, 2001).

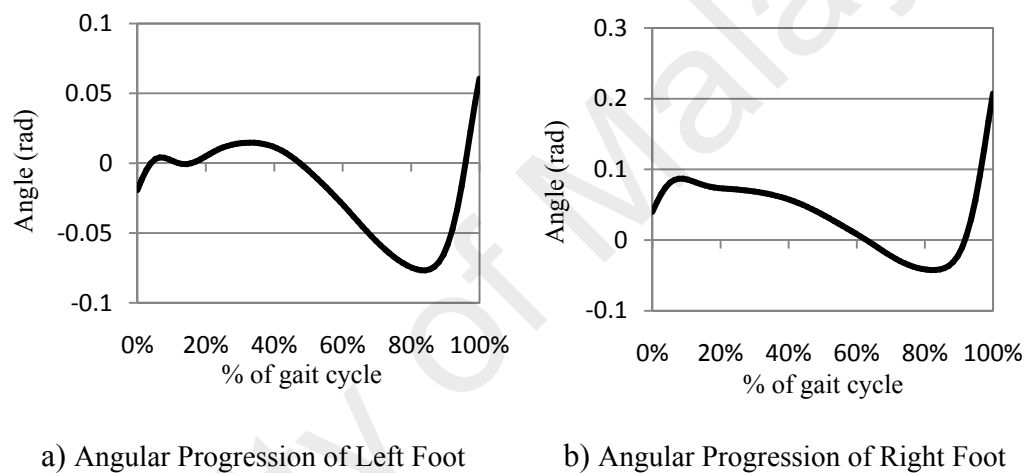
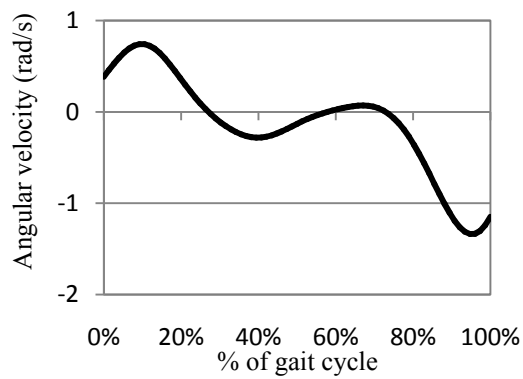
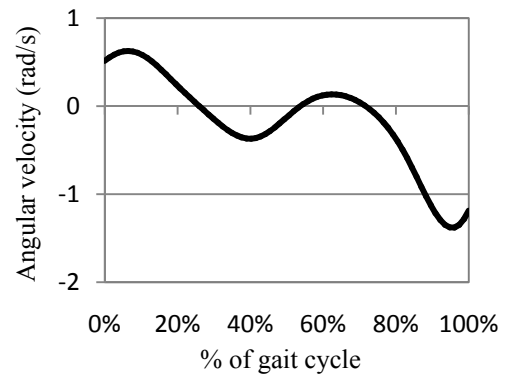


Figure 5.2: Angular displacement of foot progression.

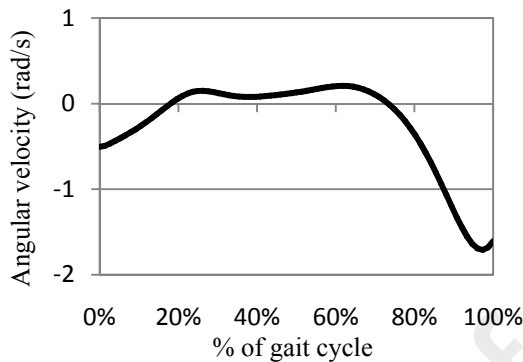
Figure 5.2 represents the angular progression of left and right foot during walking. From the figures, despite the trend of the angular foot progression is largely alike; the extent of angular foot progression of right foot is considerably higher than that of the left foot.



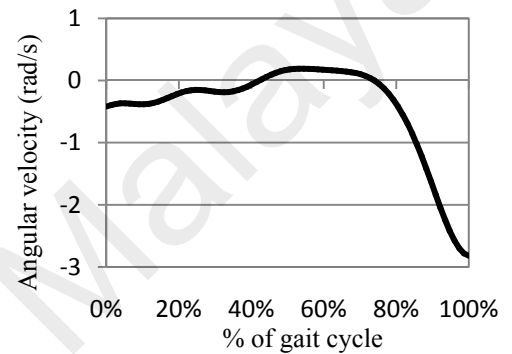
a) Angular Velocity of Left Hip



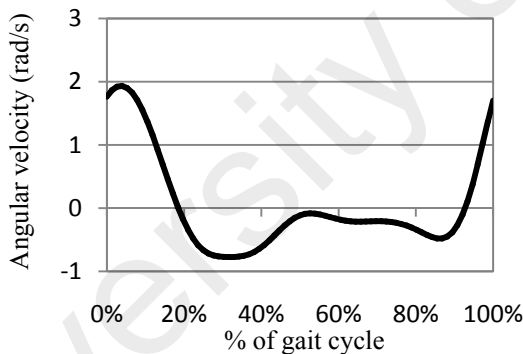
b) Angular Velocity of Right Hip



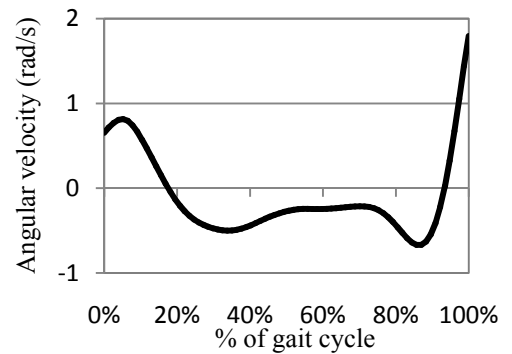
c) Angular Velocity of Left Knee



d) Angular Velocity of Right Knee



e) Angular Velocity of Left Ankle



f) Angular Velocity of Right Ankle

Figure 5.3: Angular velocity of lower limb joints during walking at normal speed.

Figure 5.3 illustrates the angular velocity of hip, knee and ankle joints of left and right legs throughout the gait cycle during normal walking on the plane field. Though pattern-wise, the graphs were quite similar for both the left and right leg joints, magnitude-wise the angular acceleration of left leg joints significantly

vary from the angular acceleration of the right leg joints. The variation of angular velocity was observed to be mixed in nature. The similar patterns and magnitude in the angular velocity graph of lower limb joints were found in the previous publications (Mills and Barrett, 2001).

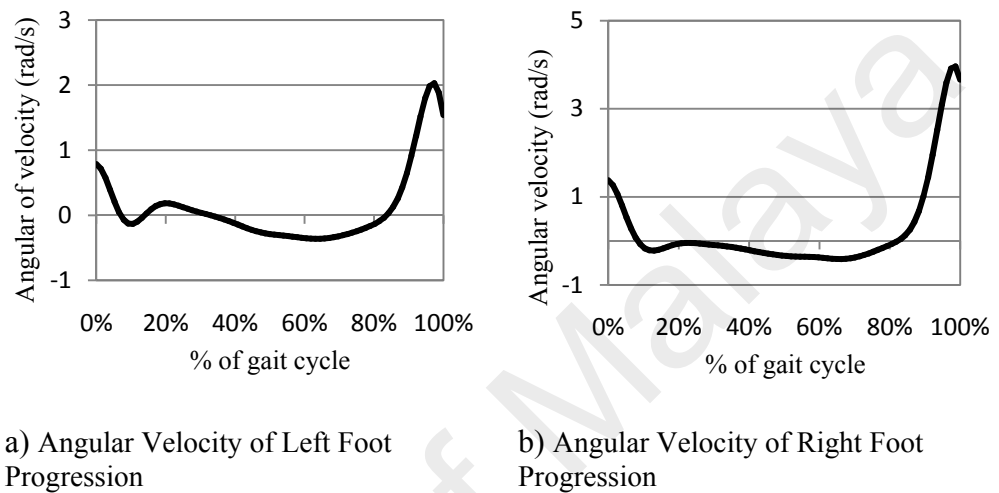
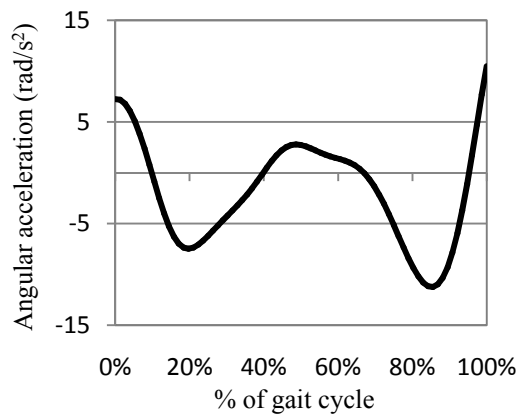
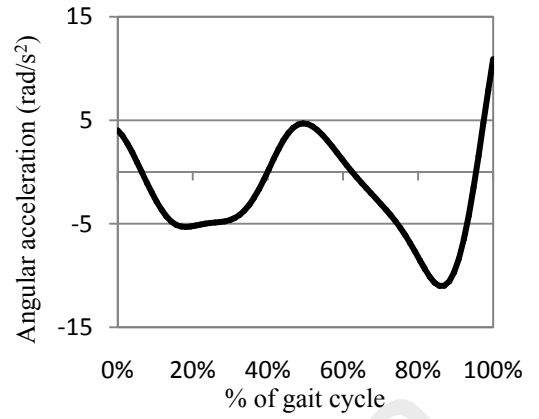


Figure 5.4: Angular velocity of foot progression during walking at normal speed.

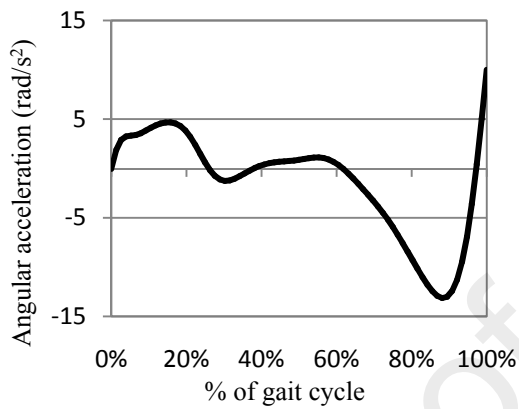
Figure 5.4, depicts the angular velocity of foot progression during normal level ground walking. From the figure, the nature of changing the angular velocity of left and right foot progression is quite similar. However, the fluctuation of angular velocity of right foot progression is significantly greater than that of left foot. Nonetheless, the shape of the angular velocity plots of foot progression resemble to the results obtained from the literature (Mills and Barrett, 2001).



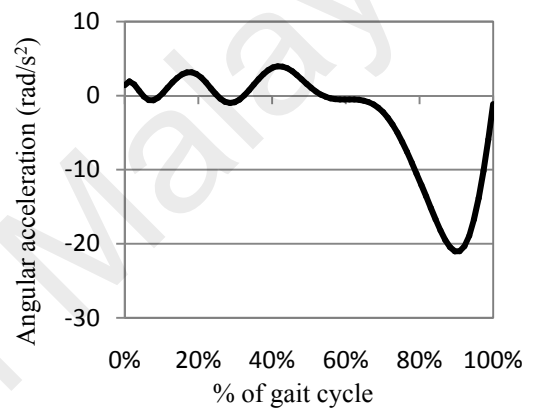
a) Angular Acceleration of Left Hip



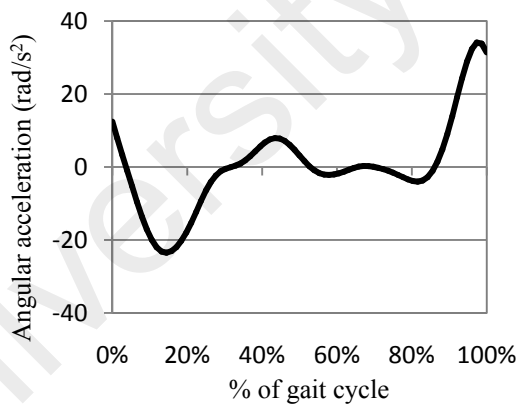
b) Angular Acceleration of Right Hip



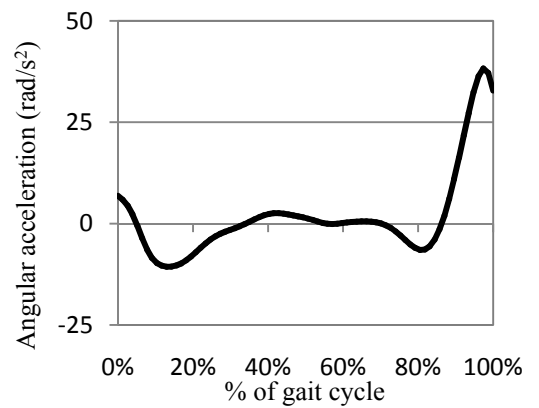
c) Angular Acceleration of Left Knee



d) Angular Acceleration of Right Knee



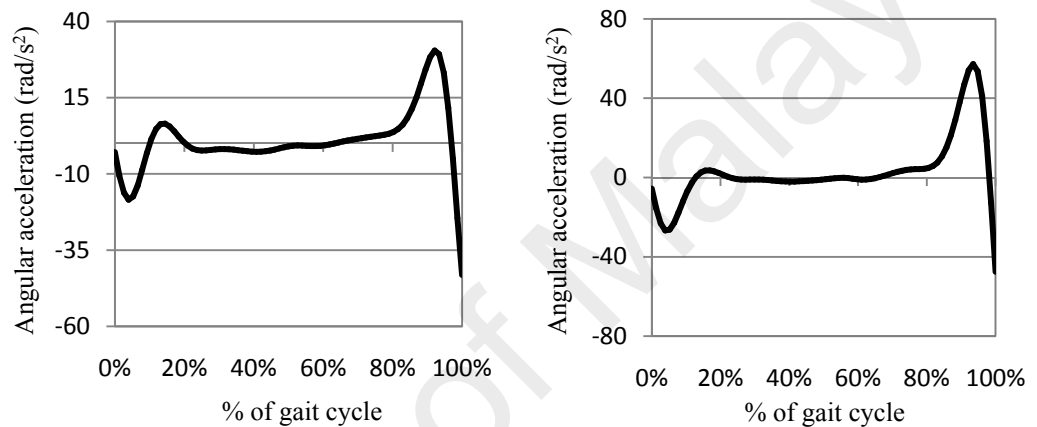
e) Angular Acceleration of Left Ankle



f) Angular Acceleration of Right Ankle

Figure 5.5: Angular acceleration of lower limb joints during walking at normal speed.

Figure 5.5 represents the angular acceleration of hip, knee and ankle joints of healthy individual throughout the gait cycle while walking in normal speed. From the figure, the angular accelerations of the left and right leg joints are found to be symmetrical. However, the degree of acceleration of some particular joint of a leg is not exactly same like that of the corresponding joint of other leg, which is rather found to be mixed in size.



a) Angular Acceleration of Left Foot Progression

b) Angular Acceleration of Right Foot Progression

Figure 5.6: Angular acceleration of foot progression during walking at normal speed.

Figure 5.6 shows the angular acceleration of foot progression during the normal gait cycle. The graphs are seen to be identical in pattern, which can be attributed to the fact that both the feet have maintained a particular style of ambulation during progression. However, there was some difference between the magnitudes of the angular accelerations of the left and right legs. Due to difference between the biomechanics of left and right legs, the pattern of graph has some alteration.

5.1.2 Kinetic analysis

The kinetic analysis provides information about the force, moment and power of the prosthesis joints and components during the gait cycle. The following figures would describe the kinetics of the prosthesis and its joints and segments.

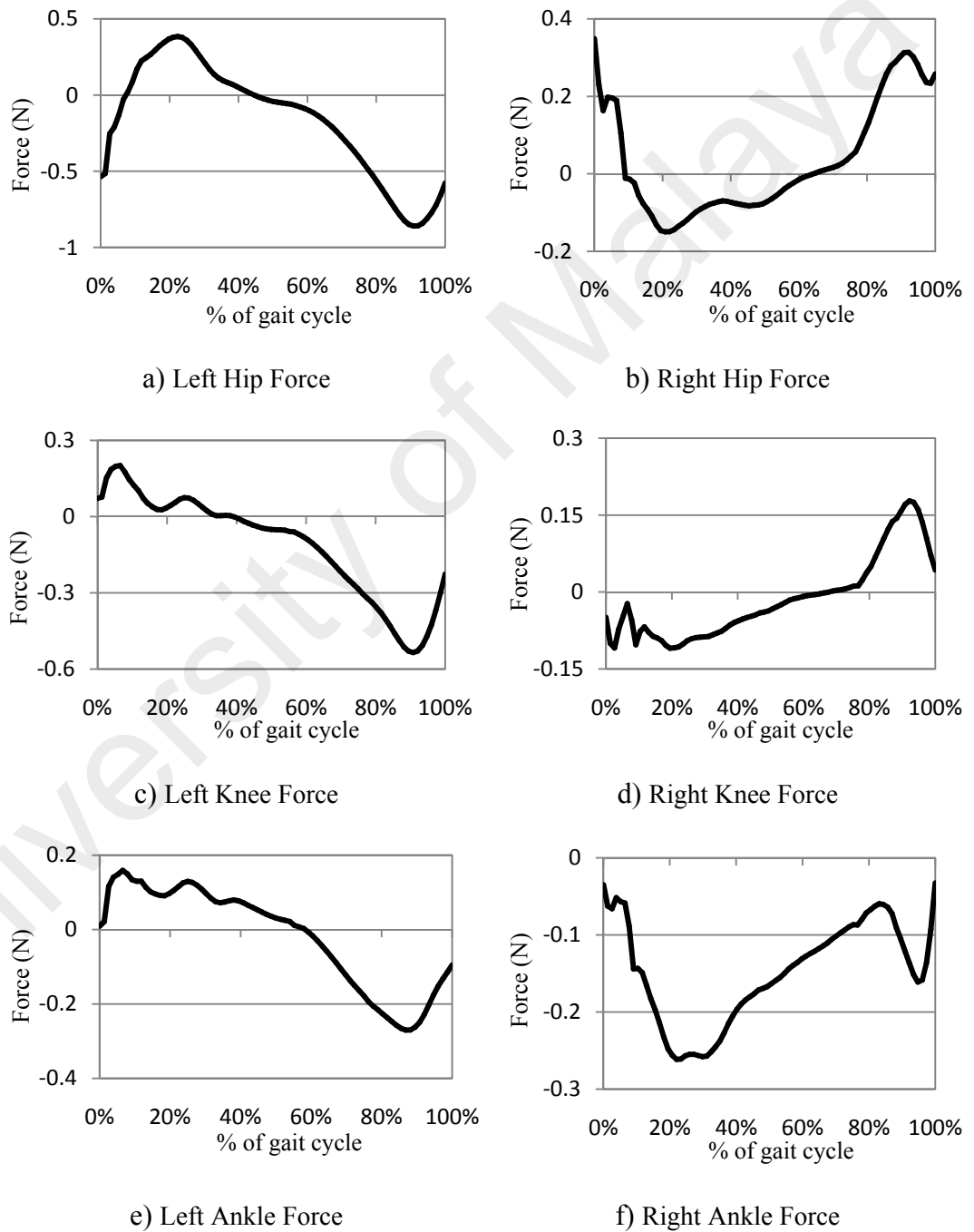
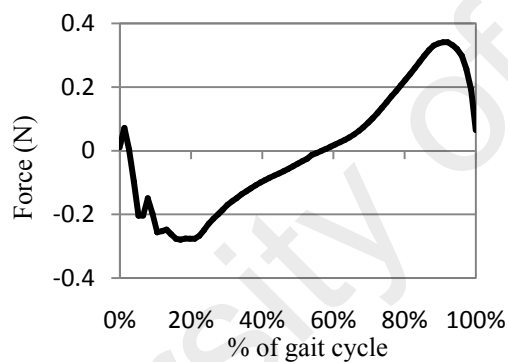
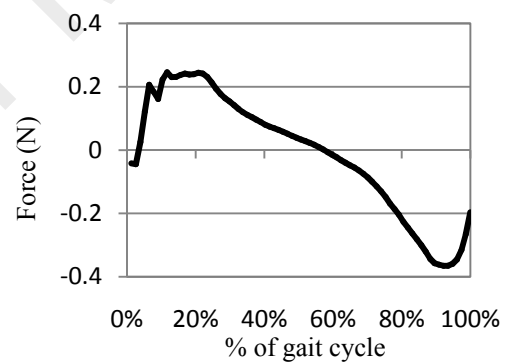


Figure 5.7: Forces in the lower limb joints.

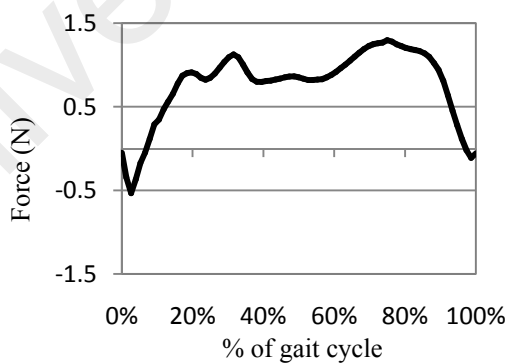
Figure 5.7 represents the changes in the hip, knee and ankle forces throughout the gait cycle. From the pattern analysis, none of the left leg joints has similarity to the corresponding right leg joints. They are found rather having opposite trend in magnitude. For the joints of left leg, the maximum forces were recorded at first 0 – 30% of the gait cycle, whereas the minimum forces were measured at last 80 – 100% of the gait cycle. However, for the right leg joints, opposite trend was observed. The minimum forces were measured in the segment of 10 – 40% of gait cycle whereas the maximum forces were recorded at the last 80 – 100% of the gait cycle. Moreover, the forces in each joints of left leg were found to be greater than the corresponding joints of right leg.



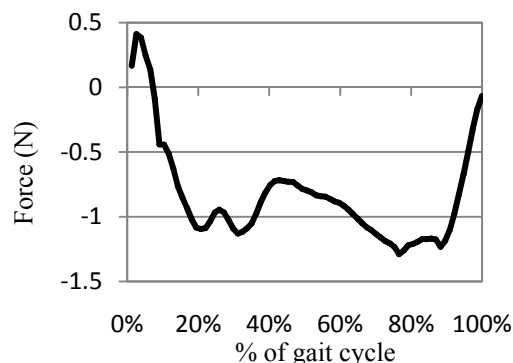
a) Left Foot Ground Reaction Force



b) Right Foot Ground Reaction Force



c) Normalized Left Foot Ground Reaction Force



d) Normalized Right Foot Ground Reaction Force

Figure 5.8: Ground reaction forces of healthy lower limb foot.

Figure 5.8 illustrates the ground reaction force of healthy lower limb foot while walking at normal speed on plane ground. From Figure 5.8 a) and Figure 5.8b), the ground reaction force of the left foot has decreased to minimum during the first 0 – 20% of gait cycle, which then gradually increased to maximum at 90% of gait cycle and followed then by a decrease. The completely reverse trend is noticed in the ground reaction force of right foot. Due to difference of biomechanics between the left and right foot, the trend of ground reaction force was different. Though, the normalized ground reaction force graphs were different in shape than the foot ground reaction force plots, they still maintain an inverse relationship between the patterns of left and right foot ground reaction forces.

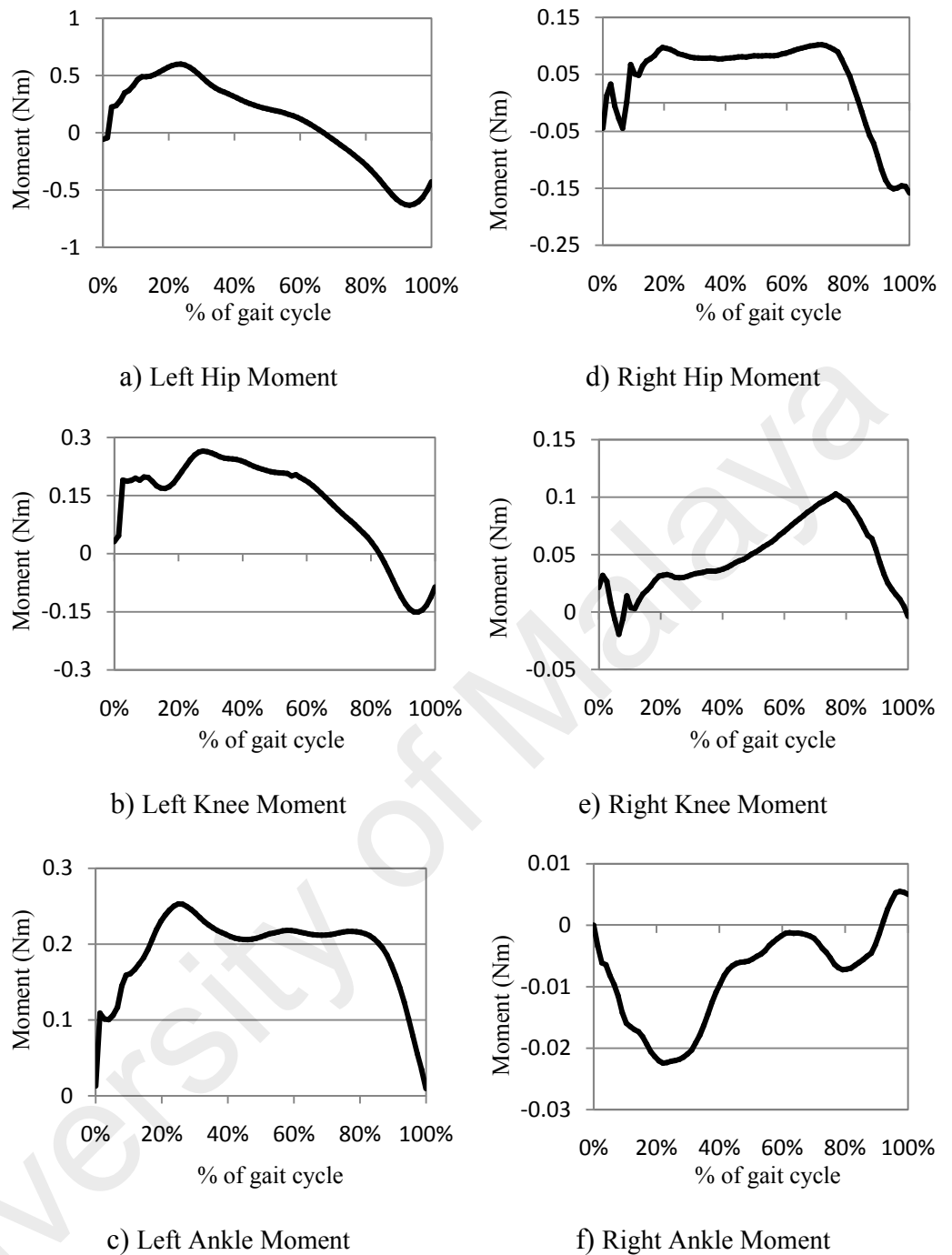
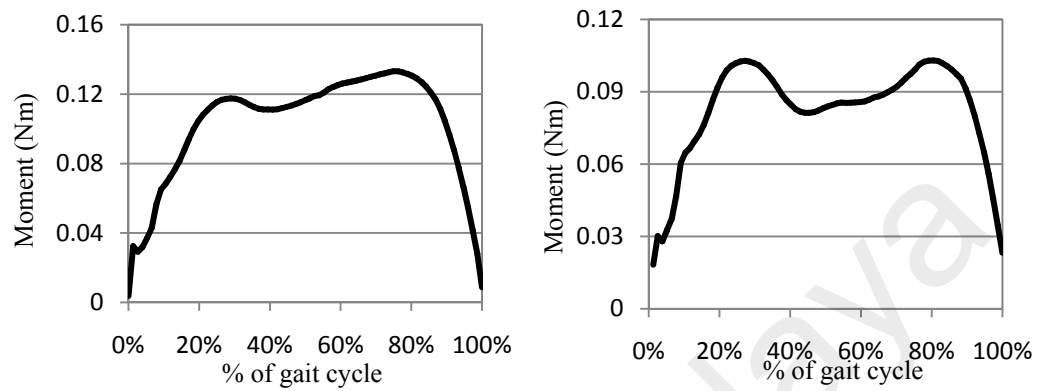


Figure 5.9: Joint moments of healthy lower limb

Figure 5.9 illustrates the moments of hip, knee and ankle joints of both legs during the gait cycle when walking at normal speed. All the moment graphs have distinct pattern, and there is no minimum resemblance found in these plots. Though there is no common pattern observed in the moment graphs, a particular trend is observed in the moment of left leg joints, the moment increase until

some 30% of gait cycle and then decrease gradually until the end of gait cycle.

For right leg joints, the fluctuation of magnitude is seen to be random.

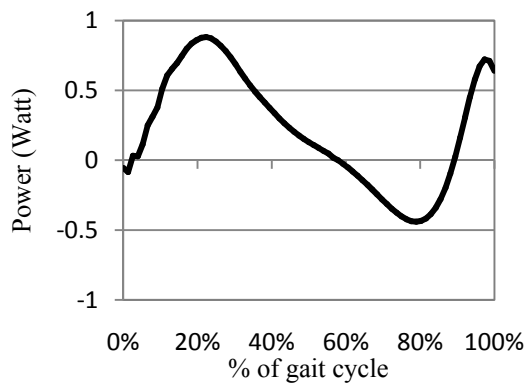


a) Left Foot Ground Reaction Moment

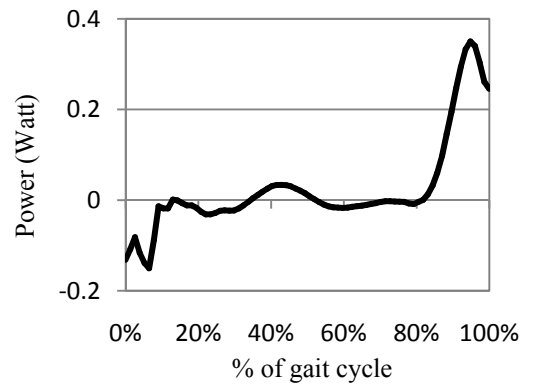
b) Right Foot Ground Reaction Moment

Figure 5.10: Ground reaction moment of healthy lower limb foot.

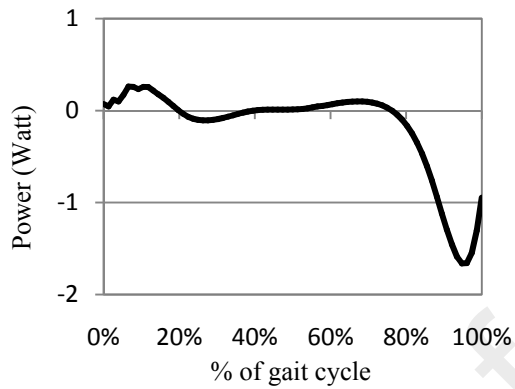
Figure 5.10 shows the ground reaction moment of left and right foot throughout the gait cycle when walking at normal speed on plane field. The peaks of the left foot ground reaction moment graph were significantly greater than that of right foot. The minimum values of the ground reaction moment of left foot at the starting and ending of the gait cycle were also lower than that of right foot. However, a similar fluctuation was observed in the ground reaction moments of the both feet.



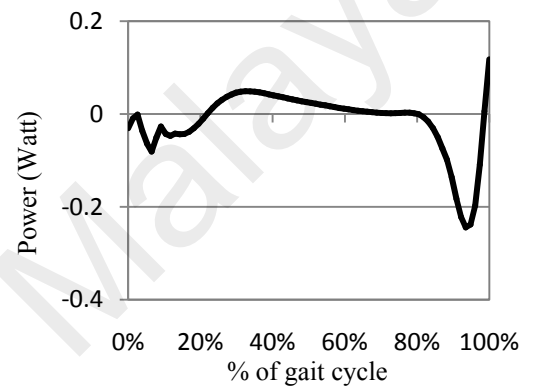
a) Left Hip Power



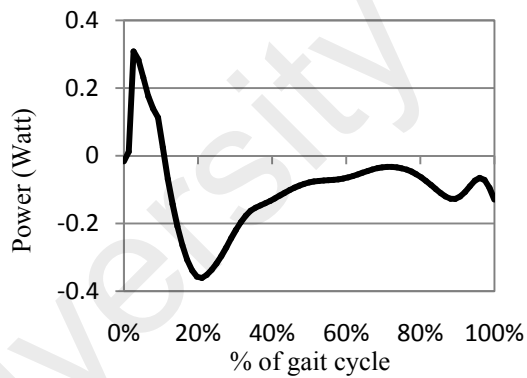
b) Right Hip Power



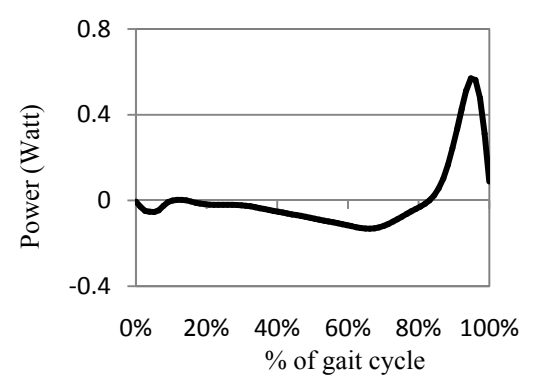
b) Left Knee Power



d) Left Knee Power



c) Left Ankle Power



e) Right Ankle Power

Figure 5.11: Joint power of healthy lower limb.

Figure 5.11 shows the power at different joints of the lower limb during normal plane ground walking. The positive segments of the power graph represents the period of energy storing by the joints during the gait cycle, whereas the negative segments of the power plots demonstrate the by the joints while producing

movement in normal gait walking. Though there is little resemblance between the left and right knee power curves, for hip and ankle joints no such relationship is found. According to the graph, both the events of energy storing and returning by the left hip joint were considerably high; however, for the right hip joint, the energy storing and returning was significantly low. For both the left and right knees, the energy storing was trivial, however, the energy returning was quite remarkable. For the ankle joints, the energy storing was moderate; the energy returning by the left ankle was substantially larger than that by the right ankle. From the figures, the energy storing and returning by the joints were most significant at the last 20% of the gait cycle (i.e. in 80 – 100% of gait cycle), except for the left ankle.

5.2 Stability test of healthy individual

Stability of individual is tested with two types of tests – i) postural stability test, and ii) fall risk test. Both the static and dynamic tests are carried out to assess the stability of the subject. Postural stability was tested for single leg and also for double leg, and the fall risk was tested only for double leg standing.

5.2.1 Postural Stability test

In double leg postural stability test, the healthy subject mounted and stood on the platform of the Biodex machine positioning the left and right feet at some angle of 20° , and placing the respective heel at E6 and E16 lines of the machine platform scale. In single leg postural stability test, the position of left foot and heel were at 5° and E11 respectively. Different levels of perturbation and disturbance have been applied to test the postural stability of the individual. Both

the static and dynamic data were recorded during the test. The postural stability test data for single leg and double leg and for both the static and dynamic analysis are tabulated in the following Table 5.3.

University of Malaya

Table 5.3: Postural stability analysis of healthy individual

Platform setting	Overall Stability Index	Anterior/Posterior Index	Medial Lateral Index	% Time in Zone	% Time in Quadrant
Double leg stability					
Dynamic 8	2.6 ± 1.46	1.8 ± 1.02	1.6 ± 1.49	A96, B4, C0, D0	I8, II5, III24, IV63
Dynamic 2	9.0 ± 4.86	5.9 ± 3.72	5.6 ± 5.00	A24, B34, C28, D14	I29, II32, III12, IV27
Static	0.3 ± 0.27	0.3 ± 0.27	0.1 ± 0.10	A100, B0, C0, D0	I1, II0, III10, IV89
Single leg stability					
Dynamic 8	1.2 ± 0.58	0.9 ± 0.57	0.6 ± 0.53	A100, B0, C0, D0	I14, II32, III30, IV24
Dynamic 2	5.7 ± 4.68	4.5 ± 4.74	2.4 ± 2.26	A55, B24, C18, D3	I17, II37, III26, IV20
Static	0.8 ± 0.58	0.6 ± 0.53	0.5 ± 0.48	A100, B0, C0, D0	I9, II8, III39, IV44

From the data shown in Table 5.3, the score of the tests varied with the platform setting. In double leg stability test, for platform setting at level 8, the overall score obtained from the dynamic stability test was 2.6, which indicated quite a good stability of the subject; while for platform setting at level 2, the score of 9.0 indicated poor stability for the subject. For static analysis, the overall score was some 0.3, which was good enough for some healthy individual. However, in single leg stability test, for platform setting at level 8 and level 2, the stability index were 1.2 and 5.7 respectively. The scores from the both level of dynamic test for single leg stability were remarkably good. The score from the static analysis of single leg stability test was 0.8, which indicated a very good static stability of the subject.

5.2.2 Fall risk test

The fall risk test was also carried out for two level of platform setting. During the fall risk test, the left foot of the subject was placed on the platform at some angle of 25° when the corresponding heel position was at E6 line of the machine platform scale. Then the right foot and heel position was at 20° and E16 respectively. For fall risk test, no single leg test was performed. The data obtained from the fall risk test are shown in Table 5.4.

Table 5.4: Fall risk test of healthy individual

Platform setting	Overall Stability Index
Dynamic 8	2.0 ± 0.46
Dynamic 2	6.0 ± 4.46
Static	1.1 ± 0.75

From the dynamic analysis results, the fall risk index for the platform setting at level 8 was found to be 2.0, which was significantly good for the individual. The fall risk score for the platform setting at level 2 was 6.0, that was also reasonable for a healthy individual. From the static analysis, the fall risk index obtained for the subject was 1.1, which was also quite acceptable for any healthy subject.

5.3 Finite element analysis of prosthesis components

A finite element analysis of the joint components would illustrate the stress, strain and deformation incurred to the components under applied load and therefore, shows the viability of the design. The finite element analysis (*FEA*) of the prosthesis includes the *FEA* analysis of knee joint components and ankle joint components.

5.3.1 Finite element analysis of knee joint components

Finite Element Analysis can efficiently optimize and validate each design step; it can ensure quality, performance, and safety. SOLIDWORKS simulation uses the displacement formulation of the finite-element method to calculate component displacements, strains, and stresses under internal and external loads. The analysis of components is carried out by linear stress analysis. It was done to ensure the geometry remains in the linear elastic range [that is, once the load is removed, the component returns to its original shape], then linear stress analysis is applied, as long as the rotations and displacements are small relative to the geometry. For such an analysis, factor of safety (*FoS*) is a common design goal. First of all, a model has to be created to perform a finite-element analysis. Several papers published elsewhere have already focused on creation of a finite-

element model either of a joint itself (knee joint, hip joint, temporo-mandibular joint, etc.) or of an implant (total knee replacement) (Zach et al., 2014). To create a finite-element model, boundary conditions had to be set at the first place; followed by mesh formation, and simulation.

5.3.1.1 Knee joint model

The finite-element model of the knee joint was developed to check the functionality of the joint designed for the prosthesis. To set up a model, connections between the components, component contacts, fixtures and external load are the primary factors to be defined accurately. The whole gear assembly is defined as global contact, where the contact between the gears (gear 1 – gear 2), gears – stoppers, and gears – bearing plates are assigned as bonded contact, the contact between the stoppers (stopper 1 – stopper 2) and bushing pins – bearings are defined as no penetration contact. The bearing-plates are set up as fixed geometry where the faces between the gears and stoppers with the bearing-plates are defined as the roller slider joint. The faces between the bushing pins and the bearing are set up as fixed hinge joints. Normal loads are applied from top and bottom of the gear 1 and gear 2 respectively. Two opposite directional torques are applied on the face of two gears. Solid curvature based high quality 16 Jacobian points mesh is formed. The minimum element size of the mesh is 1.3238 mm where the maximum element size of the mesh is 6.61898 mm. Total nodes in the meshed model is 95294, total elements in the model is 53492 where the maximum aspect ratio is 26.613.

All components are considered to be solid body. The Aluminum Alloy 1060-H16 is chosen for all components except the for ball bearing, sleeve bearing and bushing pin, for which Alloy Steel (SS), Copper Alloy – Brass, and Alloy Steel

AISI 4140 are respectively selected. The properties of these materials are given in Table C1.

The key features of *FE* modeling of the knee joint components are tabulated in Table 5.5.

Table 5.5: Key features of finite element modeling of knee joint components

Various features of the <i>FE</i> model	
Software used	: SOLIDWORKS
Solver type	: FFEPlus
Mesh type	: Solid Mesh
Mesher Used	: Curvature based mesh
Jacobian points	: 16 Points
Element type	: Triangular (2D)
Maximum element size	: 6.61898 mm
Minimum element size	: 1.3238 mm
Mesh Quality	: High
Remesh failed parts with incompatible mesh	: On
Total Nodes	: 95294
Total Elements	: 53492
Maximum Aspect Ratio	: 26.613

The loading conditions were determined by calculation.

A transfemoral amputee with a mass of 69 Kg and height of 166.5 cm was taken as subject and the prosthesis was designed accordingly. Therefore, at the stance phase of the gait cycle, the applied load on the knee gears was entirely from the body weight of the amputee, i.e. equal to the body weight of the amputee and the value of applied torque will be zero. However, at the swing phase, the applied load would be the Y-component of the amputee body weight for the accrued knee/gear rotation angle, and the value of the applied torque would be the torque due to the X-component of amputee weight for that particular rotation angle. The variables used in the simulation were based on the features of subject presented in Table 3.1 of Chapter 3.

The weight of the subject was 676.9 N.

Applied load = weight of the subject + weight of the thigh rod socket arrangement = resultant weight = $W_r = 679.9 + 1.5 * 9.81 = 691.6N$

For the sake of simplifying the calculation, it is presumed that the weight is shared equally by the two legs; therefore, the weight should be divided by two. However, at the event of balance loosing, the body weight becomes 1 to 4 times of real body weight. Therefore, the total weight is considered as the applied load.

The total body height of subject = 166.5 cm

The length of Femur, $l = 51.5$ cm, and

Therefore, the length of Tibia = 41.0 cm

Torque arm length for Femur at 15^0 and 70^0 of rotation is, $l_1 = 515$ mm; torque arm length for Tibia at 15^0 and 70^0 of rotation is $l_2 = 410$ mm

During the swing phase of the gait cycle, the subject knee is found to rotate from 15^0 to 70^0 , which to be imitated by the prosthetic knee joint. The angle of rotation is resultant angle of both the gears. Therefore, to generate 15^0 of rotation, each gear has to rotate 7.5^0 ; and to create 70^0 of rotation, each gear has to rotate 35^0 .

Therefore, value of Y-component of subject weight at 15^0 of rotation angle can be derived as follows:

At stance phase of gait cycle, 0^0 of rotation of knee joint:

The applied load on both the gears of the knee joint = Y-component of the resultant weight = applied load = 691.6 N.

The X-component of the subject body weight = 0 N;

Therefore, the applied torque on both the gears of the knee joint = 0 Nm.

At swing phase of gait cycle, 15^0 of rotation of knee joint:

The applied load on the gear-1 of the knee joint = Y-component of the resultant weight at 7.5° of rotation

$$F_{Y15deg} = F \cos 7.5 = 691.6 * \cos 7.5 = 685.7N$$

The applied load on the gear-2 of the knee joint = Y-component of the subject body weight at 15° of rotation,

$$F_{Y15deg} = F \cos 7.5 = 691.6 * \cos 7.5 = 685.7N$$

The X-component of the subject body weight at 15° of rotation,

$$F_{X15deg} = F \sin 7.5 = 691.6 * \sin 7.5 = 90.3N$$

Therefore, the applied torque on gear-1 of knee joint at 15° of rotation,

$$\tau_{X15deg} = F_{X15deg} * l_1 = 90.3 * 0.515 = 46.5 Nm .$$

The applied torque on gear-2 of knee joint at 15° of rotation,

$$\tau_{X15deg} = F_{X15deg} * l_2 = 90.3 * 0.410 = 37.0 Nm$$

At swing phase of gait cycle, 70° of rotation of knee joint:

The applied load on the gear-1 of the knee joint = Y-component of the subject body weight at 35° of rotation,

$$F_{Y70deg} = F \cos 35 = 691.6 * \cos 35 = 566.5N$$

The applied load on the gear-2 of the knee joint = Y-component of the subject body weight at 70° of rotation,

$$F_{Y70deg} = F \cos 35 = 691.6 * \cos 35 = 566.5N$$

The X-component of the subject body weight at 70° of rotation,

$$F_{X70deg} = F \sin 35 = 691.6 * \sin 35 = 396.7N$$

Therefore, the applied torque on gear-1 of knee joint at 70° of rotation,

$$\tau_{X70deg} = F_{X70deg} * l_1 = 396.7 * 0.515 = 204.3Nm .$$

The applied torque on gear-2 of knee joint at 70° of rotation,

$$\tau_{X70deg} = F_{X70deg} * l_2 = 396.7 * 0.410 = 162.6Nm$$

Boundary conditions used in the simulation of prosthetic knee joint are shown in the following Table 5.6.

Table 5.6: Boundary conditions of knee joint simulation

Constraints	Values	
	at 15 ^o of rotation	at 70 ^o of rotation
Load applied	691.6N to 685.7 N	691.6N to 566.5 N
Moment	Gear-1: 0 Nm to 46.5 Nm, Gear-2: 0 Nm to 37.0 Nm	Gear-1: 0 Nm to 204.3 Nm, Gear-2: 0 Nm to 162.6 Nm

The knee joint model of Figure 5.12a) shows the loads and constrains applied to the different component, and Figure 5.12b) illustrates the meshing of the knee components.

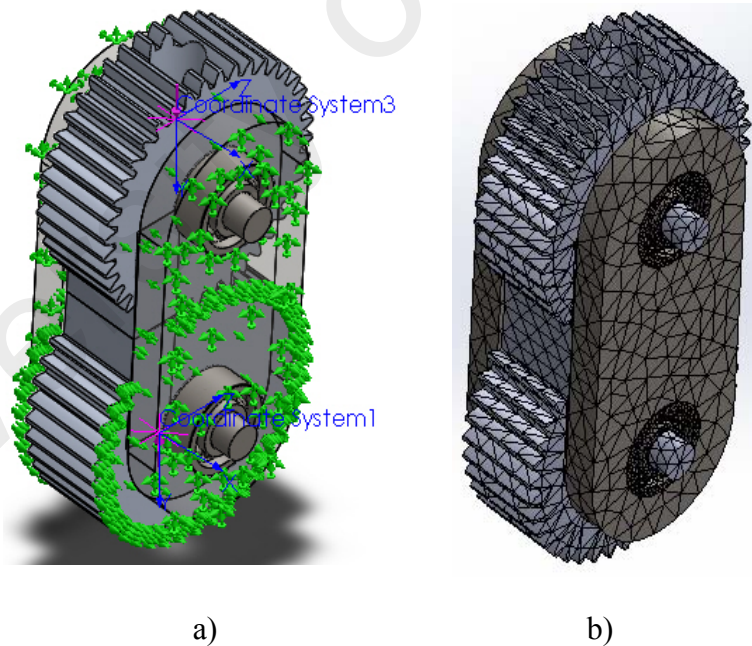


Figure 5.12: a) Model of gear based knee joint, b) Solid mesh of the model.

In the finite-element analysis, the stress, strain and displacement of the knee components are studied to check the viability of the design. In most of the engineering design, the maximum von Mises stress is calculated as a mean of

design safety. The maximum von Mises stress criterion is based on the von Mises-Hencky theory, also known as the Shear-energy theory or the Maximum distortion energy theory.

In terms of the principal stresses $\sigma_1, \sigma_2, \sigma_3$, the von Mises stress is expressed as (Zach et al., 2014):

$$\sigma_{vonMises} = \{[(\sigma_1 - \sigma_2)^2 + (\sigma_2 - \sigma_3)^2 + (\sigma_1 - \sigma_3)^2]/2\}^{1/2} \quad (5.1)$$

The theory states that a ductile material starts to yield at a location when the von Mises stress becomes equal to the stress limit. The yield strength is generally used as the stress limit.

$$\sigma_{vonMises} \geq \sigma_{limit} \quad (5.2)$$

Yield strength is a temperature-dependent property. This specified value of the yield strength should consider the temperature of the component. The factor of safety at a location is calculated from:

$$\text{Factor of Safety, } (FoS) = \sigma_{limit} / \sigma_{vonMises} \quad (5.3)$$

The equivalent strain or the von Mises equivalent strain is a scalar quantity, which is another important factor for the design and is often used to describe the state of strain in solid components. The equivalent strain is commonly defined on plasticity, which is expressed as following (Zach et al., 2014).

$$\varepsilon_{eq} = \sqrt{\frac{2}{3} \varepsilon^{dev} : \varepsilon^{dev}} = \sqrt{\frac{2}{3} \varepsilon_{ij}^{dev} \varepsilon_{ij}^{dev}}; \varepsilon^{dev} = \varepsilon - \frac{1}{3} tr(\varepsilon) \mathbf{1} \quad (5.4)$$

This quantity is work conjugate to the equivalent stress defined as (Zach et al., 2014)

$$\sigma_{eq} = \sqrt{\frac{3}{2} \sigma^{dev} : \sigma^{dev}} \quad (5.5)$$

The displacement analysis allows one to assess the displacement and reaction force results for static, nonlinear, dynamic, drop test studies, or mode shapes for buckling and frequency studies.

5.3.1.2 FEA results of knee joint components

The von Mises stress of different knee components found from the finite element analysis are shown in Figure 5.13.

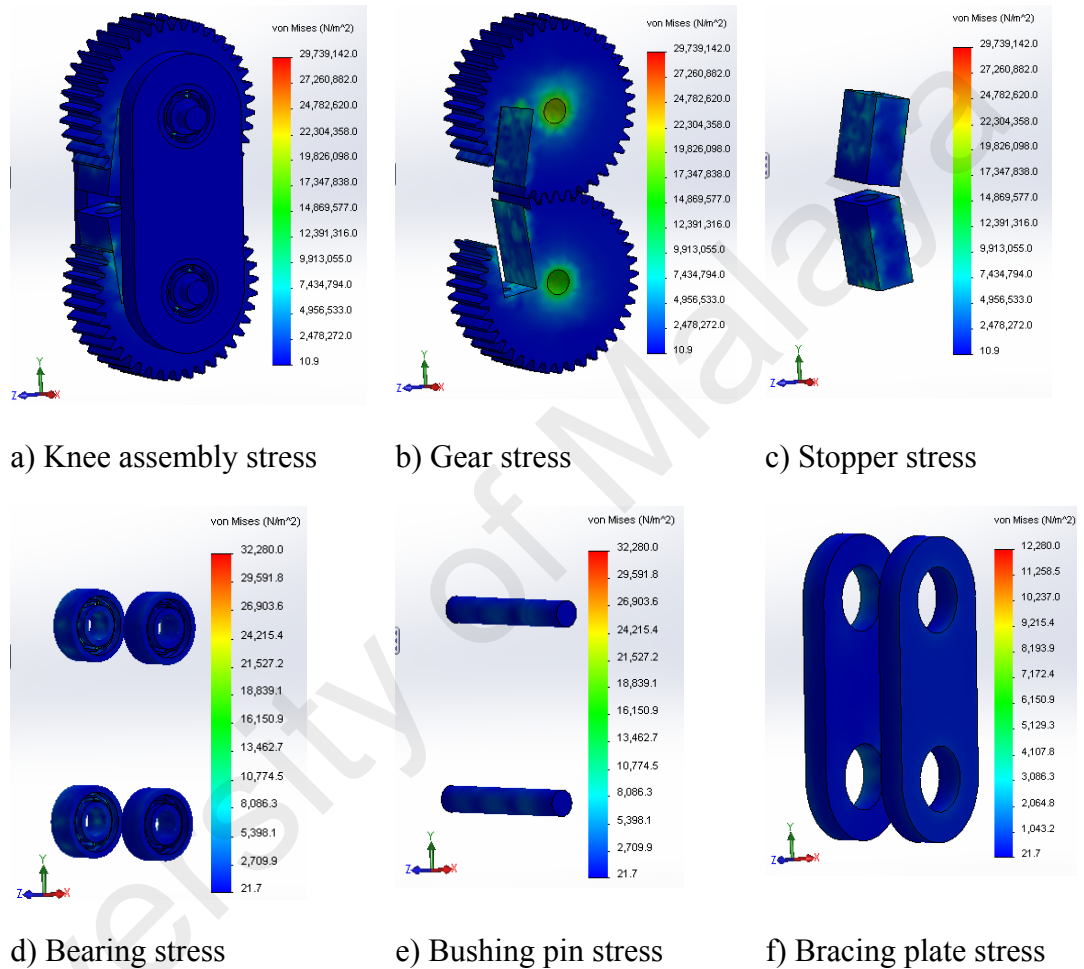


Figure 5.13: von Mises stress of knee joint components.

The primary focus of von Mises stress analysis was on the condition of plastic stability. From the *FEA* results, the maximum von Mises stress value was achieved of 29.74 MPa was achieved in the gear set (Figure 5.13), which did not exceed the *PEEK* material yield strength of 105 MPa (according to material properties of 1060-H12 Aluminum Alloy). The factor of safety was $105.00/29.74 = 3.5$, which was adequate to ensure the safety of the designed

components. Therefore, no plastic deformation of the knee joint occurred and the condition of plastic stability was met.

The main focus of work was to design a knee joint *FE* model and to confirm its functionality; for this purpose, the Solidworks software was used. The model was validated using the gait cycle data obtained from the healthy subject.

The equivalent strains of different components of knee joints are shown in Figure 5.14.

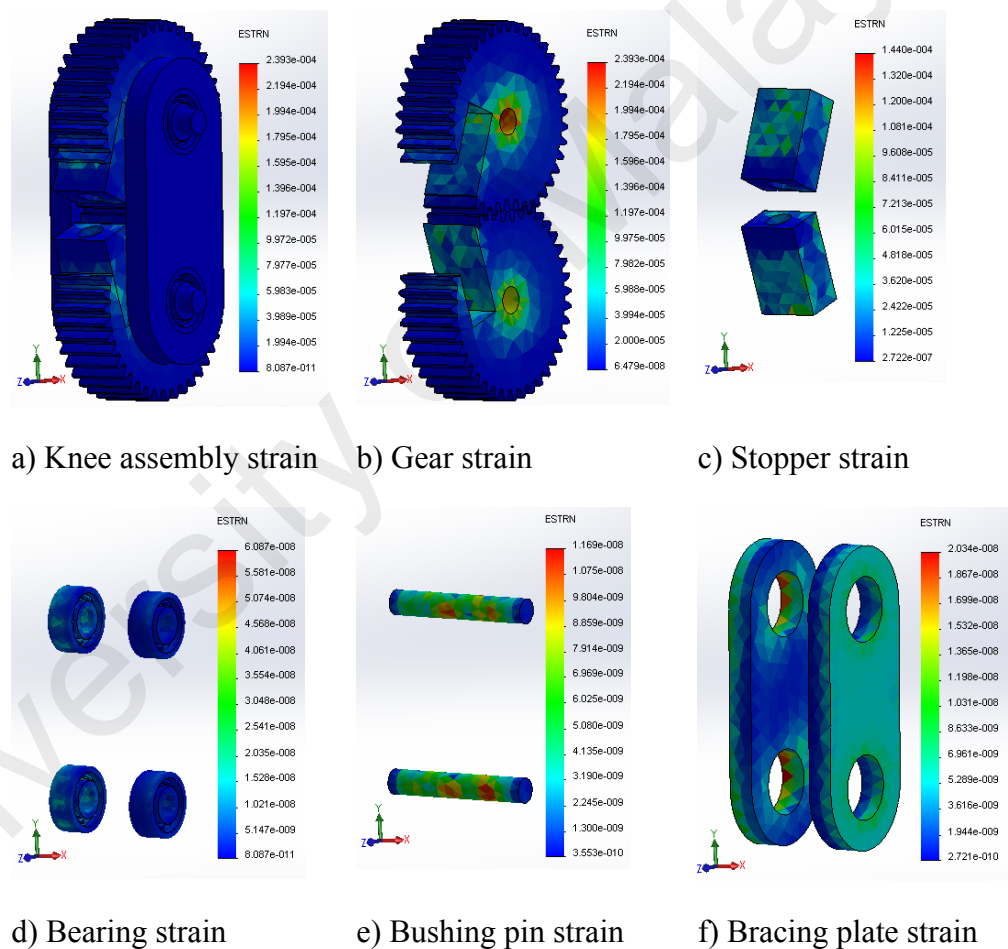


Figure 5.14: Strain analysis of knee joint components.

From the equivalent strain analysis, the maximum strain of $2.393e-004$ was occurred in gear, which was insignificant to be appeared as distortion on the

shape of component and therefore, could be neglected. Hence the components of the knee joint have met the condition of rigidity.

The results of static displacement studies are shown in the following Figure 5.15.

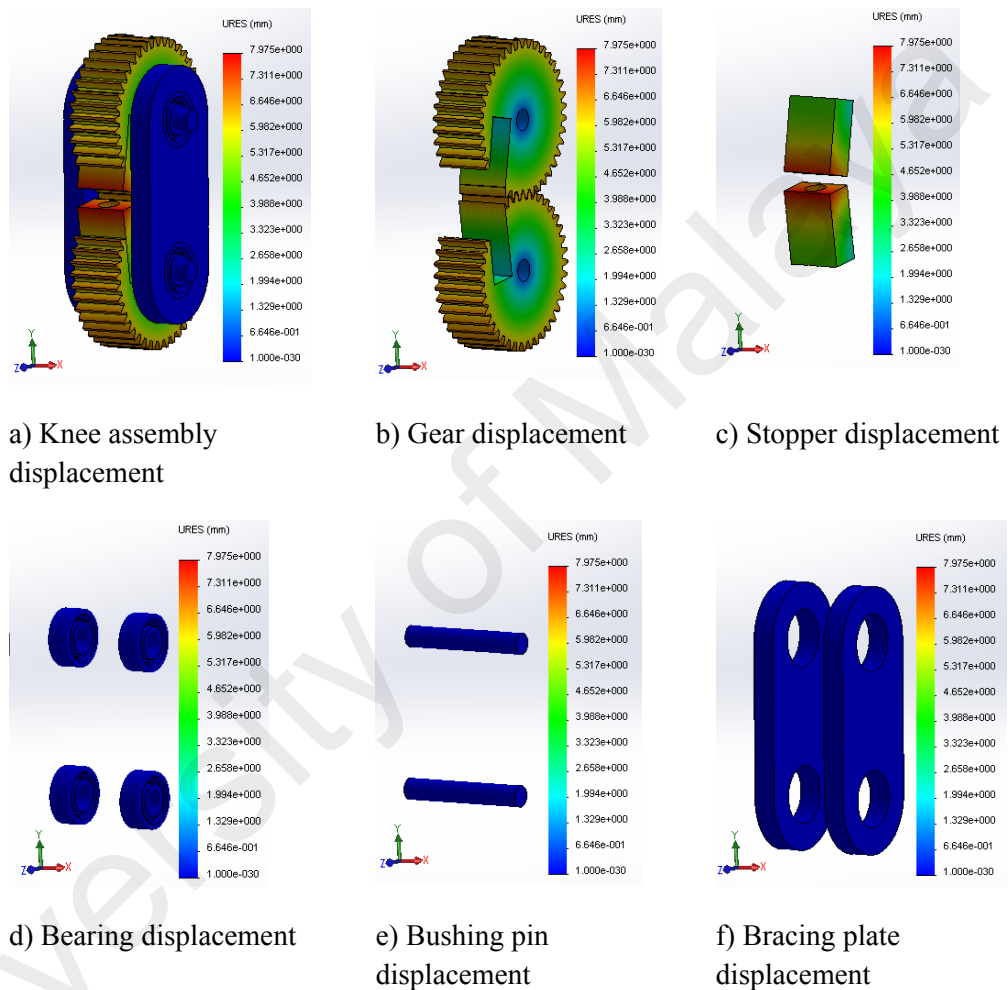


Figure 5.15: Displacement analysis of knee joint components.

From Figure 5.15, the maximum static displacement of aluminum alloy made components was 7.97549 mm occurred in the stopper, which was trivial in magnitude and thus was acceptable. Therefore, the design has complied the condition of stiffness as well.

From the finite-element analysis, the maximum von Mises stress, equivalent strain and displacement of the components occurred during the gait cycle movement of the knee joint were found to remain quite below than the material yield strength, permissible strain and displacement limits respectively. Therefore, the proposed design was safe for the particular application, and no unexpected failure would take place.

5.3.2 Finite element analysis of ankle joint components

The boundary conditions have been calculated and assigned to the different components of the prosthetic ankle joint to develop a *FEA* model. Then the model was meshed, and simulation was run to obtain the stress, strain and displacement values under applied loading conditions.

5.3.2.1 Ankle joint model

Different constraints like connections between the components, component contacts, fixtures and external load have been defined at the first place. The whole ankle assembly is defined as global contact, where the contacts between the shank – sleeve bearing is set as roller sliding contact; sleeve bearing – bushing pin as fixed hinge joint; knuckle – bushing pin as bearing support connection. The connections between the components like shank – knuckle, and upper foot plate – lower foot plates are assigned as spring connection. The inner face of bearing hole of the knuckle frame and the outer face of the ball bearing are defined as bonded contact. The contacts between knuckle and upper foot plate, upper foot plate and spring guide, and lower foot plate and spring holder are defined as fixed geometry. The lower foot plate is set up as fixed geometry

whereas the face between upper foot plate and lower foot plate is defined as a roller slider joint. The maximum displacement was set to the components (shank) at 30 mm. Both the normal force and torque are applied as external load on to the shank tip.

All components of ankle joint are considered to be the solid body. The Aluminum Alloy 1060-H16 is chosen for all ankle joint components except the for ball bearing, sleeve bearing and bushing pin, for which Alloy Steel (SS), Copper Alloy – Brass, and Alloy Steel AISI 4140 are respectively selected. The properties of selected materials are represented in Table C.1.1 of Appendix C.

The key features of *FE* modeling of the ankle joint components are tabulated in Table 5.7.

Table 5.7: Key features of finite element modeling of ankle joint components

Various features of the <i>FE</i> model	
Software used	: SOLIDWORKS
Solver type	: FFEPlus
Mesh type	: Solid Mesh
Mesher Used	: Curvature based mesh
Jacobian points	: 16 Points
Element type	: Triangular (2D)
Maximum element size	: 8.45233 mm
Minimum element size	: 1.69047 mm
Mesh Quality	: High
Remesh failed parts with incompatible mesh	: On
Total Nodes	: 81671
Total Elements	: 45754
Maximum Aspect Ratio	: 33.911

For ankle-foot design, similar load calculation was carried out.

During the normal level ground walking, the subject ankle was found to rotate from -15° to 34° , which has to be imitated by the prosthetic ankle joint. The load applied to the torsional spring was equal to the proportion of amputee weight

shared by the torsional spring during swing phase and flexion and extension movements.

During swing phase of a biological lower limb, the finger joints help to produce desired rotation in the foot. However, as there was no finger joint incorporated in the proposed design, the ankle joint had to yield that movement in the foot arrangement.

The rotation angle varies depending on the mode and speed of walking and also on the type of activities performed. The maximum possible angles of rotation were considered as the design parameter for the torsional spring design. Therefore, the forces applied on the spring at those particular angles were casual and could not consider as dynamic load, and thus should not apply dynamic loading condition during the spring design. The maximum angle of rotation produced by the ankle joint at different phases of the gait cycle is shown in Figure 5.16.

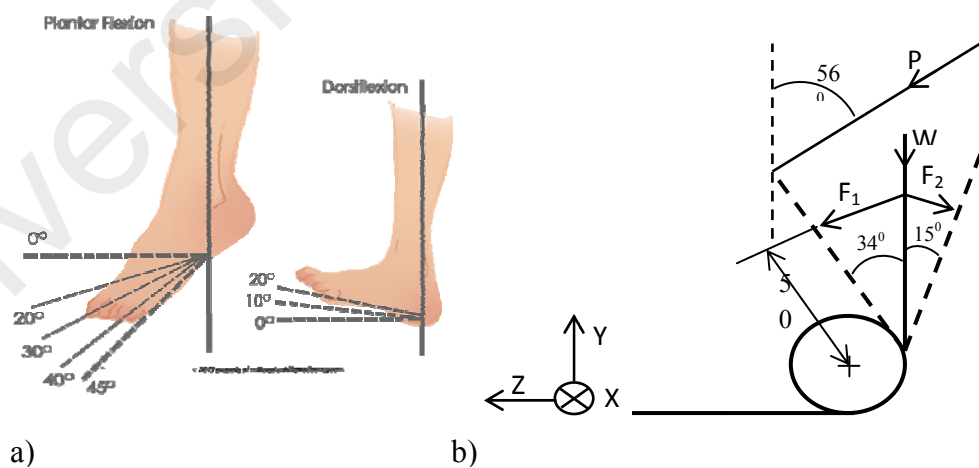


Figure 5.16: The angle of rotation produced by a) the ankle joint, and b) shank of the prosthetic ankle.

During swing phase, no significant rotation occurred at the ankle joint. However, the range of rotation during performing different daily activities is quite large

when both the feet are usually in contact with the ground. In this case, the body weight of amputee (W) is shared by the healthy leg and the prosthesis. The proportion of load shared by the prosthesis, and the unimpaired leg vary based on the rotation ankle. However, for the sake of simplifying the calculation; the load is assumed to be shared equally by the healthy limb and the prosthesis.

Due to the same reason of taking the event of balance losing into consideration, the load is not divided by two.

Therefore, Applied load $F = ma = (69 + 2.5) * 9.81 = 701.4 N =$ weight of the subject + weight of prosthesis component up to ankle joint = resultant weight = W_r

When the shank produces 34° of rotation angle at the ankle joint, a corresponding angle of 56° is produced at the knee joint.

Therefore, the weight component transmitted to the shank from the hip is

$$P_{34deg} = W_r \cos 56 = 701.4 * \cos 56 = 392.0 N$$

When the shank produces -15° of rotation angle at the ankle joint, a corresponding angle of -75° is produced at the knee joint.

Therefore, the weight component transmitted to the shank from the hip is

$$P_{-15deg} = W_r \cos 56 = 701.4 * \cos(-75) = 181.5 N$$

The applied load on the shank rod integrated to the spring arm at 34° clockwise rotation is $F_1 = 392.0 N$

The applied load on the shank rod integrated to the spring arm at 15° anti-clockwise rotation is $F_2 = 181.5 N$

The length of torque arm, $l = \text{length of shank (including spring arm)} = 410 mm$

The torque applied at counterclockwise direction,

$$M_{max} = M_1 = F_1 \times l = 392 \times 0.410 = 160.7 Nm \text{ (anticlockwise)}$$

The torque applied at counterclockwise direction,

$$M_{min} = M_2 = F_2 \times l = 181.5 \times 0.410 = 74.4 \text{ Nm, (clockwise)}$$

$$\text{Total angle of rotation, } \theta = (\theta_1 - \theta_2) = 34^\circ - (-15^\circ) = 49^\circ$$

In simulation, the springs are substituted by setting the connections between the components from the two ends of the spring as spring joint where the spring constant/spring rate is used same as of the replaced spring. Therefore, the spring contacts/spring rates are to be calculated to input in the simulation. This has been done to simplify the simulation and reduce the simulation time.

The spring constant (spring rate/turn) of the torsional spring that chosen for the ankle joint is $k = 152.66 \text{ N.mm/turn}$

Motion analysis of the ankle joint is carried out to see the movements of the ankle-foot assembly and its different components under applied external load. The movements and forces calculated for the ankle-foot system will help to carry out a structural analysis of the ankle components and thus to ensure ankle performance. Two types of analysis are carried out in motion analysis – kinematic analysis and dynamic analysis. Boundary conditions used in the simulation of prosthetic ankle joint are shown in the following Table 5.8.

Table 5.8: Boundary conditions of ankle joint simulation

Constraints	Values	
	at 34° of rotation	at -15° of rotation
Load applied	701.4 N to 392 N	701.4 N to 181.5 N
Moment	0 Nm to 160.7 Nm,	0 Nm to 74.4 Nm
Spring constant	152.66 N.mm/turn	

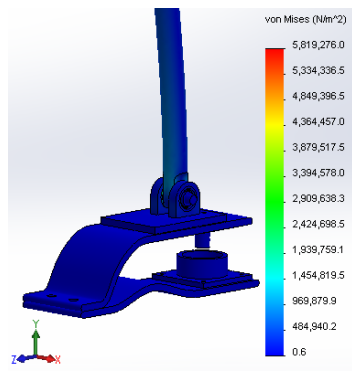
The ankle joint model of Figure 5.17a) shows all the constraints and the external loads applied to the different component, and Figure 5.17b) illustrates the meshing of the ankle components.



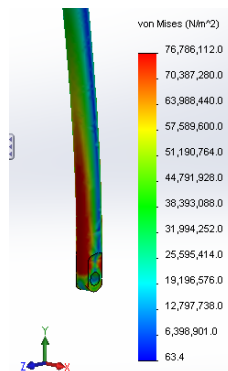
Figure 5.17: a) Model of spring based ankle joint, b) Solid mesh of the model.

5.3.2.2 FEA results of ankle joint components

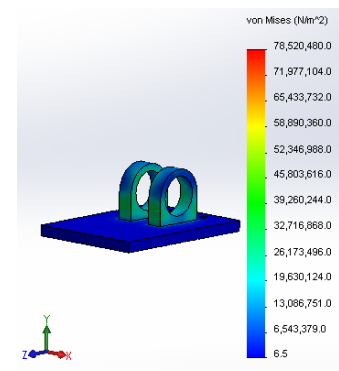
In the finite-element analysis, the stress, strain and displacement of the ankle joint components were studied to check the viability of the design. The von Mises stress of different ankle components found from the finite element analysis are shown in Figure 5.18.



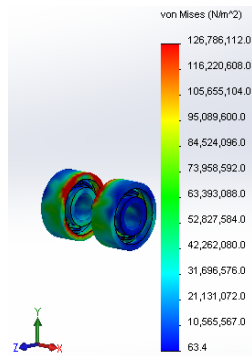
a) Ankle assembly stress



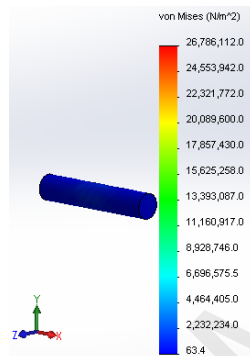
b) Shank stress



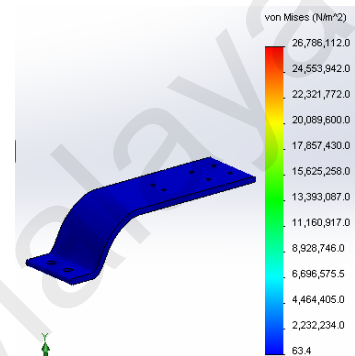
c) Knuckle stress



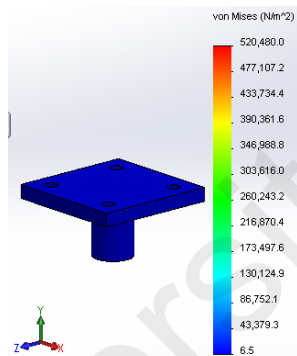
d) Bearing stress



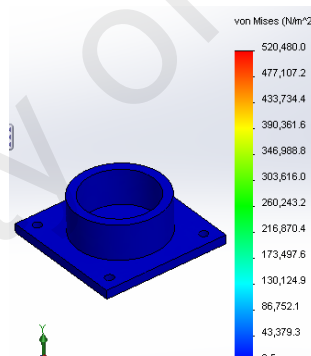
e) Bushing pin stress



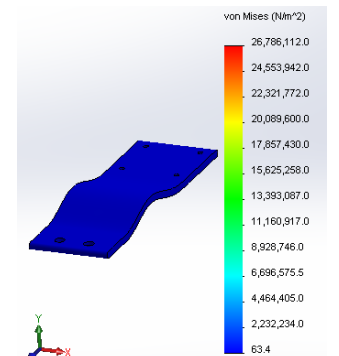
f) Upper foot plate stress



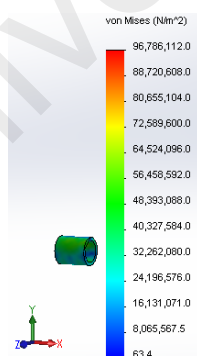
g) Spring guide stress



h) Spring holder stress



i) Lower foot plate stress



j) Sleeve bearing stress

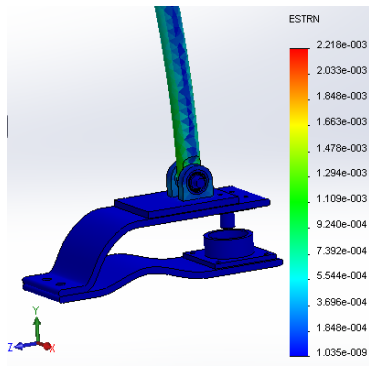
Figure 5.18: von Mises stress of different components of ankle joint.

From stress analysis (Figure 5.18), the maximum von Mises stress value of 126.79 MPa was obtained in ball bearing, which did not exceed the *PEEK* material yield strength of 620.42 MPa (according to material properties of Alloy steel (*SS*)). The factor of safety for shank rod was $620.42/126.79 = 4.9$, which was sufficient to ensure the safety of components. Therefore, no plastic deformation of the ankle joint components occurred, and the condition of plastic stability was conformed.

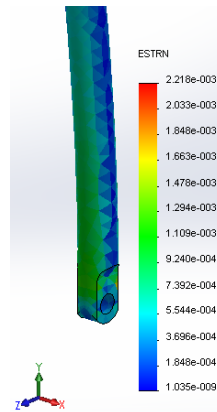
The main focus of work was to design an ankle joint *FE* model and to confirm its functionality; for this purpose, the Solidworks software was used. The model was validated using the gait cycle data obtained from the healthy subject.

The equivalent strain or the von Mises equivalent strain is another important factor for the design and is often used to describe the state of strain in the design components.

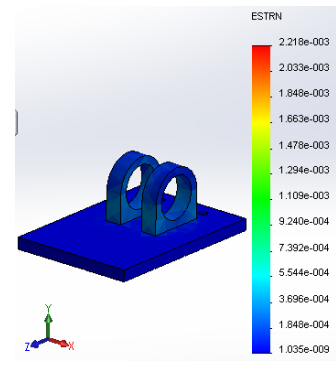
The equivalent strains of different components of ankle joint are shown in Figure 5.19.



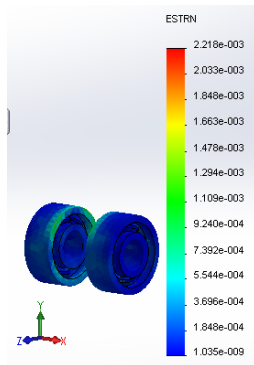
a) Ankle assembly strain



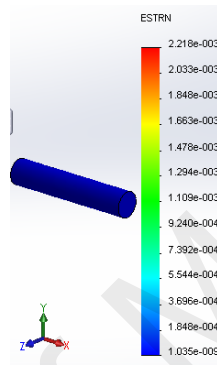
b) Shank strain



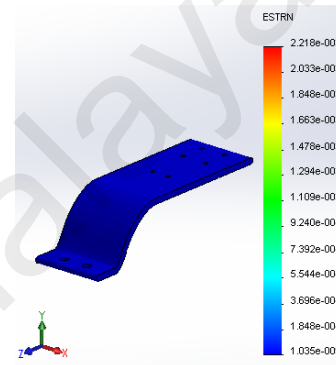
c) Knuckle strain



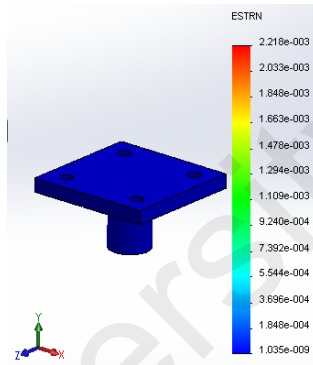
d) Bearing strain



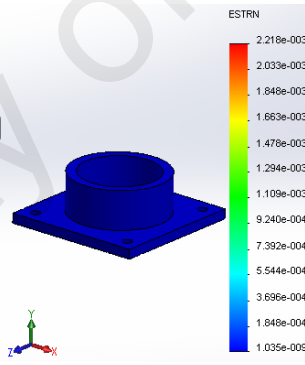
e) Bushing pin strain



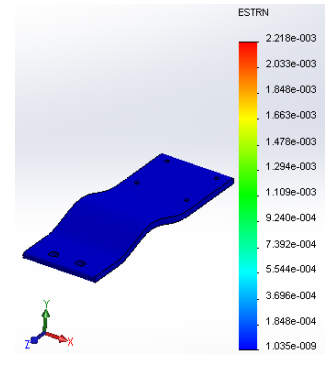
f) Upper foot plate strain



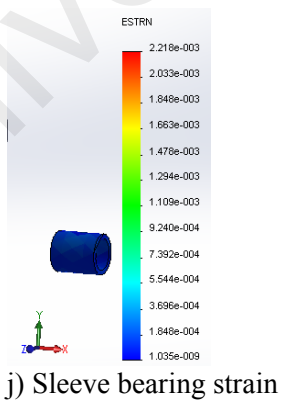
g) Spring guide strain



h) Spring holder strain



i) Lower foot plate strain



j) Sleeve bearing strain

Figure 5.19: Strain analysis of ankle joint components.

From the equivalent strain analysis (Figure 5.19), it was obvious that the maximum strain of $2.218e-003$ was occurred in the ball bearing. The value of maximum strain occurred in the ankle components were insignificant to be appeared as distortion to the shape of component and therefore, could be neglected. Hence the components of the ankle joint have met the condition of rigidity.

The static displacement analysis was carried out to assess the displacement and reaction force results for static, nonlinear, dynamic, drop test studies, or mode shapes for buckling and frequency studies.

The results of static displacement studies are shown in following Figure 5.20

University of Malaya

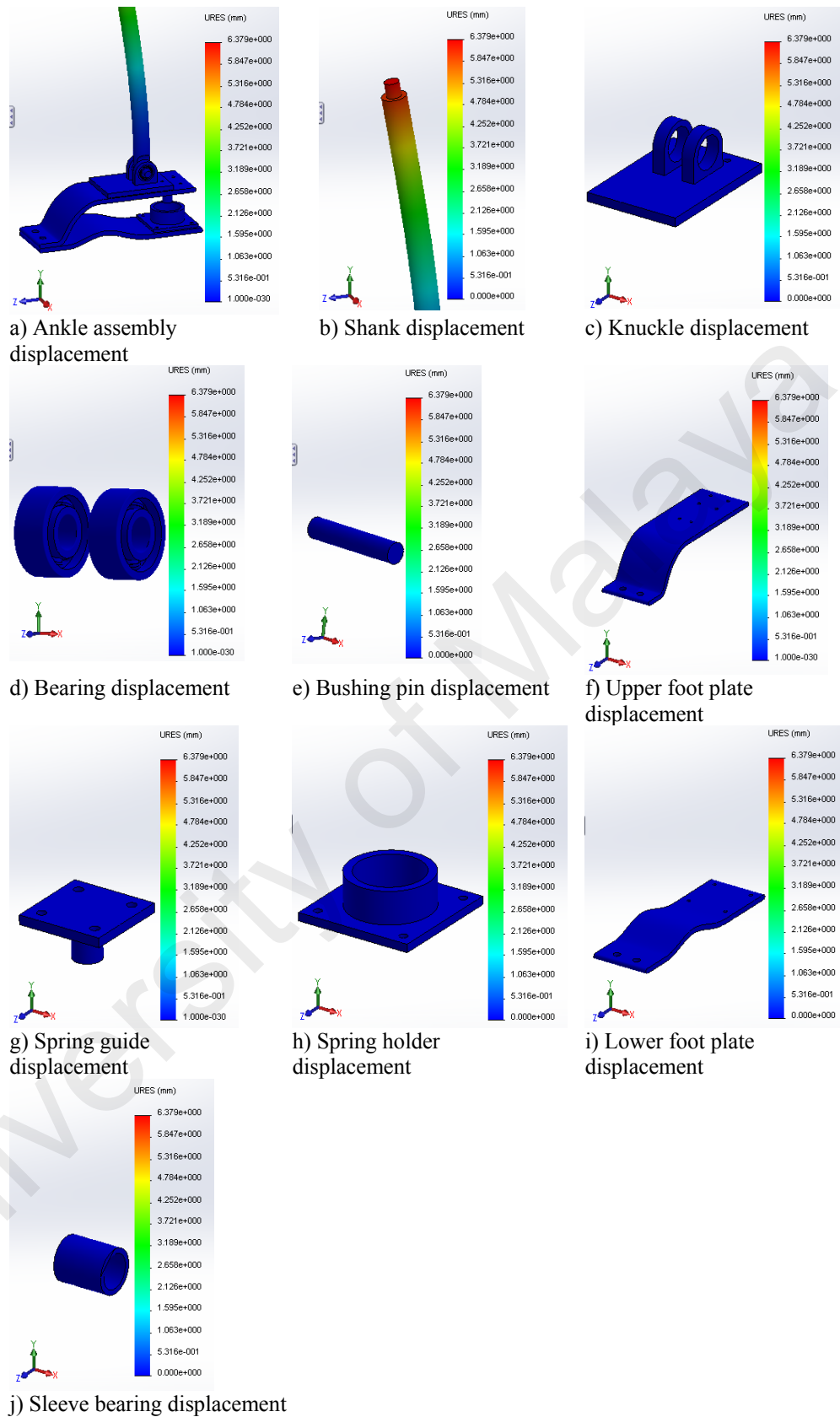


Figure 5.20: Displacement analysis of ankle joint components.

From Figure 5.20, the maximum static displacement of 6.37870026 mm was occurred in the shank rod. For the ankle components, the maximum displacement values were considerably lower than the maximum allowable displacement by the material used for making the components. Therefore, the design has complied the condition of stiffness as well.

In addition to this, the elastic property of the spring materials helped the ankle – foot arrangement to store and return energy during the gait cycle. Since the springs in the ankle – foot arrangement has been substituted with some spring constants of the same value; the *FEA* of the springs was not performed in the simulation. The finite-element analysis results of other ankle joint components were obtained for the equivalent spring constant and for the spring life of 10^6 cycles. The entire results for the ankle joint components obtained from the *FEA* showed that the components were safe. The life cycle used in the simulation was quite big, which indicated the springs were good enough to store and return energy effectively for long without experiencing any fatigue failure.

From the finite-element analysis, the maximum von Mises stress, equivalent strain and displacement of the components occurred during the gait cycle movement of the ankle joint were found to remain quiet below than the material yield strength, permissible strain and displacement limits respectively. Therefore, the proposed design was safe for the particular application, and no unexpected failure would take place.

5.4 Simulation results of the prosthesis joints

Motion analysis of the different prosthetic joints has been performed to predict the performance of the designed lower limb prosthesis. The knee joint and the ankle–foot complex play the most important role in human locomotion. Both the kinematic and

kinetic analyses of the prosthetic knee joint and ankle-foot arrangement were conducted to evaluate the performance of the designed prosthesis.

Motion analysis of the ankle joint was carried out to see the movements of the ankle-foot assembly and its different components under applied external load. The movements and forces calculated for the ankle-foot system would help to carry out a structural analysis of the ankle components and thus to ensure ankle performance. Two types of analysis were carried out in motion analysis – kinematic analysis and kinetic analysis.

5.4.1 Results of kinematic analysis

The angular displacement, angular velocity and angular acceleration of the gears of the knee joint were simulated for the possible movements of the joint during the gait cycle. This was done to predict the performance of the designed prosthetic knee joint. For knee joint, the simulation was carried out for 0° to 70° of gear rotation. Boundary conditions used in the simulation of prosthetic knee joint are shown in the following Table 5.9.

Table 5.9: Boundary conditions of knee joint simulation

Constraints	Values
Motor rotation	Oscillating
Frequency	0.5 Hz
Angle of rotation by each gear	$0^{\circ} \sim 7.5^{\circ}$, and $0^{\circ} \sim 35^{\circ}$

The angular displacements of the gears at different phases of the gait cycle are shown in Figure 5.21.

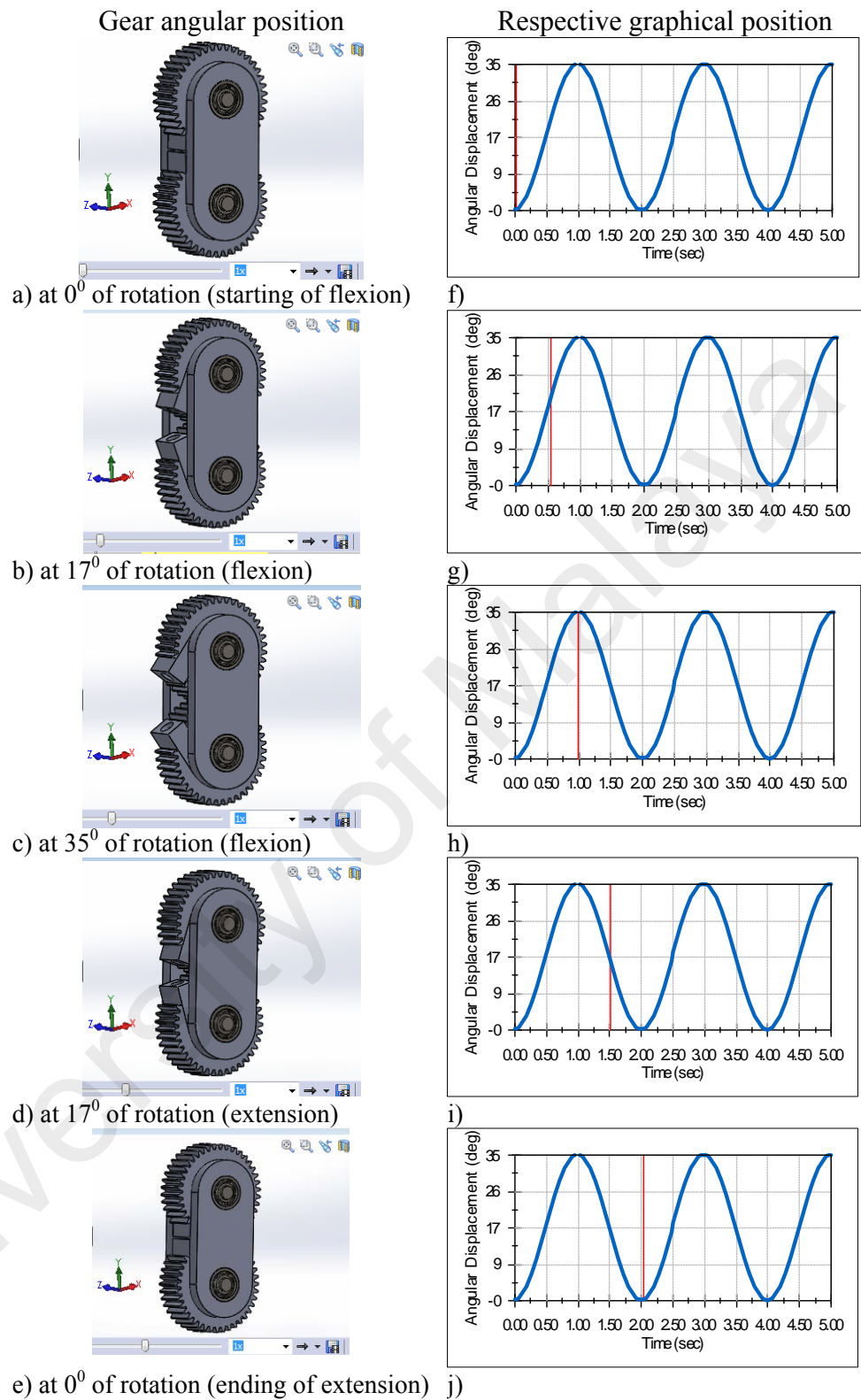


Figure 5.21: Angular displacement of gears at different phases of gait cycle.

From Figure 5.21, the angular position of the gear at standing position was 0° , which gradually changed to 70° when walking at the level ground. From Figure

5.21, the gait cycle started from Figure 5.21a and continued until Figure 5.21e, when some angular rotation was observed in the gear assembly of the knee joint. All these angular displacements are represented as the graph in the same figure from Figure 5.21g to 5.21j. The different phases of gait cycle could be identified from the graphs of Figure 5.21g – 5.21j.

The angular displacement, angular velocity, and angular acceleration of different ankle joint components under applied force and torque have been simulated for expected angle of rotation during level ground walking. For ankle joint, the simulations were carried out once for 0° to 34° shank rotation, and again for 0° to -15° of shank rotation. Two types of analysis were carried out in motion analysis – kinematic analysis and kinetic analysis.

Boundary conditions used in the simulation of prosthetic ankle joint are shown in following Table 5.10.

Table 5.10: Boundary conditions of ankle joint simulation

Constraints	Values
Motor rotation	Oscillating
Frequency	0.5 Hz
Angle of rotation	$0^{\circ} \sim -15^{\circ}$, and $0^{\circ} \sim 34^{\circ}$

The angular displacement of the ankle joint at different phases of gait cycle is shown in Figure 5.22 and Figure 5.23.

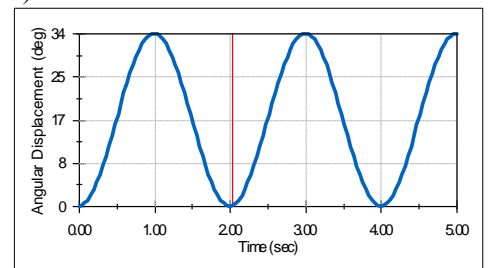
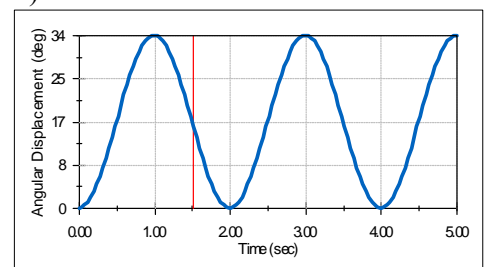
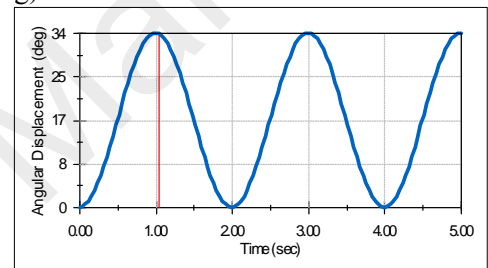
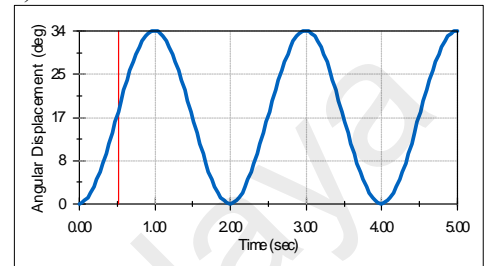
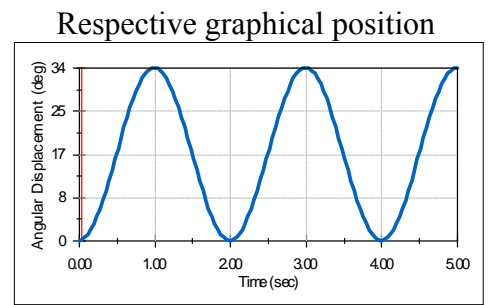
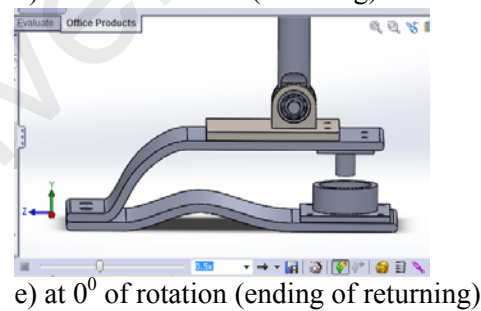
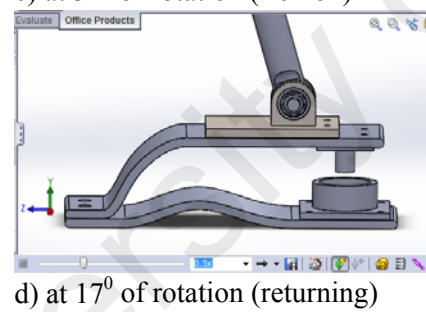
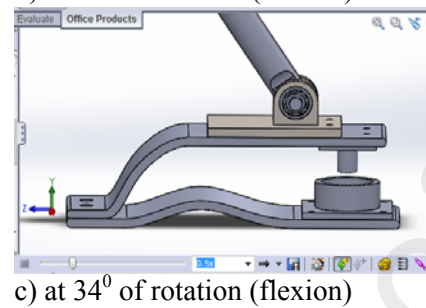
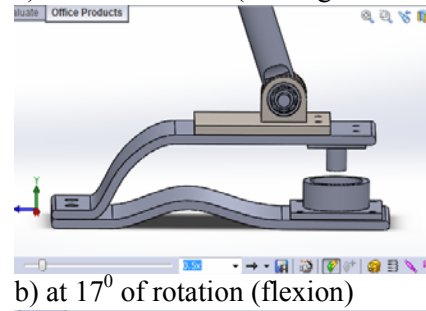
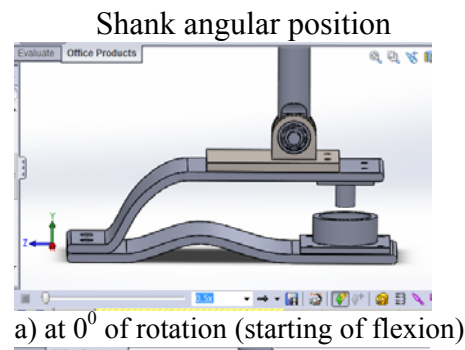


Figure 5.22: Angular displacement of shank during flexion of ankle joint.

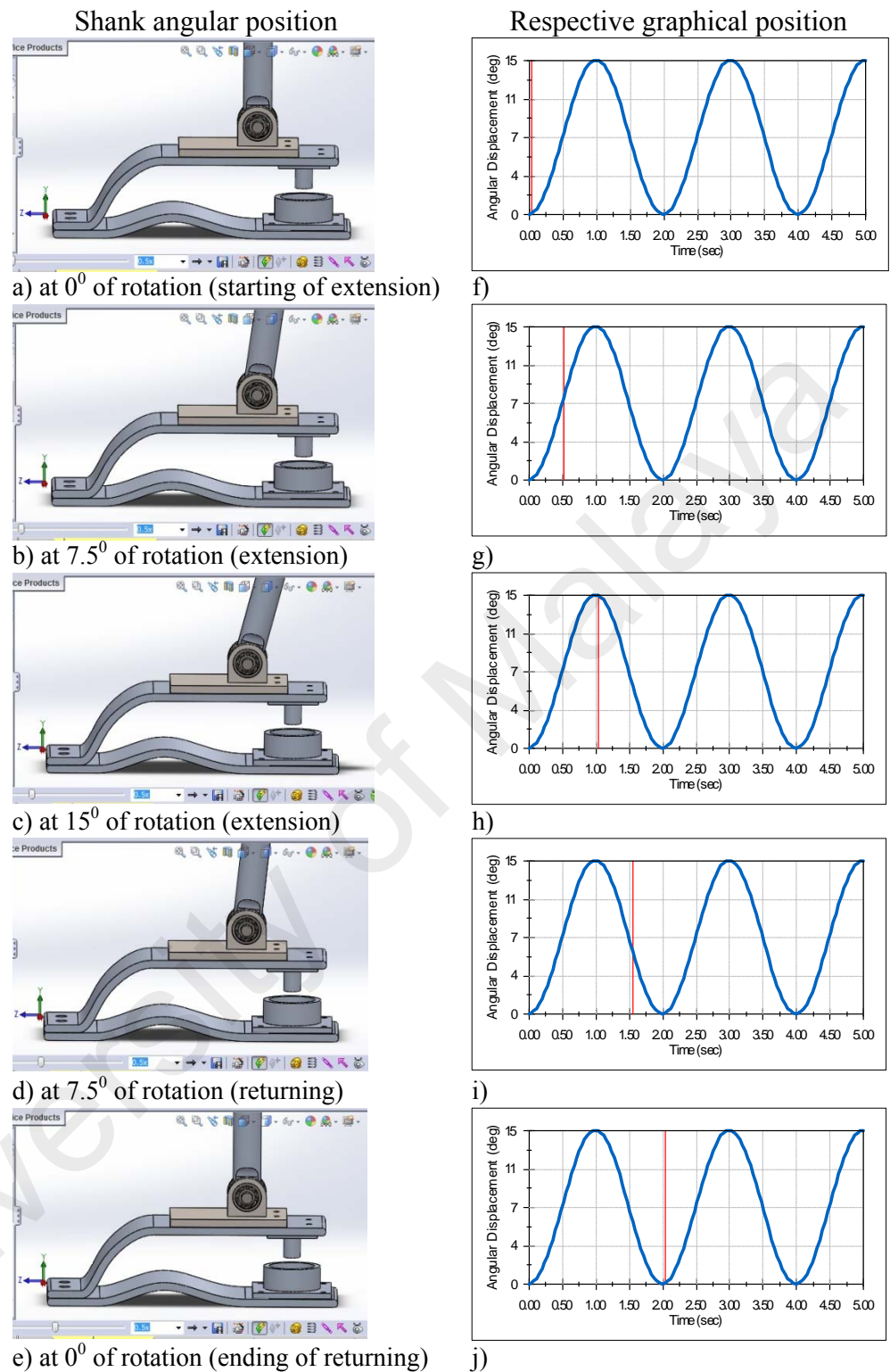
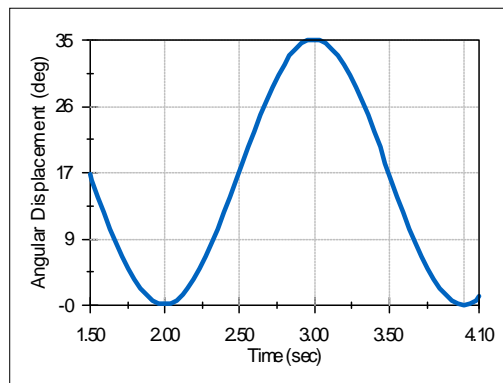


Figure 5.23: Angular displacement of shank during extension of ankle joint.

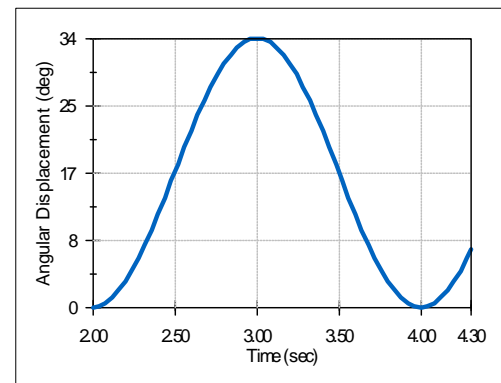
From Figure 5.22 and Figure 5.23, the angular position of the shank was 0° when standing, which varied between 34° and -15° at different phase of the gait cycle. Figure 5.22a – 5.22e shows the different angular position of the shank

while producing angular displacement from 0° to 34° . The corresponding angular displacements are represented in the plot of the same figure from Figure 5.22g – 5.22j. Figure 5.23a – 5.23e show the different angular position of the shank while producing angular displacement from 0° to -15° . The corresponding angular displacements are represented in the plot of the same figure from Figure 5.23g – 5.23j. From Figure 5.22g – 5.22j and Figure 5.23g – 5.23j, the patterns of the angular displacement graphs were quite similar; therefore, any of these angular displacement graphs can be compared with the ankle joint graph obtained from the healthy subject.

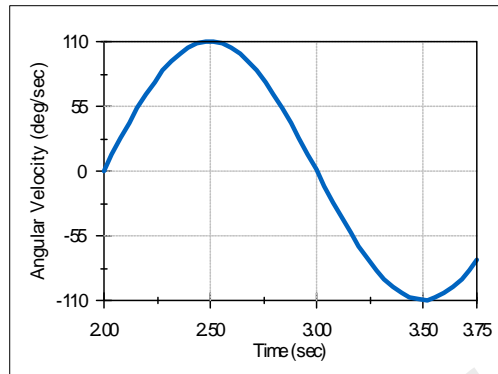
The results of prosthetic knee and ankle joints simulation are shown in following Figure 5.24.



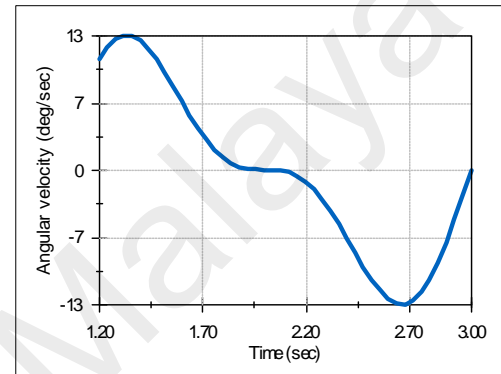
a) Knee angular displacement



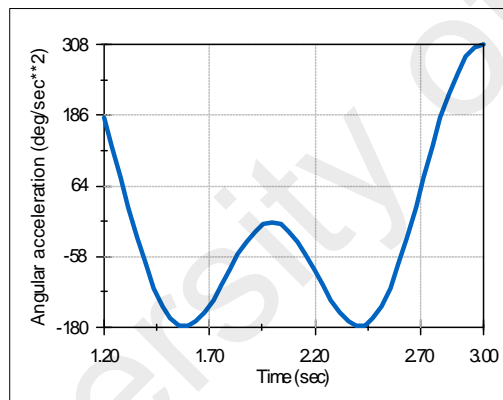
b) Ankle angular displacement



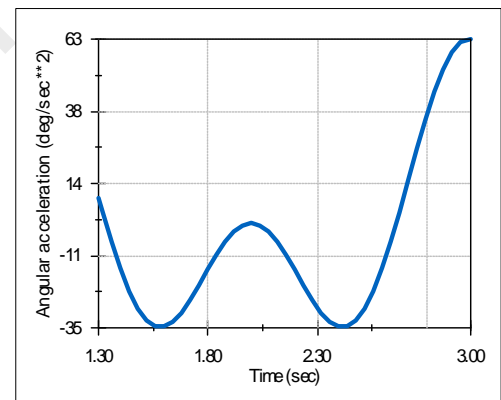
c) Knee angular velocity



d) Ankle angular velocity



e) Knee angular acceleration



f) Ankle angular acceleration

Figure 5.24: Angular displacement, velocity and acceleration of the prosthetic knee and ankle joints.

Figure 5.24a represents the angular displacement of the gears of the prosthetic knee joint, and Figure 5.24b shows the angular displacement of the prosthetic ankle joint. Figure 5.24c and Figure 5.24d, illustrates the changes of angular velocities of the prosthetic knee and ankle joints. Figure 5.24e and Figure 5.24f shows the variation of angular acceleration of the prosthetic knee and ankle

joints. From Figure 5.24a and Figure 5.24b and Figure 5.1c and Figure 5.1e, the pattern of changing the angular positions of the prosthetic knee and ankle joints were quite similar to the pattern of the respective gait cycle graphs of the healthy knee and ankle joints. Though, the angles of rotation were not same, the patterns of the graphs were observed to be identical. This was because of the angle of rotation varied based on walking speed, stepping length/stride length, etc.; however, they still maintained a similar trend throughout the swing phase. Therefore, it can be deduced that the proposed gear based knee joint is capable of reproducing the movement of a healthy biological knee and ankle joints effectively.

Figure 5.24c and Figure 5.24d and Figure 5.3c and Figure 5.3e shows the similarity or dissimilarity between the patterns of angular velocity graphs of prosthetic gear and ankle joints obtained from the simulation, and those recorded from the healthy subject. The graph of Figure 5.24c and Figure 5.24d were obtained from the motion analysis data whereas Figure 5.3c and Figure 5.3e were plotted based on the real data recorded from the healthy subject. From the figures, the pattern of the angular velocity graphs of the prosthetic knee joint (Figure 5.24c) and ankle joint (Figure 5.24d) were similar to the pattern of the angular velocity graphs of Figure 5.3c and Figure 5.3e respectively. Though the exact values of both the graphs were not same, their patterns had quite similarity. Both the graphs were dynamic; however, there were some phase differences, which could be attributed to the fact of different rates of walking speed. Since, the similar velocity wasn't maintained during simulation and subject's walking, there was some phase difference between the angular velocity graphs obtained from real data and from the motion analysis. Besides, there were some disturbances noticed in the sinusoidal pattern of the angular velocity

graphs captured from the healthy individual, which was not evident on the simulation results. It could be attributed to the fact that in simulation, the loads applied were steady and uniform whereas in real limb joints it was impractical.

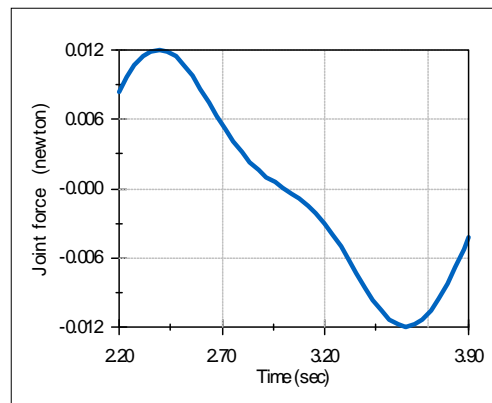
Figure 5.24e and Figure 5.24f, and Figure 5.5c and Figure 5.5e shows the difference between the patterns of angular acceleration graphs of prosthetic gear and ankle joints obtained from the simulation and those from the healthy subject. The graph of Figure 5.24e and Figure 5.24f were plotted based on the motion analysis data whereas Figure 5.5c and Figure 5.5e were obtained from the healthy subject.

From the figures, the pattern of the angular acceleration graphs of the prosthetic knee joint (Figure 5.24e) and ankle joint (Figure 5.24f) were similar to the pattern of the angular acceleration graphs of Figure 5.5c and Figure 5.5e. Though, both signals were dynamic in nature and had similarity in pattern, they exact shape and amplitude did not match. There was some disturbance in the sinusoidal pattern of the healthy knee and ankle joints graphs, which was not seen in the graphs obtained from the simulation results. It was due to the deflection of the boundary conditions used in the simulation from that of real biological knee and ankle joint biomechanics. Since the gait cycle data were captured when walking on the plain ground instead of treadmill, a particular walking speed, thus certain acceleration could not maintain. However, in simulation, steady load was applied to simplify the calculation which was impractical in real application. Therefore, there was some phase difference between the acceleration graphs obtained from real data and from the motion analysis.

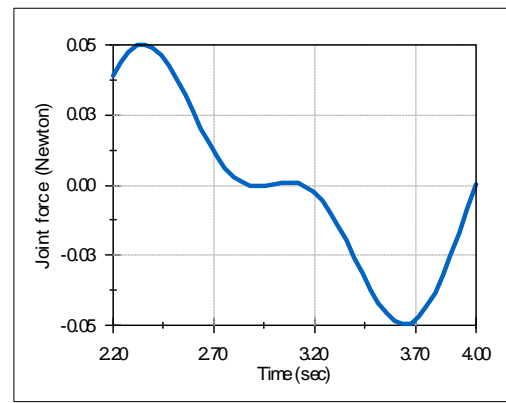
5.4.2 Results of kinetic analysis

The forces involved with the movement of the components are evaluated by the kinetic analysis. The joint force, joint moment, and joint power are the important factors to be investigated in the kinetic analysis of the knee joint. The joint force, joint moment, and joint power graphs plotted with the real data (recorded from the healthy subject) were compared with the joint force, reaction moment and joint power curves (obtained from the motion analysis of the prosthetic knee and ankle joints). The performance of the prosthetic knee and ankle joints has been predicted from that comparative study.

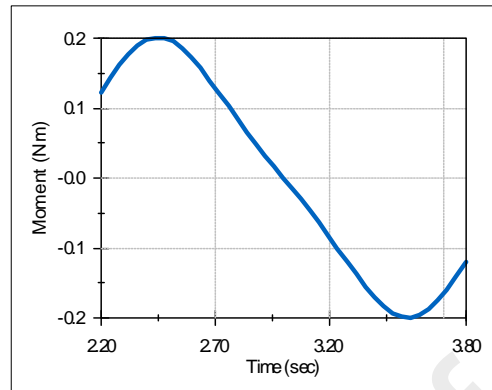
University of Malaya



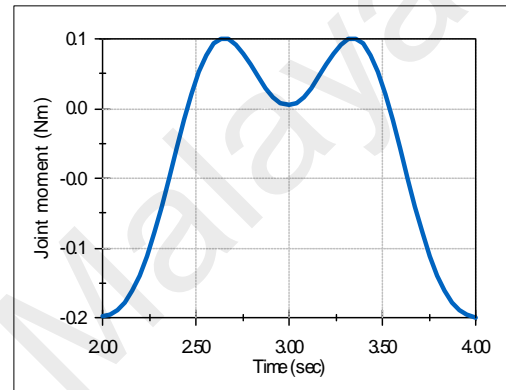
a) Knee joint force



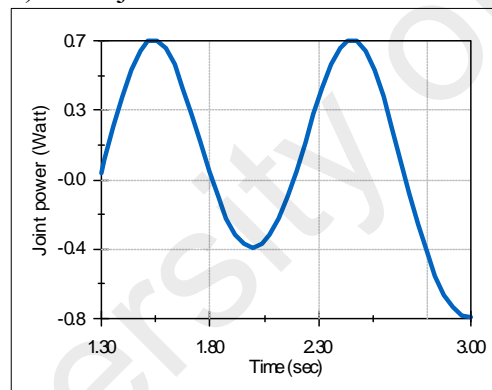
b) Ankle joint force



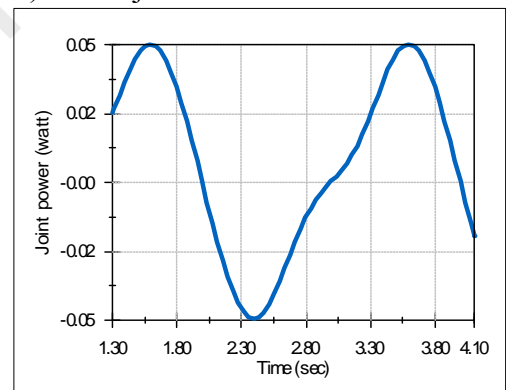
c) Knee joint moment



d) Ankle joint moment



e) Knee joint power



f) Ankle joint power

Figure 5.25: Joint force, joint moment and joint power of the prosthetic knee and ankle joints.

Figure 5.25a and Figure 5.25b show the fluctuation of joint force in the prosthetic knee and ankle joints respectively during the gait cycle. The curves were plotted based on the simulation data, which were compared with the respective joint force profiles obtained from the healthy subject of Figure 5.7c and Figure 5.7e. Figure 5.25c and Figure 5.25d illustrate the changes in the

prosthetic knee and ankle joints reaction moments, which were correlated with the corresponding joint moment graphs of Figure 5.9c and Figure 5.9e. Figure 5.24e and Figure 5.24f depict the variation in the knee and ankle joints power, which were also evaluated with respect to the corresponding joint power curves obtained from the healthy subject of Figure 5.11c and Figure 5.11e.

From Figure 5.24a and 5.24b, the pattern of the knee and ankle joint force curves were dynamic type; however, nature of this graph had great resemblance to the joint force profiles obtained from the healthy knee and ankle joints of Figure 5.7c and Figure 5.7e respectively. Though, the magnitude of variation was not exactly same, the trend of the joint force graph obtained from simulation and from the healthy individual was similar. There was some disturbance on the pure sinusoidal profiles of the knee and ankle joints force, which was not evident on the joint force curves obtained from the simulation. The graphs obtained from the simulation were rather symmetric.

This disturbance could be attributed to the fact that during simulation, a particular load was applied to the simulation, and the boundary condition was maintained in the system, which was impractical for real gait cycle analysis. As the subject was walking on the plain ground instead of walking on the treadmill, a certain speed of walking could not maintain. Therefore, there was some deflection between the joint force graphs from simulation and real gait analysis.

From Figure 5.24c and Figure 5.24d, and Figure 5.9c and Figure 5.9e, the pattern of the joint moment curves obtained from the simulation had great similarity to that of healthy knee and ankle joint moment graphs. Though, the magnitude and the shape of the graphs were not exactly same, their trend of fluctuation largely resembled each other. The similar justification that made for joint force profiles can be made for the joint moment curves also.

From Figure 5.24e and Figure 5.24f, and Figure 5.11c and Figure 5.11e, the joint power curves were dynamic in nature. From the figures, the joint power at the different points of gait cycle varied both in positive and negative directions. The positive amplitude of the power graph represented the power generation by the knee joint whereas the negative amplitude showed the power absorption by the joint. The patterns of the joint power curve obtained from the kinetic analysis of the prosthetic knee and ankle joints were found to have a similar trend like that of healthy knee and ankle joints. Though, the magnitude of the joint power was not same, the pattern of the knee and ankle power curve of Figure 5.24e and Figure 5.24f were similar to the pattern of the joint power curves of Figure 5.11c and Figure 5.11e of healthy joints. Due to the differences between the boundary conditions used for collecting data from the subject and simulation, there was some phase difference in the graphs. There was some disturbance in the joint power curves of healthy knee and ankle joints, whereas the joint power graphs from the simulation had a quite periodical pattern. However, they were found to maintain a similar trend throughout the gait cycle.

5.5 Gait analysis of lower limb prosthesis

In the prosthesis arrangement, the knee and ankle are two main joints where rotations are created and thus enable the prosthesis to accomplish the gait cycle. The mechanics of prosthetic knee and ankle joints plays the most important role in lower limb locomotion. The efficiency of the prosthesis depends on how much the prosthetic joints can assimilate the biomechanics of a corresponding healthy biological limb. Both the stance and swing phases of walking involve an intricate dynamical behavior of the lower limbs and its interaction with the floor. A motion analysis of the hip, knee and ankle joints when using prosthesis (able-body subject was used to capture the gait

analysis data) would allow one to look into the ability of a shank in following residual limb movement during gait cycle. This could evaluate the prosthesis capacity of imitating the gait cycle of a healthy limb. The data recorded during the gait analysis of the able-body subject with prosthesis are presented in following Table 5.11.

Table 5.11: Gait analysis data from normal speed walking of subject with prosthesis

ANALYSIS				
Subject	Context	Name	Value	Units
With prosthesis	Right	Cadence	45.62736	steps/min
With prosthesis	Right	Walking Speed	0.19605	m/s
With prosthesis	Right	Stride Time	2.63	s
With prosthesis	Right	Foot Off	88.98305	%
With prosthesis	Right	Stride Length	0.515611	m
With prosthesis	Left	Cadence	48	steps/min
With prosthesis	Left	Walking Speed	0.19579	m/s
With prosthesis	Left	Stride Time	2.5	s
With prosthesis	left	Foot Off	88.99975	%
With prosthesis	Left	Stride Length	0.489476	m

The cadence, walking speed, stride time, foot off, stride length, etc. for both the left and right lower limbs are tabulated in Table 5.11. From the data, there are some differences between the data obtained from left and right limbs for a particular type of parameter and also some deviation from the data captured without prosthesis. According to the gait data, the cadence of right leg was lower than that of left leg; however, the walking speed was almost same for the both legs. The stride length and stride times of right leg were found to be a little greater than that of left leg. The proportion of left foot off is observed to be almost similar to that of right foot off. Table 5.12 represents the different events in gait cycle of lower limb prosthesis while walking at normal speed.

Table 5.12: Real events involved in prosthesis gait during normal speed walking

EVENTS				
Subject	Context	Name	Time (s)	Description
With prosthesis	Left	Heel Strike	2.48	The instant the heel strikes the ground
With prosthesis	Left	Toe Off	7.26	The instant the toe leaves the ground
With prosthesis	Right	Heel Strike	3.33	The instant the heel strikes the ground
With prosthesis	Right	Toe Off	6.10	The instant the toe leaves the ground

The time elapsed for the events of foot strike and foot off by left prosthetic foot and the right healthy foot during normal speed walking are shown in Table 5.12. From the data, the lengths of time for these events are not identical for both limbs. A mixed nature is observed in the elapsed time length for different events performed by left prosthetic leg and right natural leg while walking.

Besides these, the angular displacement, the forces, moments and power of the limb joints and segments are also recorded to analyze the gait cycle of the prosthetic lower limb. Two types of data were also obtained from the motion analysis of the prosthetic lower limb. One type of data described the angular displacement, velocity and acceleration of the prosthesis joints and components whereas the other type of data illustrated the force, moment and power of the same entities. All these data fall under the categories of kinematic and kinetic data.

5.5.1 Kinematic analysis

The kinematic analysis includes information about the linear and angular position, velocity and acceleration of the prosthesis joints and components during the gait cycle.

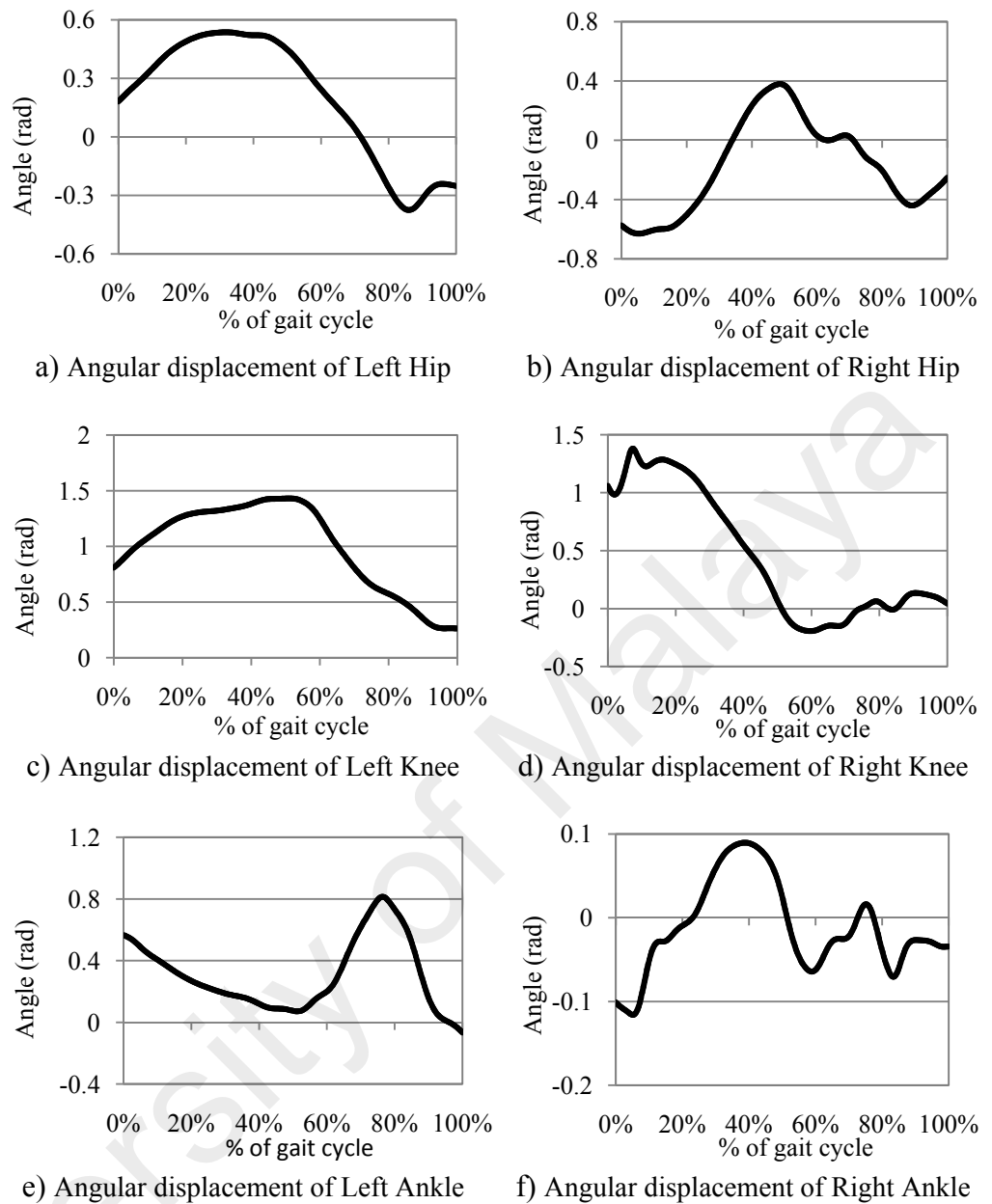


Figure 5.26: The angular displacement of the prosthetic joints.

Figure 5.26 a – Figure 5.26f shows the angular displacement of hip, knee and ankle joints of left and right legs throughout the gait cycle. From Figure 5.26a and Figure 5.26b, though both the angular displacement graphs of left and right hip joints were dynamic in nature, they were different in pattern and amplitude. Similar observation was made for the graphs from the healthy lower limbs. The maximum amplitude of the left hip angular displacement was little higher than

that of right hip. According to Figure 5.26c and Figure 5.26d, despite the angular displacement curve of left knee joint was different in shape than that of the right knee joint, the trend of changing the angular displacement had still similarity. The range of magnitude variation for left knee joint was slightly higher than that of the right knee joint. The angular displacement graph of the left and right ankle joints (Figure 5.26e and Figure 5.26f) shows a remarkable disparity between them. The patterns of the curves were different; the magnitude of the left ankle angular displacement was considerably higher than that of right ankle angular displacement.

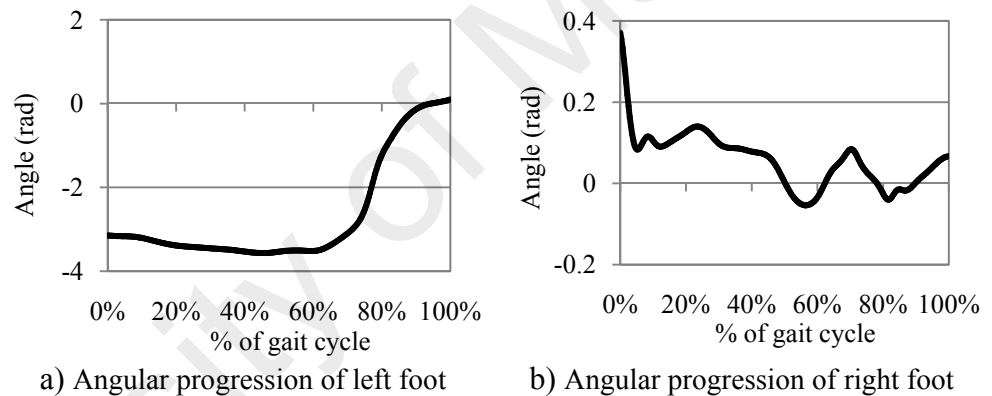


Figure 5.27: Angular progression of foot.

Figure 5.27 represents the angular progression of left and right feet while walking at normal speed. The angular progression of left and right feet was different in shape and magnitude. For left foot, the magnitude was times higher than that of right foot.

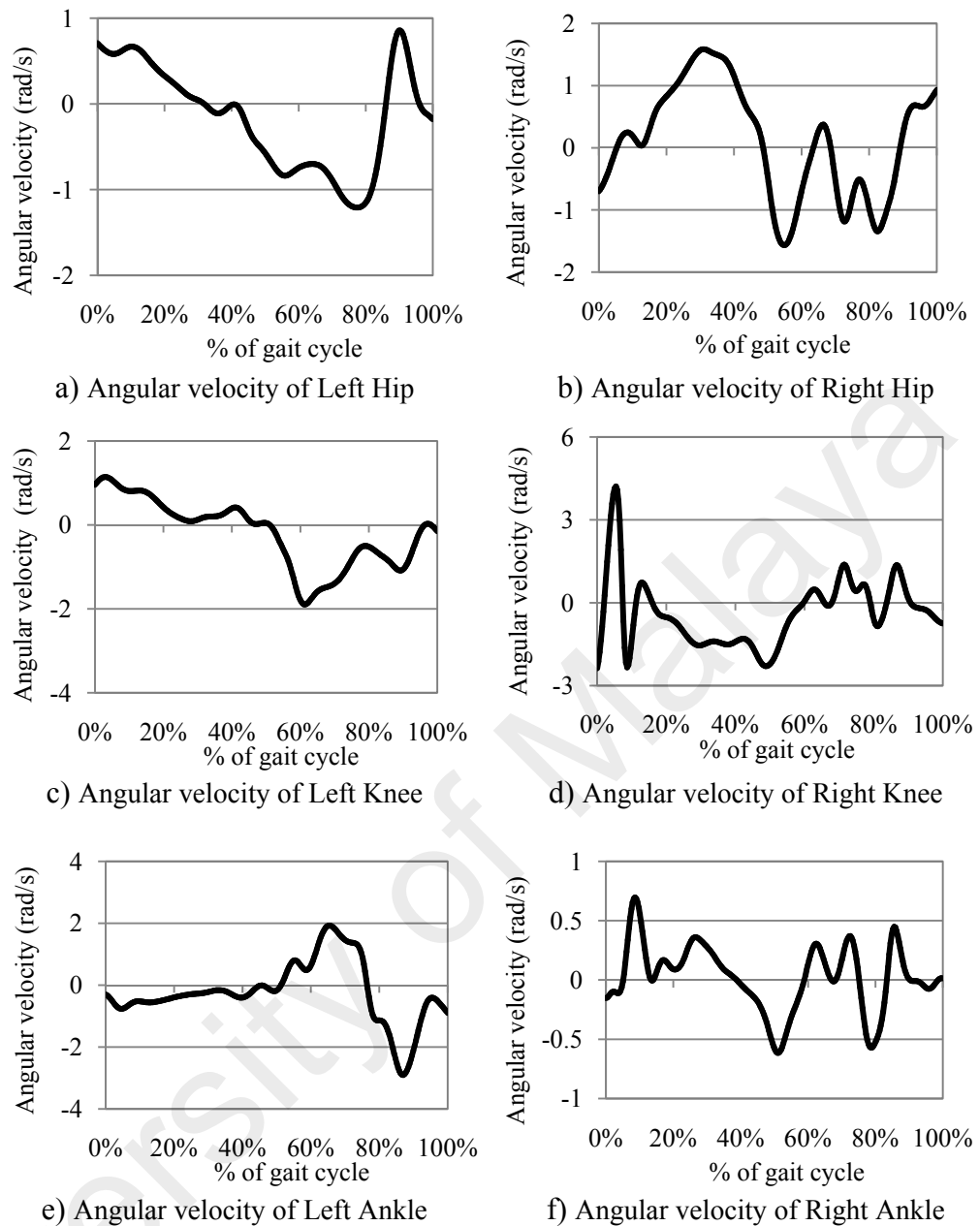


Figure 5.28: Angular velocity of lower limb joints during walking at normal speed.

Figure 5.28 illustrates the variation in the velocity of left leg and right leg joints. From Figure 5.28a and Figure 5.28b, the angular velocity graphs of the left hip differ in shape and magnitude from that of right foot while using prosthesis. The magnitude of angular velocity and its fluctuation of left hip were lower than the right hip velocity and its fluctuation. It was because of the left hip instrumented with prosthesis has maintained almost a steady velocity until changing from one

phase to another phase of gait cycle. During the transition, the right hip had to change velocity to compensate the limitation of the left hip incurred from the prosthesis arrangement.

From Figure 5.28c and Figure 5.28d, the amplitude of angular velocity graphs of left and right knees were similar throughout the entire gait cycle except the beginning of the cycle. Then the right knee velocity had a sudden high velocity, which was unlike to the left knee velocity graph. The shapes were also little different, however, both of them fluctuated about the mean value of zero for the whole cycle.

From Figure 5.28e and Figure 5.28f, the fluctuation of the left ankle velocity varied from the right ankle velocity. Though, the magnitudes of the left and right ankle velocity graphs were different, the pattern of these had some similarity except the starting part. There were some variation noticed in the velocity pattern at the first half of the cycle, however at last half of the gait cycle, the velocity has changed following a similar pattern.

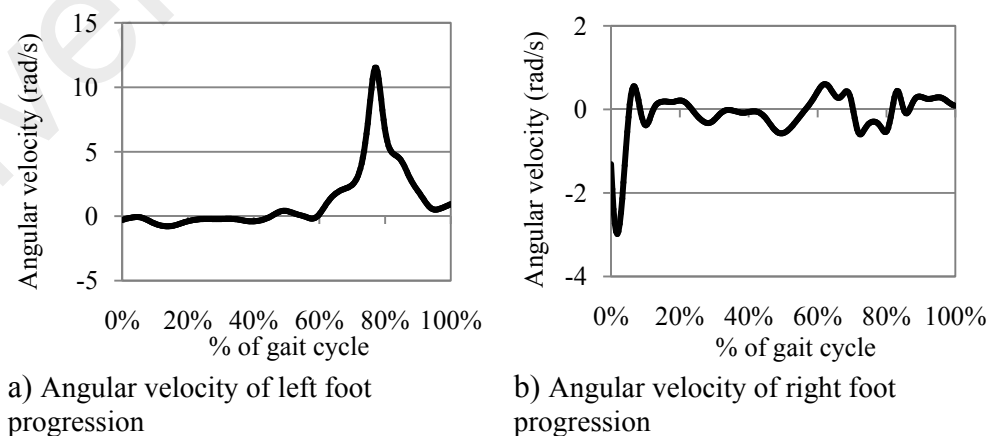


Figure 5.29: Angular velocity of foot progression during walking at normal speed.

Figure 5.29 shows angular velocity of foot progression for left and right feet during the gait cycle. From the figure, the angular velocities of left foot and right foot progression were not much different in shape except a spike at some 80% of left foot gait cycle and at the beginning of the right foot gait cycle. The amplitude varies slightly about the mean value of zero in the remaining cycle for the both foot. However, the velocity spike went times higher for left foot than that of the right foot.

University of Malaya

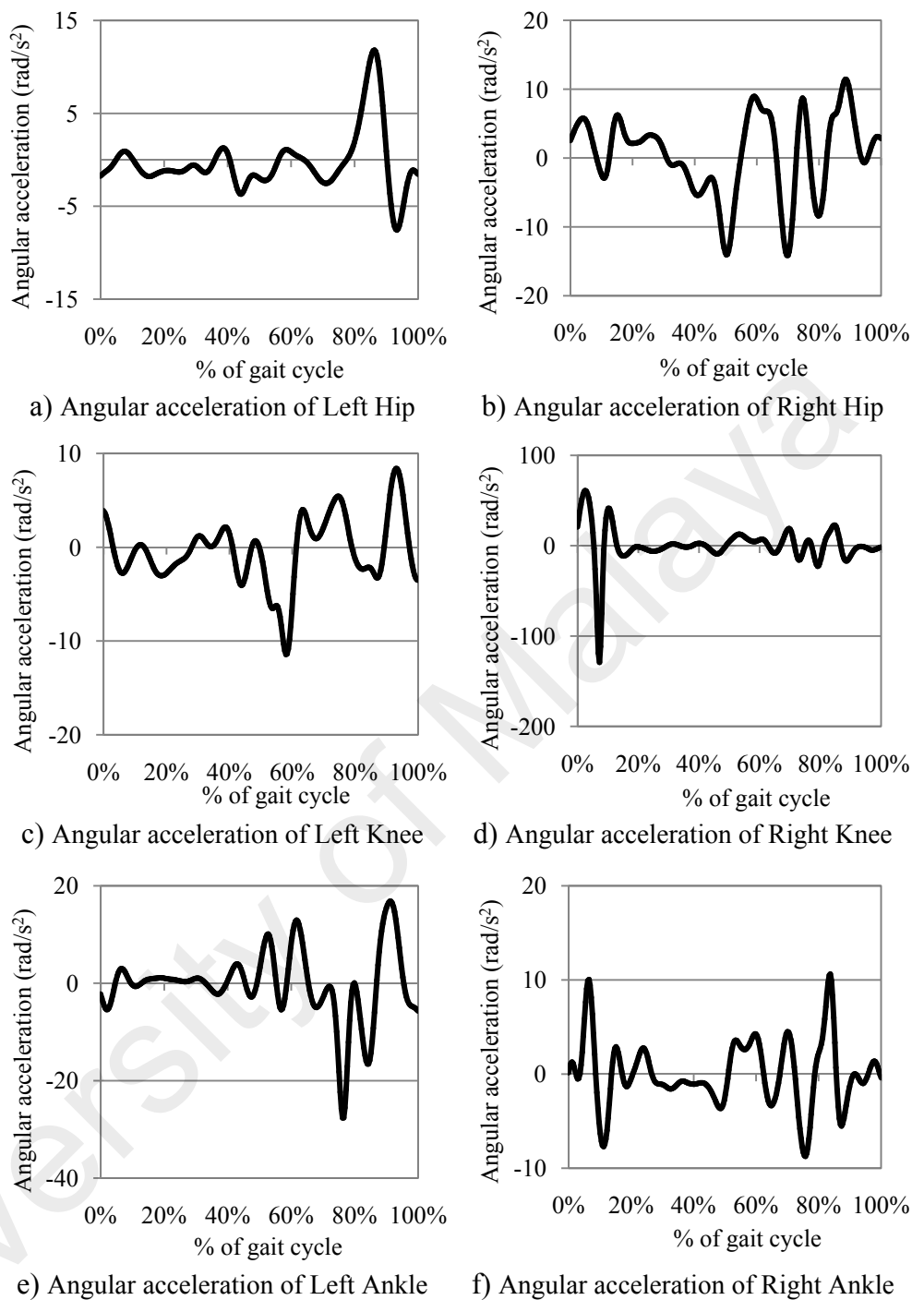
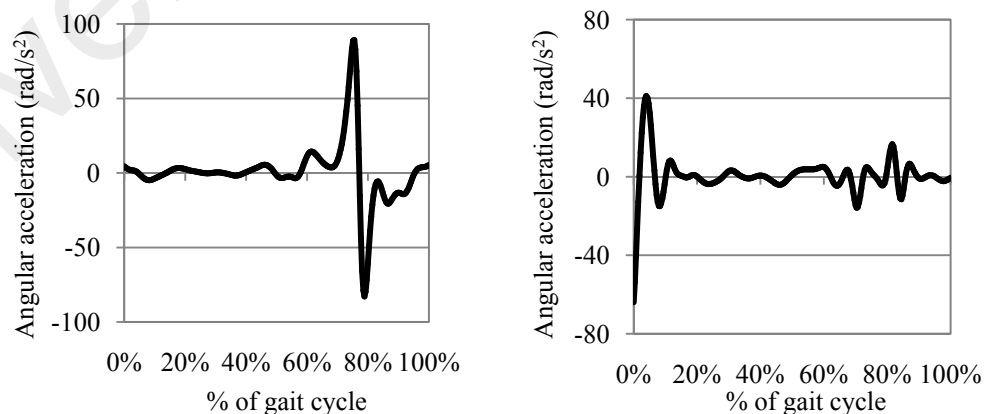


Figure 5.30: Angular acceleration of lower limb joints during walking at normal speed.

Figure 5.30 represents the fluctuation of angular acceleration in different joints of lower limb when using the prosthesis. From Figure 5.30a and Figure 5.30b, the angular acceleration of left and right hip joints had large similarity in pattern; however the magnitude of right hip was greater than that of left hip. From Figure

5.30c and Figure 5.30d, the angular acceleration graph of left prosthetic knee joint and right knee joint were dynamic in nature. The magnitude of the left knee acceleration was almost same to that of right knee except the spikes at the first 20% of right knee gait cycle. The sudden increase in the right knee gait cycle was followed by a steady fluctuation until the end of the gait cycle. This sudden increase can be attributed to the event of the sudden knee rotation to compensate the difficulties in adopting the prosthesis by the able body subject. The fluctuation of left knee acceleration was steady all through the gait cycle. From Figure 5.30e and Figure 5.30f, the angular acceleration of the left and right ankles when using prosthesis had similar pattern, however, the magnitude of the left ankle was found having steadier acceleration than that at the beginning of the right ankle which became unstable at later stage. Then the maximum acceleration of the left prosthetic ankle was higher than that of right ankle. That was because of the resultant effect of angular position and properties of prosthetic ankle joint making material. For prosthetic ankle joint, no muscle and tendon acted to operate the ankle, which did function in natural right ankle joint.



a) Angular acceleration of left foot progression b) Angular acceleration of right foot progression

Figure 5.31: Angular acceleration of foot progression during walking at normal speed.

Figure 5.31 shows the angular acceleration of left and right feet progression while using prosthesis. From the figure, the angular acceleration of left foot progression was almost steady until 70% of gait; it had a sudden increase to some level and then attenuated in the following stage until the end of the cycle. For right foot progression, the pattern was little different while a sudden increase was seen at the beginning of the cycle. This exception can be attributed to the unexpected movement of the leg due to some unwanted disturbance.

5.5.2 Kinetic analysis

A closer imitation of the flexion and extension movements of the knee and ankle joints would make the prosthesis moving in more natural way. Kinematic analysis is performed to determine the changes in the position, velocity and acceleration of joints and segments without taking the associated forces into consideration. The key results of interest are the assembly range of motion and determining the displacements, velocities, and accelerations of different prosthetic elements.

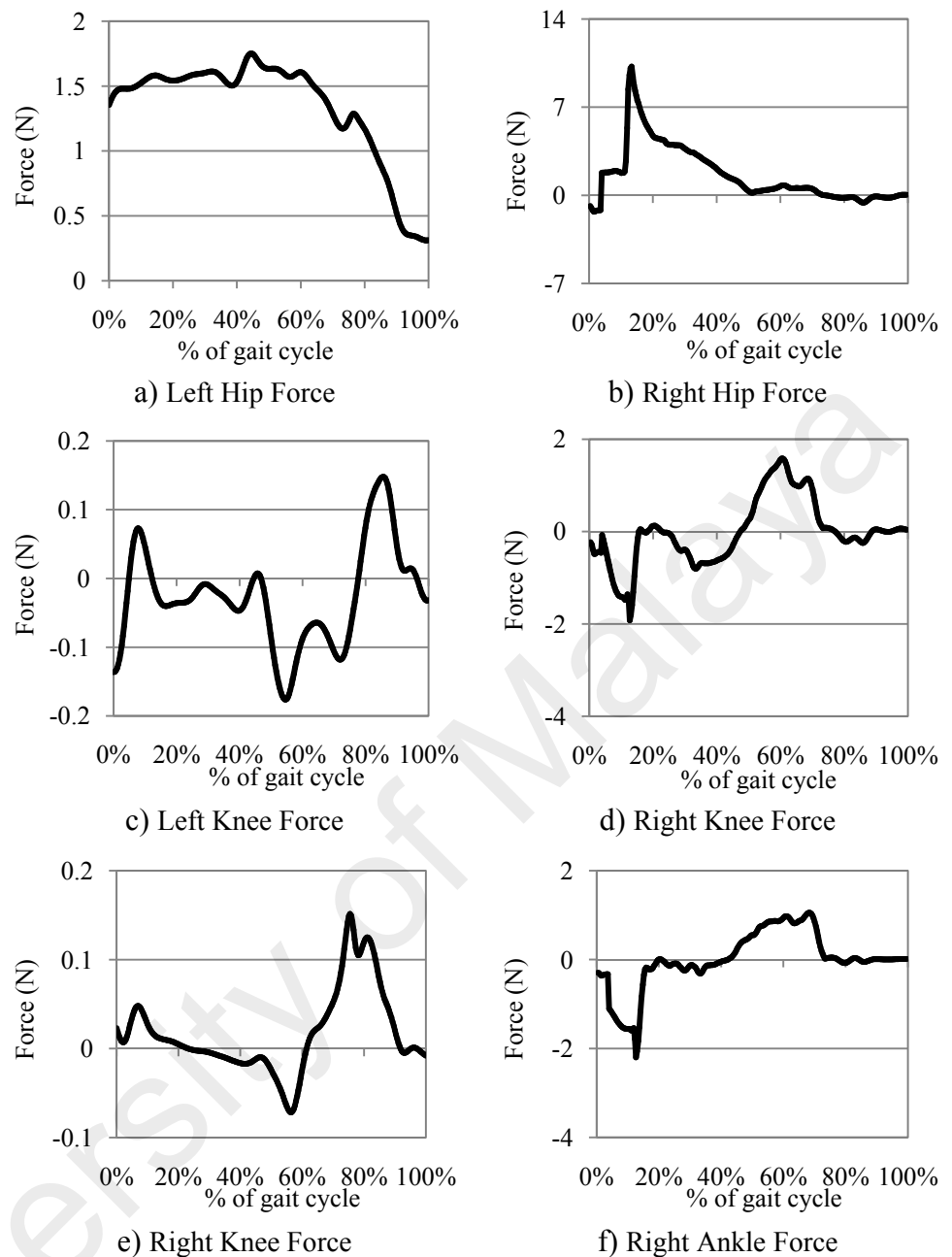


Figure 5.32: Forces in the lower limb prosthetic joints.

Figure 5.32 illustrate the variation in the joint forces when using prosthesis. From Figure 5.32a and Figure 5.32b, the pattern of the left hip and right hip forces were quite different. The magnitude of left hip force was recorded to be considerably greater than that of right hip force. The left hip force was steady until 70% of cycle and then decreased exponentially rest of the cycle. The right hip force has suddenly increased at some 20% of gait and then decreased

exponentially until the end of the gait cycle. From Figure 5.32c and Figure 5.32d, both the left and right knee force graphs were dynamic type; they fluctuated about the mean value of zero both in positive and negative directions. However, the maximum magnitude of knee force was lower than right knee force. From Figure 5.32e and Figure 5.32f, the left prosthetic ankle and right ankle forces had no obvious similarity, so did between the forces of healthy ankle joints. The maximum amplitude of left ankle force was significantly lower than that of right ankle. That was due to the change in biomechanics while using prosthesis.

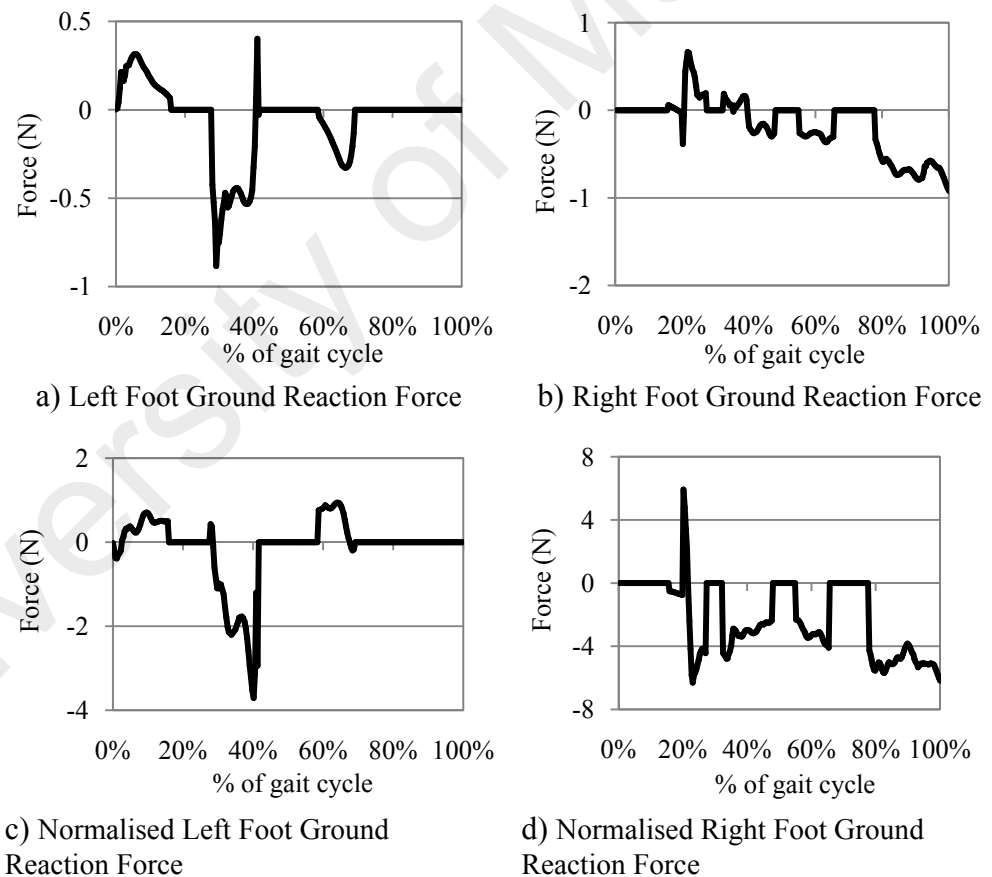


Figure 5.33: Ground reaction forces of prosthetic foot.

Figure 5.33 represents the foot ground reaction force when using the prosthesis. From the figure, the ground reaction force of left and right feet fluctuated about the mean value of zero throughout the gait cycle. The extent of right foot ground reaction force was higher than that of left foot. That was incurred by the compensation mechanics due to change in the left foot biomechanics associated with the properties of material used for making the prosthesis. For normalized force, the pattern did not change much; however, the magnitude increased significantly.

University of Malaya

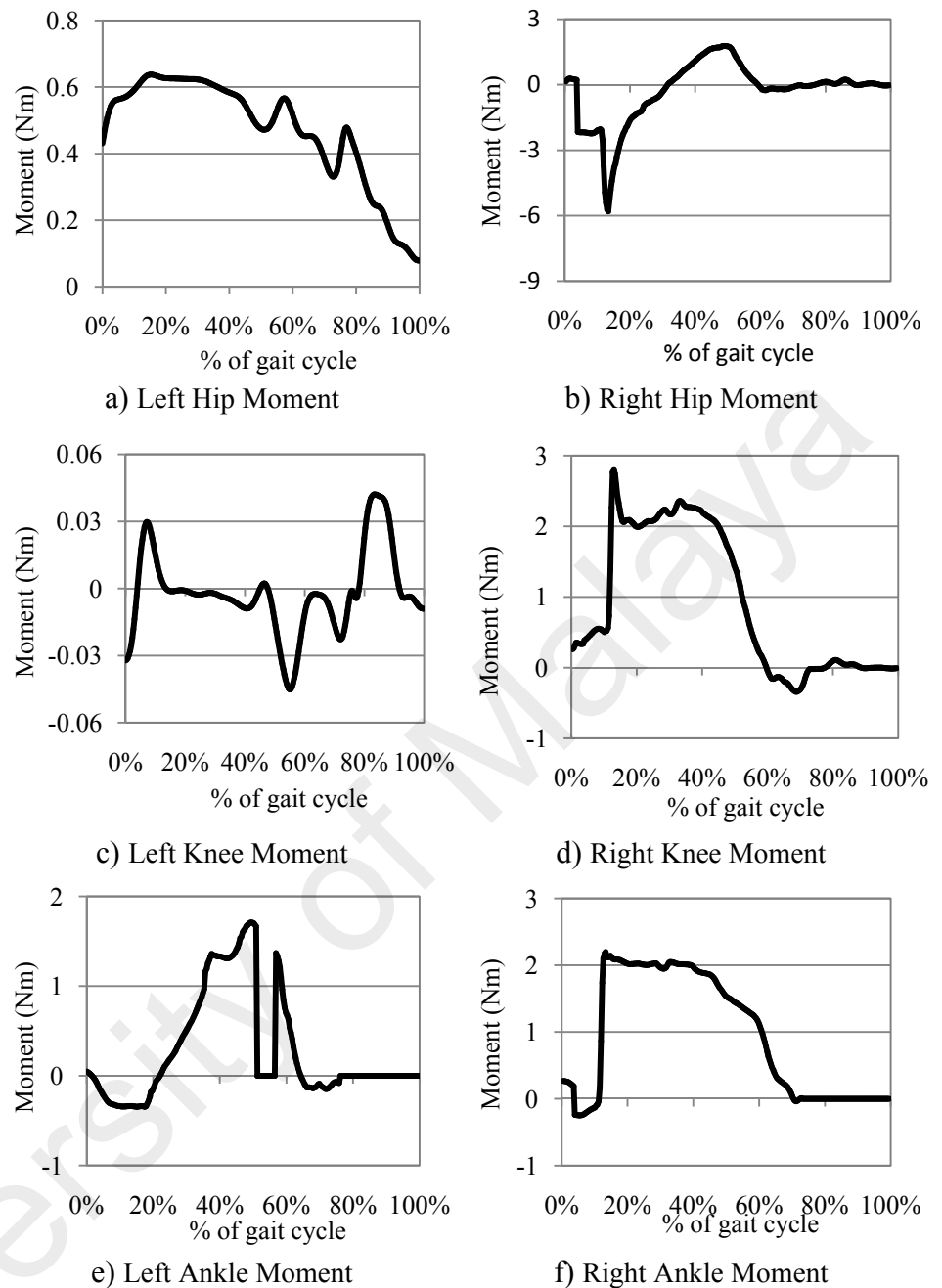


Figure 5.34: Joint moments of prosthetic lower limb.

Figure 5.34 shows the moments of different lower limb joints when using prosthesis. From Figure 5.34a and Figure 5.34b, the moment graphs of the left and right hip had some resemblance except a sudden drop in the right hip moment profile. The amplitude of the right hip moment was greater than left hip moment. According to Figure 5.34c and Figure 5.34d, the left and right knee

moment curves fluctuated randomly at different points of the gait cycle. The amplitude of the left knee moment was considerably lower than the right hip moment. From Figure 5.34e and Figure 5.34f, the moment graphs of the left and right ankles had little similarity in pattern; however, in magnitude, the right ankle moment was greater than the left ankle moment. The left ankle moment had some abrupt drop whereas a sudden rise was observed in the right ankle moment. That abrupt drop and rise could be attributed to the sudden change in the biomechanics at the ankle joint while using prosthesis.

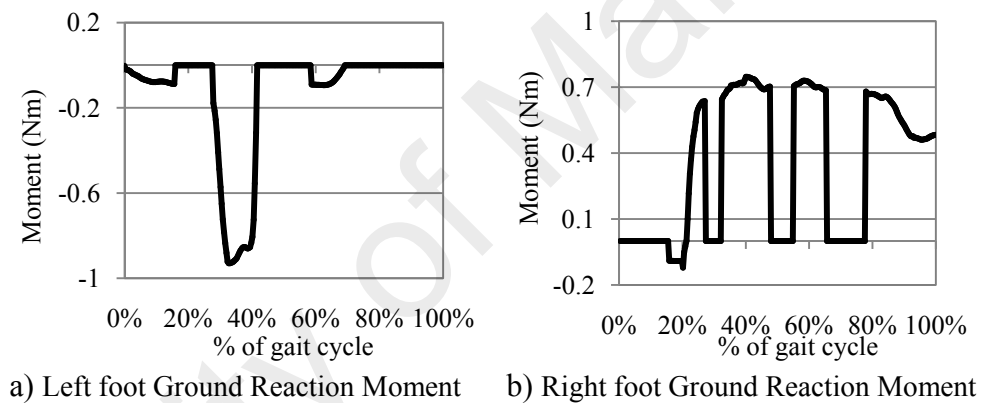


Figure 5.35: Ground reaction moment of prosthetic foot.

Figure 5.35 illustrates the ground reaction moment profiles of left and right feet. From the figure, the pattern of left foot ground reaction moment has somewhat matched with the right foot ground reaction moment; however, the magnitude-wise, the right foot moment was quite higher than the left foot moment.

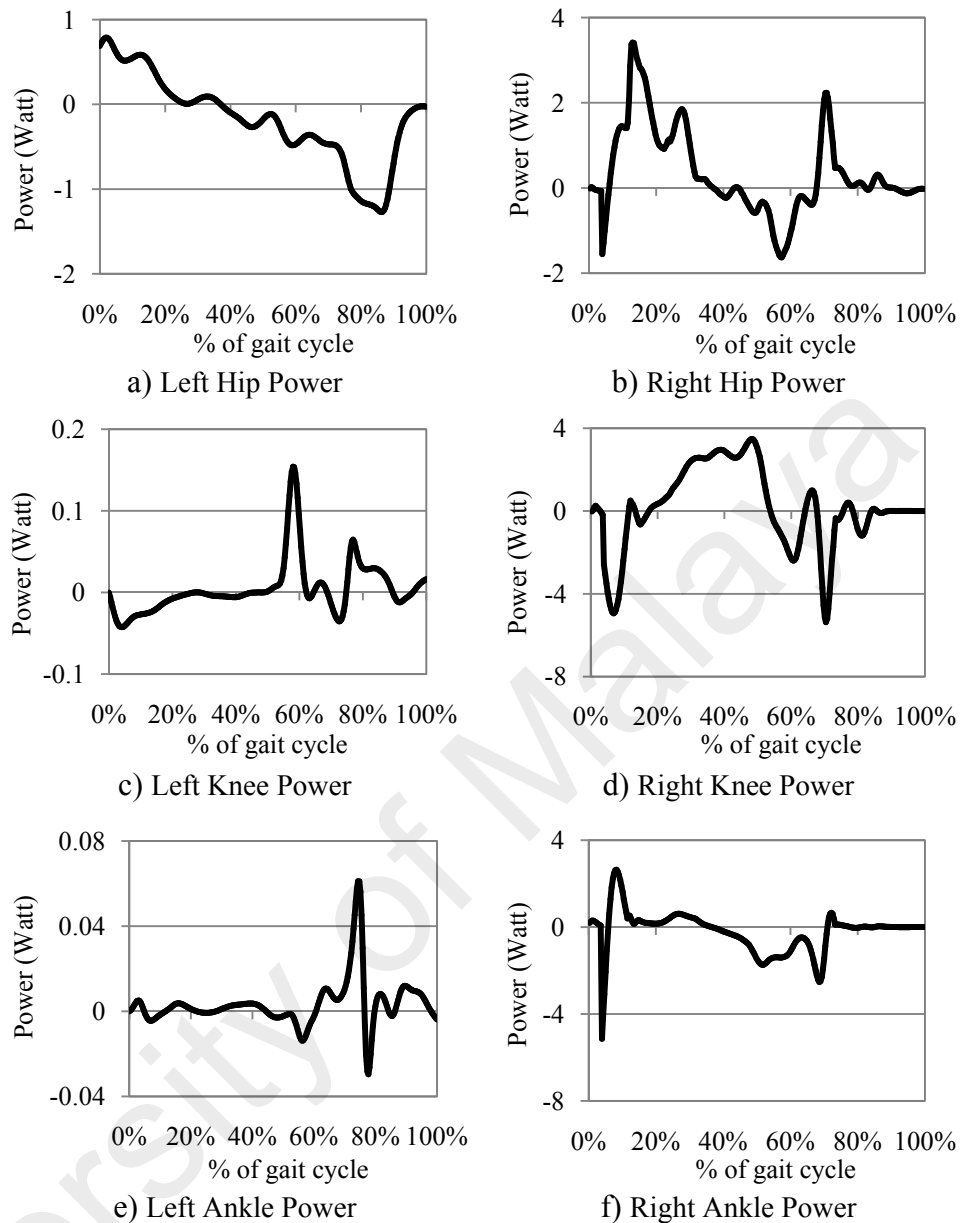


Figure 5.36: Joint power of prosthetic lower limb

Figure 5.36 shows the power of different lower limb joints while using prosthesis. From Figure 5.36a and Figure 5.36b, the power graphs of the left and right hips have no obvious similarity. The left hip power curve has gradually decreased whereas for right hip the power fluctuated more in a cyclic pattern. From Figure 5.36c and Figure 5.36d, the left and right knee power profiles had little resemblance in pattern; however, in magnitude the right knee power was

significantly larger than that of the left knee. From Figure 5.36e and Figure 5.36f, the ankle power curves of the left and right ankles had more likely an opposite pattern. A sudden spike was observed after 70% of the gait cycle on the left ankle power graph, whereas a spike followed by a steady decrease was found on the right ankle power profile within first 20% of the gait cycle.

5.6 Stability test of the subject with prosthesis

Stability of subject when using prosthesis was tested. The postural stability test, and fall risk test data were recorded during the stability assessment. Both the static and dynamic tests were conducted to evaluate the stability of the subject with the prosthetic lower limb. Postural stability and fall risk were tested for double leg standing. For prosthesis stability and fall risk assessment, no single leg test was performed.

5.6.1 Postural Stability test

During postural stability test, the subject instrumented with prosthetic lower limb has mounted and stood on the Biodex machine platform in such a way that the center of mass remained at the center of the machine platform. Then the position of the left and right feet were at some angle of 0° each, and the respective heel position were at E2 and D17 respectively. Different levels of perturbation and disturbance have been applied to test the postural stability of the subject with the prosthesis. Both the static and dynamic data were recorded during the test. The postural stability test data for both the static and dynamic analysis are shown in following Table 5.13.

Table 5.13: Postural stability analysis of subject with prosthesis

Platform setting	Overall Stability Index	Anterior/Posterior Index	Medial Lateral Index	Double leg stability	
				% Time in Zone	% Time in Quadrant
Dynamic 8	0.8 ± 0.31	0.7 ± 0.34	0.2 ± 0.15	A100, B0, C0, D0	I2, II0, III45, IV53
Dynamic 2	1.8 ± 1.02	1.4 ± 1.06	0.9 ± 0.66	A100, B0, C0,D0	I9, II5, III53, IV33
Static	0.4 ± 0.22	0.3 ± 0.24	0.2 ± 0.15	A100, B0, C0, D0	I0, II0, III22, IV78

From the data shown in Table 5.13, the score of the tests varied with the platform setting. In double leg stability test, for platform setting at level 8, the overall score obtained from the dynamic stability test was 0.8, which was quite good for someone using prosthesis; for platform setting at level 2, the score was 1.8, which was also good for the subject. For static analysis, the overall score was some 0.4, which was good enough for subject with prosthesis. The scores of the dynamic tests for double leg stability were remarkably good.

5.6.2 Fall risk test

The fall risk of the subject with the prosthesis was also tested for two level of platform setting. During the test, the subject was mounted on the platform in such a way that the location of the left and right feet was at some angle of 0° and 10° when the corresponding heel positions were at E5 and D17 respectively. The data obtained from the fall risk test are tabulated in following Table 5.14.

Table 5.14: Fall risk test of subject with prosthesis

Platform setting	Overall Stability Index
Dynamic 8	1.7 ± 0.88
Dynamic 2	1.8 ± 1.52
Static	2.0 ± 2.14

From the dynamic analysis results, the fall risk index for the platform setting at level 8 was found to be 1.7, which was significantly good for the subject with prosthesis. The fall risk score for the platform setting at level 2 was 1.8; that was also great for someone using prosthesis. From the static analysis, the fall risk index obtained for the subject was 2.0, which was quite acceptable for any amputee with prosthesis.

5.7 Performance analysis of the prosthesis

Due to difficulty in having transfemoral amputee subject, an able body had to become the subject, who had simulated to being an above knee amputee during the experiment. A special arrangement was designed and developed to do the performance test of the prosthetic limb with the able body individual. Some braces and brackets are used to fit the prosthesis to the leg of the subject, and to hold the shank of the biological leg up and thus to enable the subject to act like an above knee amputee.

The performance analysis was carried out by doing a comparative study between the kinematic, and the kinetic analysis results obtained from the healthy subject without prosthesis and those with prosthesis. The changes in the angular displacement, angular velocity, angular acceleration, force, moment and power of hip, knee and ankle joints are the parameters were looked into and compared with that of the natural prosthesis. The similarity and dissimilarity between the variables recorded at different points of gait cycles from the subjects without prosthesis and with prosthesis would evaluate the performance of the prosthesis successfully.

In addition, a comparison was conducted between the stability data obtained from the healthy subject without prosthesis and with prosthesis to evaluate the stability performance of the prosthesis. Besides, a comparative study between the results obtained from the motion analyses of the designed prosthesis and that from some existing mechanical type prosthesis would make the performance test even more effective.

5.7.1 Kinematic performance analysis

For kinematic performance analysis of the prosthesis, the angular displacement, angular velocity, and angular acceleration profiles of different joints and

segments of healthy lower limb were compared with those of the lower-limb prosthesis. Though, the prosthesis was fit to the left leg, there were significant changes observed in both leg mechanics while using prosthesis. Therefore, both the left and right legs data have been compared to test the performance of the prosthesis. The following figures would represent a picture of comparative analysis.

A comparative study between Figure 5.1 and Figure 5.26 showed the similarity, dissimilarity and deflection between the hip, knee and ankle data obtained from healthy subject without prosthesis and that from the subject with prosthesis. From the figures, the angular displacement of the lower limb joints when using prosthesis deflected from that without prosthesis. Though, there was a big difference in phases and amplitudes of left hip displacements graphs, there were still some similarities in pattern. The magnitude of angular displacement of joints was significantly larger than that from the displacement without prosthesis. This was due to the increased resistance in producing movements in prosthesis. The phase shift of the angular displacement graphs to the right was comparatively bigger for the right leg joints than that for left leg joints. However, the angular displacement graph of the right ankle joints had some irregularities. The phase shift could be attributed to the event of elapsing longer time in creating movements due to changes in biomechanics produced from the extra stiffness of the prosthetic ankle. The graphs showed that the displacement graph with the prosthesis has deflected much for the right leg joints than for the left leg joint. This could be associated to the fact that the right leg had to compensate much of the change in the biomechanics due to adopting the prosthesis.

Figure 5.2 and Figure 5.27 shows the difference between the angular foot progression data obtained from healthy subject without prosthesis and that from the subject with prosthesis. From the figures, the angular progression of left foot without prosthesis and with prosthesis was quite different. This was because of the prosthesis used by the able body subject was an extra load rather being a support to the subject. The magnitude was quite higher than that of the natural angular foot progression. It could be justified by the resistance in bending the ankle against the stiffness of the material, which was quite greater than the muscle and tendon stiffness of the biological ankle joint. The shape of the right foot angular progression profile was disturbed for the sake of compensating the limitation of the left prosthetic foot.

Figure 5.3 and Figure 5.28 shows the difference between the angular velocity data of different lower limb joints captured from healthy subject without prosthesis and that from the subject with prosthesis. From Figure 5.3a and Figure 5.28a, the magnitude and pattern of the left hip velocity (with prosthesis) resembled a lot to that from the healthy hip joint (without prosthesis) until 80% of the gait cycle. A sudden increase was noticed in the left hip velocity graph at the end of the cycle. That was due to disturbance in ambulation caused by difficulty in adjusting and adopting the prosthesis by the able body subject. The right hip (Figure 5.3b and Figure 5.28b) on the other hand, fluctuated to a greater extent than the respective right hip joint without prosthesis. However, the patterns of the right feet velocity profiles were quite similar in shape. From Figure 5.3c and Figure 5.28c, the phase of the left knee angular velocity curve has deflected more than its magnitude. The magnitude of the left knee velocity was remained within a certain range for both the prosthetic knee and natural knee joints.

For the right knee joints (Figure 5.3d and Figure 5.28d), the amplitude variation for the major portion of the cycle was almost same except the beginning 20% of the cycle when the velocity fluctuation was nearly double. That was due to lack of stability in the right knee experienced from the alteration of the left knee biomechanics. From Figure 5.3e and Figure 5.28e, though shape wise, there was significant difference between the velocity graphs from the natural ankle and prosthetic ankle joints, magnitude-wise, those were remained within a similar range for the respective leg ankles joints. The fluctuation in the pattern was owing to the difficulties in complementing limitations of each other leg joints caused by the able-body subject.

Figure 5.4 and Figure 5.29 shows the difference between the angular velocity of foot progression data recorded from the healthy subject without prosthesis and that from the subject with prosthesis. From the figures, the pattern of the left prosthetic foot progression had considerable similarity with that of normal foot; however, the magnitude was significantly greater. That could be attributed to the fact of compensation of velocity in order to overcome the limitation in adapting the prosthesis by the able-body subject. For the right prosthetic foot, the angular velocity graph had similar fluctuation in terms of magnitude; however, the pattern was deflected. The similar justification could be made for that deflection also.

Figure 5.5 and Figure 5.30 illustrate the similarities and dissimilarities between the angular acceleration of left and right leg joints without prosthesis and with prosthesis respectively. From the figures, the angular acceleration of left and right hip joints had similarity to the pattern of fluctuation of corresponding acceleration profile of normal hip joints without prosthesis. However, the frequency of the acceleration curves obtained from the hip joints with prosthesis

was more than that without prosthesis. Magnitude-wise, the acceleration of the hip joint with prosthesis have emulated to their respective acceleration when no prosthesis was used.

For prosthetic knee acceleration, the pattern and magnitude of the left knee acceleration curve had some resemblance to that of natural knee acceleration. However, for right knee, though the pattern had a lot similarity except the initial burst pattern, the magnitude increased significantly when the subject adopted the prosthesis on his left leg. That was due to the change of angular position when to adjust the difficulties of the left knee with help of the right knee.

The trend of the prosthetic ankle acceleration graphs had large similarity with that of natural ankle acceleration curves. However, there was some small fluctuation in the prosthetic ankle acceleration profiles, which was caused by the compensation and adaptation activities by the ankle joint when using prosthesis. The magnitude of both the left and right ankle acceleration when using prosthesis were greater than that of acceleration without prosthesis.

Figure 5.6 and Figure 5.31 shows the difference between the angular acceleration of foot progression data recorded from the healthy subject without prosthesis and that from the subject with prosthesis. From the figures, both the left and right feet progression angular acceleration had similar steady trend followed by a sudden increase at last part of the gait cycle, except an initial disturbance for the right foot. The fluctuation of magnitude for the right foot remained within a same range for both cases; however, for left prosthetic foot, the magnitude was quite higher than that without prosthesis. That deflection was associated with the change of prosthetic foot biomechanics.

From the data shown in the previous sections, it has been seen that the magnitude of the angular displacement deflected 0.5 to 7 times than the healthy

gait cycle data when using prosthesis. The angular velocity data were also found to vary between 0.4 times and 4.7 times, whereas the angular acceleration data had a deflection from 0.1 to 2.5 times. These deflections would significantly reduce when a real amputee is employed as a subject.

5.7.2 Kinetic performance analysis

Kinetic performance analysis of the prosthesis has been accomplished by carrying out a comparative study between the forces, moment and power profiles of different joints and segments of the lower prosthesis with that of healthy lower limb. Both the left and right legs data have been compared to test the performance of the prosthesis. The following figures would demonstrate the distinguished similarities and dissimilarities between the kinematic parameters.

Figure 5.7 and Figure 5.32 shows the difference between the forces of various lower limb joints when using prosthesis and those without prosthesis. From Figure 5.7a and Figure 5.32a, the pattern of the left hip force profiles when using prosthesis had great similarity with that of force profile without prosthesis. The magnitude of the left hip force had maintained a steady increasing trend in the majority of the gait cycle unlike to the corresponding natural left hip force graph. That was due to the changed biomechanics of the lower limb when used prosthesis by the able-body subject. For the right hip force (Figure 5.7b and Figure 5.32b), the patterns of the graphs had some resemblance, except the sudden spike in the force profile when using prosthesis. That could be attributed to some compensation events associated with the adaptation of prosthesis by the able-body subject. The fluctuation of right hip force magnitude has remained in some certain range except for the moment of spike when the force was exceptionally high.

For the knee force (Figure 5.7c and Figure 5.32c), the left prosthetic knee force fluctuated in some particular limits like that of the natural knee joint; however, the pattern of fluctuation has changed. The force varied at different points of the gait cycle due to the deflection in the biomechanics of the knee joints when using prosthesis. For right knee force (Figure 5.7d and Figure 5.32d), the patterns of the knee force profile were also deflected from the natural force profile for the same reason. However, the amplitude in this case was quite greater than that of the natural knee joint. That was due to sharing uneven force by the right knee when using prosthesis on left leg. From Figure 5.7e and Figure 5.32e, though the fluctuation of the left ankle force was remained within a same band for both the biological and prosthetic ankle, the pattern of the prosthetic ankle force graphs had a similar pattern up to some 60% of gait cycle and then changed following an opposite trend. For right ankle joint force (Figure 5.7f and Figure 5.32f), despite the shape was not exactly same, their pattern had quite similarity. The magnitude was quite higher than that of the healthy ankle joint. That was due to the disturbance in the biomechanics of ankle joints when using prosthesis.

Figure 5.8 and Figure 5.33 show the difference between the ground reaction forces of prosthetic foot and those of normal foot. From the figures, the fluctuation of the ground reaction force of the left foot has remained in the same band for both the normal and prosthetic foot. However, their pattern has changed significantly. For the right prosthetic foot, both the pattern and the magnitude have deflected from that of normal foot. Though, the magnitude has increased, the graph has still maintained a similar trend. The same conclusion that made for other cases could be made here also. For the normalized forces, both pattern and

the magnitude of left and right feet ground reaction force matched more with ground reaction force graphs of normal feet.

Figure 5.9 and Figure 5.34 shows the difference between the moments of various lower limb joints when using prosthesis and those without prosthesis. From the figures, both the left and the right hip moment graphs have followed the similar trend like that of natural hip joint moment. However, for the left hip moment, the amplitude of the moment without prosthesis was greater than the moment with prosthesis. Opposite scenery was observed for the right hip moment. That could be attributed to the fact of compensation of altered biomechanics.

For knee moments, the left knee moment fluctuated much lower than that of natural knee joint moments. The shape of the graph was found to have a similar pattern until 70% of the gait cycle except some disturbance, which was associated with changes in the biomechanics of the prosthetic knee joint. That was because of the difference in the characteristics of the material used for making prosthesis and that of natural muscle and tendon of the natural knee joint. For right knee joint, both the shape and amplitude of the moment changed because of extra dependency on the right knee by the able-body subject when using prosthesis.

In case of ankle joints, the left and right prosthetic ankle moments graphs had a lot similarity in pattern to the respective natural ankle moment curves. In natural gait, a gradual decrease was found in left ankle moment profile; however, in the prosthetic ankle, it was replaced by a sudden drop. The similar justification that made for knee joint moment could be given for the deflection in the ankle joint moments. The magnitude of moment was much higher in the prosthetic left ankle than in respective natural left ankle joint. For right ankle joint, despite there was some sudden increase in amplitude, the pattern had some similarity to

that of natural ankle moment. The similar justification can be made for the sudden increase of the ankle moment. However, the magnitude was much higher than the respective ankle moment without prosthesis. That was associated with the extra resistance of the prosthesis material and thus the moment caused by the altered biomechanics.

Figure 5.10 and Figure 5.35 shows the difference between the ground reaction moment of prosthetic foot and those of normal foot. From the figures, the left foot and right feet ground reaction moment curves had no obvious similarity with the normal foot ground reaction moment graphs. However, some subtle similarities were there; they fluctuated following a similar trend with their respective natural moment graphs. Amplitude-wise, both the left and right feet ground reaction moments when using prosthesis were greater their respective normal moment profiles.

Figure 5.11 and Figure 5.36 shows the difference between the powers of various lower limb joints when using prosthesis and those without prosthesis. From Figure 5.11a and Figure 5.36a, the left hip power curve of the when using prosthesis was different than that without prosthesis. However, the joints power maintained nearly a similar trend throughout the gait cycle when using prosthesis and that without prosthesis. The magnitude of left hip power fluctuation for both the cases was same. For right hip power profiles (Figure 5.11b and Figure 5.36b), the trend and the magnitude have changed significantly. The magnitude of the right hip power when using prosthesis was quite higher than that of normal right hip power.

From Figure 5.11c and Figure 5.36c, the left prosthetic knee power graphs had deflected from that of the healthy knee joint. The trend of the prosthetic knee power curves had some similarity to the natural knee power graph except a rise

on the profile. That rise was associated with the alternation of knee joint biomechanics while fitting the prosthesis with the able-body subject instead of an amputee. The amplitude remained almost in same limits except when there was a drop in the natural left knee power profile. From Figure 5.11d and Figure 5.36d, for the right knee, the pattern of the right knee power had little similarity with that of knee power without prosthesis; however the exact shape was not same. The magnitude of the right knee power when using prosthesis was several times greater than that of knee power without prosthesis. For the right knee power curves, opposite scenery to the left knee power profiles was observed. The power of the knee joint has changed inversely when the prosthesis was used. That could be attributed to that the use of prosthesis has increased dependency on the healthy side of the subject in sharing the load and creating ambulation during the gait cycle.

From Figure 5.11e and Figure 5.36e, the left prosthetic ankle power graph had significant resemblance to that of the respective natural ankle power graph. Both the pattern and the magnitude were similar for the left ankle power curves. For the right ankle power curves (Figure 5.11f and Figure 5.36f), the pattern of the ankle power graph when using prosthesis had no remarkable similarity with that of power curves obtained without prosthesis. The magnitude was also considerably greater than that of without prosthesis. Most importantly, in the event of disturbance, an opposite picture was seen between the left and right ankle power curves; the amplitude had changed inversely in both the cases when using prosthesis and without prosthesis.

The results were expected to be better if the able-body subject trained up with the prosthesis quite a number of times. This has been seen from the few trials

carried out by the subject; in each trial, the results were observed improving a lot due to the increased adaptability.

The employment of real amputee subject would improve the performance test results significantly. This would eliminate the limitation associated with fitting and adopting the prosthesis with the healthy leg. This statement can be justified with help of some previous work carried out by Frank Sup (2009). The researcher has tested the prosthesis with able-body subject before applying it to a real amputee subject. He has obtained significantly greater values of the measurand from the able-body subject than that from the real amputee subject. Though the prosthesis was advanced type, the nature of resistance in the joints and prosthesis should be similar like that in mechanical type. Hence, the deflection between of data obtained from the able-body subject and the real-amputee subject should be regardless of the prosthesis type. Therefore, the data deflection should be equally applicable to the mechanical type prosthesis.

From the data presented in the previous sections, it has been observed that the magnitude of the joint force deflected 2.5 to 12 times than the healthy gait cycle data when using prosthesis. The joint moment data were found to vary between 0.9 times and 15 times, whereas the joint power data had a deflection from 1 to 14 times. These deflections would decrease significantly when the prosthesis is tested with a real amputee.

5.7.3 Stability performance analysis:

The performance of the subject stability was evaluated by comparing the stability data obtained from the prosthesis with that from the healthy subject. Both the postural stability and fall risk data were analyzed during the assessment of stability performance.

5.7.3.1 Postural Stability performance

In postural stability performance analysis, the postural stability data recorded from the healthy individual without prosthesis were compared with the data obtained from the subject with prosthesis. The performance was tested for both the static and dynamic postural stability. The postural stability data from healthy individual without prosthesis and subject with prosthesis have shown in the previous sub-sections in Table 5.3 and Table 5.13 respectively.

From the data shown in Table 5.3 and Table 5.13, for platform setting at difficulty level 8, the dynamic postural stability index of the subject with prosthesis was increased 3.3 times than that of the healthy subject without prosthesis, for platform setting at level 2, the postural stability was improved 5 times. For static platform setting, the postural stability was decreased 1.3 times than that of the healthy subject without prosthesis. Both the overall index and the standard deviation scores indicated that the use of prosthesis improved the postural stability of the subject.

5.7.3.2 Fall risk performance

The performance of fall risk when using prosthesis was analyzed comparing to the fall risk without the prosthesis. Unlike to postural stability, the fall risk performance was also evaluated both for the dynamic and static data. The fall risk data obtained from the subject without prosthesis and with prosthesis are tabulated in Table 5.4 and Table 5.14 respectively.

From Table 5.4 and Table 5.14, for the platform setting at level 8, the dynamic fall risk of the subject with prosthesis was increased 1.2 times than that of the healthy subject. Though, the overall index was lower for the fall risk data with

prosthesis, the standard deviation of the fall risk score was slightly higher for the subject with prosthesis. That means, the fall risk reduced when the prosthesis was used, however, the score was not steady. That indicated the demand of more trial by the subject to adopt the prosthesis. For platform setting at level 2, the dynamic fall risk of subject with prosthesis was improved 3.3 times than that without prosthesis. Both the overall index and the standard deviation indicated that the use of prosthesis reduced the fall risk significantly. For static platform setting, the overall fall risk score and the deviation both were behaving like that of postural stability. The static fall risk with prosthesis was decreased 1.8 times than that without prosthesis.

There was some deflection in the results due to the dummy amputee subject. As the subject was not real amputee and acted as an above knee amputee, the real performance of the prosthesis could not assess. Even though there was some deflection in the result because of the able body subject, at least the approximate performance of the prosthesis was well reflected in the motion analysis results. A peek look on the differences between the results from able body subject and from real amputee subject would provide some idea about the real performance of the prosthesis.

Due to unavailability of a real transfemoral amputee, and having a able-body subject instead for the performance analysis, it was not possible to obtain accurate results from the gait performance and stability test analyses. This was the weakness of the performance analysis of this study. However, some ideas on nature of gait cycle and stability test data have been obtained from the performance analysis.

5.8 Cost analysis of the prosthesis development

The total cost of the above knee prosthesis development has been calculated by summing up the cost of making the components of the prototype. The materials and making cost of different elements of the designed above knee prosthesis are as following:

Table 5.15: Cost of prototype development

Particulars	Prices (USD)
Cost of materials	: 90
Component making cost	: 160
Accessories cost	: 30
Assembly and testing cost	: 20
Total	: 300

From the Table A1, the price of a basic above knee prosthesis is USD 37,000.00 which is much higher than the per capita spending on healthy in Malaysia of USD 676 and some other least developed countries where amputation is prevalent (Figure A2). On the other hand, the development cost of prototype is USD 300 which is significantly below than the per capita spending on health in Malaysia and very cheap comparing to the existing basic above knee prosthesis. Choosing some cheaper composite material for the prosthesis components will reduce the price of the prosthesis. The price of the prosthesis will considerably decrease when to go for mass production.

CHAPTER 6: CONCLUSIONS AND RECOMMENDATIONS

Conclusions have been stated based on the results of the experiment and recommendations have been made based on the experience for the future development of the prosthesis.

6.1 Conclusions

The cost of quasi-active type above knee prosthesis designed for a lower limb amputee was found considerably cheap and thus available for mass proportion of amputee. The gear based knee joint and the spring based ankle joint designed for a transfemoral amputee was found capable of recreating gait cycle movement of a healthy biological limb and can be used compatibly with adequate safety.

The salient features of the research are as following:

- The gait cycle analysis of the healthy lower limb has shown that
 - The angular displacement, angular velocity, and angular acceleration profiles of different joints obtained from the healthy subject were agreed with those from the literature.
 - The kinetic analysis results of the healthy lower limb also remained in good agreement with those from the literature.
- The simulation results showed that
 - Though there were some deflection in magnitude, the pattern of the angular displacement, angular velocity, and angular acceleration graphs obtained from the kinematic analysis of the knee and ankle joints were imitating the pattern of those of healthy limb.

- The kinetic analysis results graphs also displayed a great resemblance to the plots obtained from the healthy subject.
- The gait performance analysis of the developed prosthesis has shown some mixed behaviors. Though there was some deviation between the gait cycles data obtained from the subject using prosthesis and that from the healthy subject, the pattern of the graphs maintained a similar trend.
- Kinematic analysis:
 - The magnitude of angular displacement of prosthesis gait cycle had some deviation of 0.5 to 7.5 times than that of healthy gait cycle.
 - The magnitude of angular velocity data of prosthesis had some deviation of 0.4 to 4.7 times than the healthy gait cycle data.
 - The magnitude of angular acceleration of prosthesis gait cycle had some deviation of 0.1 to 2.5 times than that of healthy gait cycle.
- Kinetic analysis:
 - The magnitude of joint force data of prosthesis had some deviation of 2.5 to 12 times than the healthy limb data.
 - The magnitude of joint moment data of prosthesis had some deviation of 0.9 to 15 times than that of healthy limb data.
 - The magnitude of joint power of prosthesis had some deviation of 1 to 14 times than that of healthy limb joint.
- Stability analysis: at dynamic platform setting, the postural stability and fall risk were found to improve while using prosthesis; whereas at static platform setting, the performance was found to decline.
 - For platform setting at level 8, the postural stability of the subject with prosthesis was increased 3.3 times than that of the healthy subject, for platform setting at level 2, the postural stability was improved 5 times.

For static platform setting, the postural stability was decreased 1.3 times than that of the healthy subject.

- For platform setting at level 8, the fall risk of the subject with prosthesis was increased 1.2 times than that of the healthy subject, for platform setting at level 2, the fall risk was improved 3.3 times. For static platform setting, the fall risk was decreased 1.8 times than that of the healthy subject.

6.2 Recommendations

- Use of lighter composite material would make the prosthesis arrangement more efficient. Choosing hollow-shaped rods for shank and thigh rod in this case would be more appropriate.
- Putting rubber cap at the faces of gear-stoppers would reduce the terminal impact on the prosthesis.
- Introducing some locking mechanism in the knee and ankle joints would improve the performance of the prosthesis.
- Having a real transfemoral amputee as the subject for the performance test would provide more authentic results and thus could evaluate the performance of the developed above knee (AK) prosthesis.

REFERENCES

- Albertini, J. N., Barral, X., Branchereau, A., Favre, J. P., Guidicelli, H., Magne, J. L., & Magnan, P. E. (2000). Long-term results of arterial allograft below-knee bypass grafts for limb salvage: a retrospective multicenter study. *J Vasc Surg*, 31(3), 426-435.
- Arampatzis, A., Morey-Klapsing, G., Karamanidis, K., DeMonte, G., Stafilidis, S., & Bruggemann, G. P. (2005). Differences between measured and resultant joint moments during isometric contractions at the ankle joint. *J Biomech*, 38(4), 885-892.
- Barnett, C. T., Vanicek, N., & Polman, R. C. (2013). Postural responses during volitional and perturbed dynamic balance tasks in new lower limb amputees: a longitudinal study. *Gait Posture*, 37(3), 319-325.
- Barton, T., Lintz, F., & Winson, I. (2011). Biomechanical changes associated with the osteoarthritic, arthrodesed, and prosthetic ankle joint. *Foot Ankle Surg*, 17(2), 52-57.
- Bayram, H. A., Chien, C. H., & Davis, B. L. (2014). Active functional stiffness of the knee joint during activities of daily living: a parameter for improved design of prosthetic limbs. *Clin Biomech*, 29(10), 1193-1199.
- Bei, Yanhong, & Fregly, Benjamin J. (2004). Multibody dynamic simulation of knee contact mechanics. *Medical engineering & physics*, 26(9), 777-789.
- Beillas, P., Papaioannou, G., Tashman, S., & Yang, K. H. (2004). A new method to investigate in vivo knee behavior using a finite element model of the lower limb. *J Biomech*, 37(7), 1019-1030.
- Boone, D. A., Kobayashi, T., Chou, T. G., Arabian, A. K., Coleman, K. L., Orendurff, M. S., & Zhang, M. (2012). Perception of socket alignment perturbations in amputees with transtibial prostheses. *J Rehabil Res Dev*, 49(6), 843-853.
- Bowker, J. H., & Michael, J. W. (1992). *Atlas of limb prosthetics: Surgical, prosthetic and rehabilitation principles*(2nd ed.): American Academy of Orthopaedic Surgeons, p. 930, ISBN 0-8016-0209-2.

- Božidar, Potočnik, Damjan, Zazula, Boris, Cigale, Dušan, Heric, Edvard, Cibula, & Tomažič, Tomaž. (2008). A Patient-specific Knee Joint Computer Model Using MRI Data and 'in vivo' Compressive Load from the Optical Force Measuring System. *Journal of Computing & Information Technology*, 16(3), 209-222.
- Burger, H., Marincek, C., & Jaeger, R. J. (2004). Prosthetic device provision to landmine survivors in Bosnia and Herzegovina: outcomes in 3 ethnic groups. *Arch Phys Med Rehabil*, 85(1), 19-28.
- Curtze, C., Hof, A. L., Postema, K., & Otten, B. (2012). The relative contributions of the prosthetic and sound limb to balance control in unilateral transtibial amputees. *Gait Posture*, 36(2), 276-281.
- Curtze, C., Hof, A. L., van Keeken, H. G., Halbertsma, J. P., Postema, K., & Otten, B. (2009). Comparative roll-over analysis of prosthetic feet. *J Biomech*, 42(11), 1746-1753.
- De Asha, Alan R., Johnson, Louise, Munjal, Ramesh, Kulkarni, Jai, & Buckley, John G. (2013). Attenuation of centre-of-pressure trajectory fluctuations under the prosthetic foot when using an articulating hydraulic ankle attachment compared to fixed attachment. *Clinical Biomechanics*, 28(2), 218-224.
- DeVita, P., Helseth, J., & Hortobagyi, T. (2007). Muscles do more positive than negative work in human locomotion. *J Exp Biol*, 210(Pt 19), 3361-3373.
- Eilenberg, M. F., Geyer, H., & Herr, H. (2010). Control of a powered ankle-foot prosthesis based on a neuromuscular model. *IEEE Trans Neural Syst Rehabil Eng*, 18(2), 164-173.
- Esquenazi, A., & Meier, R. H., 3rd. (1996). Rehabilitation in limb deficiency. 4. Limb amputation. *Arch Phys Med Rehabil*, 77(3 Suppl), S18-28.
- Ferris, A. E., Aldridge, J. M., Rabago, C. A., & Wilken, J. M. (2012). Evaluation of a powered ankle-foot prosthetic system during walking. *Arch Phys Med Rehabil*, 93(11), 1911-1918.
- Gao, K., Chen, S., Wang, L., Zhang, W., Kang, Y., Dong, Q., . . . Li, L. (2010). Anterior cruciate ligament reconstruction with LARS artificial ligament: a multicenter study with 3- to 5-year follow-up. *Arthroscopy*, 26(4), 515-523.
- Geil, Mark D., Parnianpour, Mohamad, Quesada, Peter, Berme, Necip, & Simon, Sheldon. (2000). Comparison of methods for the calculation of energy storage

and return in a dynamic elastic response prosthesis. *Journal of Biomechanics*, 33(12), 1745-1750.

Ghorbani, Reza, & Wu, Qiong. (2009). Adjustable stiffness artificial tendons: Conceptual design and energetics study in bipedal walking robots. *Mechanism and Machine Theory*, 44(1), 140-161.

Godest, A. C., Beaugonin, M., Haug, E., Taylor, M., & Gregson, P. J. (2002). Simulation of a knee joint replacement during a gait cycle using explicit finite element analysis. *J Biomech*, 35(2), 267-275.

Goldberg, E. J., Requejo, P. S., & Fowler, E. G. (2008). The effect of direct measurement versus cadaver estimates of anthropometry in the calculation of joint moments during above-knee prosthetic gait in pediatrics. *J Biomech*, 41(3), 695-700.

Halloran, J. P., Petrella, A. J., & Rullkoetter, P. J. (2005). Explicit finite element modeling of total knee replacement mechanics. *J Biomech*, 38(2), 323-331.

Hansen, A. H., Childress, D. S., & Knox, E. H. (2000). Prosthetic foot roll-over shapes with implications for alignment of trans-tibial prostheses. *Prosthet Orthot Int*, 24(3), 205-215.

Herr, H. M., & Grabowski, A. M. (2012). Bionic ankle-foot prosthesis normalizes walking gait for persons with leg amputation. *Proc Biol Sci*, 279(1728), 457-464.

Hofstad, C. J., Weerdesteyn, V., van der Linde, H., Nienhuis, B., Geurts, A. C., & Duysens, J. (2009). Evidence for bilaterally delayed and decreased obstacle avoidance responses while walking with a lower limb prosthesis. *Clin Neurophysiol*, 120(5), 1009-1015.

Hsu, M. J., Nielsen, D. H., Lin-Chan, S. J., & Shurr, D. (2006). The effects of prosthetic foot design on physiologic measurements, self-selected walking velocity, and physical activity in people with transtibial amputation. *Arch Phys Med Rehabil*, 87(1), 123-129.

Hsu, R. W., Sim, F. H., & Chao, E. Y. (1999). Reoperation results after segmental prosthetic replacement of bone and joint for limb salvage. *J Arthroplasty*, 14(5), 519-526.

- Jimenez-Fabian, R., & Verlinden, O. (2012). Review of control algorithms for robotic ankle systems in lower-limb orthoses, prostheses, and exoskeletons. *Med Eng Phys*, 34(4), 397-408.
- Karmarkar, A. M., Collins, D. M., Wichman, T., Franklin, A., Fitzgerald, S. G., Dicianno, B. E., . . . Cooper, R. A. (2009). Prosthesis and wheelchair use in veterans with lower-limb amputation. *J Rehabil Res Dev*, 46(5), 567-576.
- Kaufman, K. R., Frittoli, S., & Frigo, C. A. (2012). Gait asymmetry of transfemoral amputees using mechanical and microprocessor-controlled prosthetic knees. *Clin Biomech (Bristol, Avon)*, 27(5), 460-465.
- Kirtley, C. (1998). Determining initial contact and toe-off from kinematic data, [ON-line]. *Clinical Gait Analysis*, Available: <http://guardian.curtain.edu.cga/faq/toe-off.html>.
- Klute, G. K., Kantor, C., Darrouzet, C., Wild, H., Wilkinson, S., Iveljic, S., & Creasey, G. (2009). Lower-limb amputee needs assessment using multistakeholder focus-group approach. *J Rehabil Res Dev*, 46(3), 293-304.
- Kobayashi, T., Orendurff, M. S., & Boone, D. A. (2013). Effect of alignment changes on socket reaction moments during gait in transfemoral and knee-disarticulation prostheses: case series. *J Biomech*, 46(14), 2539-2545.
- Kobayashi, T., Orendurff, M. S., Zhang, M., & Boone, D. A. (2012). Effect of transtibial prosthesis alignment changes on out-of-plane socket reaction moments during walking in amputees. *J Biomech*, 45(15), 2603-2609.
- Lian, Qin, Li, Dichen, Jin, Zhongmin, Wang, Zhen, & Sun, Yuhuan. (2014). Patient-Specific Design and Biomechanical Evaluation of a Novel Bipolar Femoral Hemi-Knee Prosthesis. *Journal of Bionic Engineering*, 11(2), 259-267.
- Major, M. J., Stine, R. L., & Gard, S. A. (2013). The effects of walking speed and prosthetic ankle adapters on upper extremity dynamics and stability-related parameters in bilateral transtibial amputee gait. *Gait Posture*, 38(4), 858-863.
- Major, M. J., Twiste, M., Kenney, L. P., & Howard, D. (2011). Amputee Independent Prosthesis Properties--a new model for description and measurement. *J Biomech*, 44(14), 2572-2575.
- Martinez-Villalpando, E. C., Weber, J., Elliott, G., & Herr, H. (2008, 19-22 Oct. 2008). Design of an agonist-antagonist active knee prosthesis. Paper presented at the

Biomedical Robotics and Biomechatronics, 2008. BioRob 2008. 2nd IEEE RAS & EMBS International Conference on.

- McGimpsey, G., & Bradford, T. (2010). Limb prosthetics services and devices. Worcester, MA: Bioengineering Institute Center for Neuroprosthetics, Worcester Polytechnic Institution. Retrieved from https://www.nist.gov/sites/default/files/documents/tip/wp/pswp/239_limb_prosthetics_services_devices.pdf
- Mills, P. M., & Barrett, R. S. (2001). Swing phase mechanics of healthy young and elderly men. *Human Movement Science*, 20(4–5), 427-446.
- Miller, Laura A., & Childress, Dudley S. (2005). Problems associated with the use of inverse dynamics in prosthetic applications: An example using a polycentric prosthetic knee. *Robotica*, 23(3), 329-335.
- Morgenroth, D. C., Segal, A. D., Zelik, K. E., Czerniecki, J. M., Klute, G. K., Adamczyk, P. G., . . . Kuo, A. D. (2011). The effect of prosthetic foot push-off on mechanical loading associated with knee osteoarthritis in lower extremity amputees. *Gait Posture*, 34(4), 502-507.
- Morrison, J. B. (1970). The mechanics of the knee joint in relation to normal walking. *Journal of Biomechanics*, 3(1), 51-61.
- Okita, Yusuke, Tatematsu, Noriatsu, Nagai, Koutatsu, Nakayama, Tomitaka, Nakamata, Takeharu, Okamoto, Takeshi, . . . Tsuboyama, Tadao. (2013). Compensation by nonoperated joints in the lower limbs during walking after endoprosthetic knee replacement following bone tumor resection. *Clinical Biomechanics*, 28(8), 898-903.
- Palmer, Michael Lars. (2002). Sagittal plane characterization of normal human ankle function across a range of walking gait speeds. (Master's degree), Massachusetts Institute of Technology, Massachusetts.
- Rajtůková, V., Michalíková, M., Bednarčíková, L., Balogová, A., & Živčák, J. (2014). Biomechanics of Lower Limb Prostheses. *Procedia Engineering*, 96, 382-391.
- Resnik, L., Meucci, M. R., Lieberman-Klinger, S., Fantini, C., Kelty, D. L., Disla, R., & Sasson, N. (2012). Advanced upper limb prosthetic devices: implications for upper limb prosthetic rehabilitation. *Arch Phys Med Rehabil*, 93(4), 710-717.

- Ribeiro, Ana, Rasmussen, John, Flores, Paulo, & F., Silva Luís. (2011). Biomechanical multibody knee model with condyle contact: Modeling, simulation and analysis (Vol. 4): Sociedade Portuguesa Biomecânica.
- Robertson, D. G., & Winter, D. A. (1980). Mechanical energy generation, absorption and transfer amongst segments during walking. *J Biomech*, 13(10), 845-854.
- Robinson, Vicky, Sansam, Kate, Hirst, Lynn, & Neumann, Vera. (2010). Major lower limb amputation – what, why and how to achieve the best results. *Orthopaedics and Trauma*, 24(4), 276-285.
- Rosenfeld, Amnon, Dvorachek, Michael, & Rotstein, Ilan. (2000). Bronze Single Crown-like Prosthetic Restorations of Teeth from the Late Roman Period. *Journal of Archaeological Science*, 27(7), 641-644.
- Rowe, P. J., Myles, C. M., Walker, C., & Nutton, R. (2000). Knee joint kinematics in gait and other functional activities measured using flexible electrogoniometry: how much knee motion is sufficient for normal daily life? *Gait Posture*, 12(2), 143-155.
- Rusaw, D., & Ramstrand, N. (2010). Sagittal plane position of the functional joint centre of prosthetic foot/ankle mechanisms. *Clin Biomech (Bristol, Avon)*, 25(7), 713-720.
- Russell Esposito, E., & Wilken, J. M. (2014). Biomechanical risk factors for knee osteoarthritis when using passive and powered ankle-foot prostheses. *Clin Biomech (Bristol, Avon)*, 29(10), 1186-1192.
- Sagawa, Y., Jr., Turcot, K., Armand, S., Thevenon, A., Vuillerme, N., & Watelain, E. (2011). Biomechanics and physiological parameters during gait in lower-limb amputees: a systematic review. *Gait Posture*, 33(4), 511-526.
- Sanders, J. E., Bell, D. M., Okumura, R. M., & Dralle, A. J. (1998). Effects of alignment changes on stance phase pressures and shear stresses on transtibial amputees: measurements from 13 transducer sites. *IEEE Trans Rehabil Eng*, 6(1), 21-31.
- Schache, Margaret B., McClelland, Jodie A., & Webster, Kate E. (2014). Lower limb strength following total knee arthroplasty: A systematic review. *The Knee*, 21(1), 12-20.

- Schipplein, O. D., & Andriacchi, T. P. (1991). Interaction between active and passive knee stabilizers during level walking. *J Orthop Res*, 9(1), 113-119.
- Schultz, A. E., & Kuiken, T. A. (2011). Neural interfaces for control of upper limb prostheses: the state of the art and future possibilities. *PM R*, 3(1), 55-67.
- Segal, A. D., Zelik, K. E., Klute, G. K., Morgenroth, D. C., Hahn, M. E., Orendurff, M. S., . . . Czerniecki, J. M. (2012). The effects of a controlled energy storage and return prototype prosthetic foot on transtibial amputee ambulation. *Human Movement Science*, 31(4), 918-931.
- Shelburne, K. B., Torry, M. R., & Pandy, M. G. (2006). Contributions of muscles, ligaments, and the ground-reaction force to tibiofemoral joint loading during normal gait. *J Orthop Res*, 24(10), 1983-1990.
- Short, C. A., O'Connell, C. M., Kirby, R. L., de Saint-Sardos, J. J., & Reid, C. A. (1999). Prostheses for persons with lower-limb amputations: an extra joint increases range of motion. *Arch Phys Med Rehabil*, 80(7), 854-856.
- Silverman, A. K., Fey, N. P., Portillo, A., Walden, J. G., Bosker, G., & Neptune, R. R. (2008). Compensatory mechanisms in below-knee amputee gait in response to increasing steady-state walking speeds. *Gait Posture*, 28(4), 602-609.
- Sup, F. C. (2009). A powered self-contained knee and ankle prosthesis for near normal gait in transfemoral amputees. Doctor of Philosophy, Faculty of the Graduate School of Vanderbilt University.
- Takahashi, K. Z., & Stanhope, S. J. (2013). Mechanical energy profiles of the combined ankle-foot system in normal gait: insights for prosthetic designs. *Gait Posture*, 38(4), 818-823.
- van Keeken, Helco G., Vrieling, Aline H., Hof, At L., Postema, Klaas, & Otten, Bert. (2012). Principles of obstacle avoidance with a transfemoral prosthetic limb. *Medical Engineering & Physics*, 34(8), 1109-1116.
- Vanicek, N., Strike, S., McNaughton, L., & Polman, R. (2009). Postural responses to dynamic perturbations in amputee fallers versus nonfallers: a comparative study with able-bodied subjects. *Arch Phys Med Rehabil*, 90(6), 1018-1025.
- Ventura, J. D., Klute, G. K., & Neptune, R. R. (2011). The effects of prosthetic ankle dorsiflexion and energy return on below-knee amputee leg loading. *Clin Biomech (Bristol, Avon)*, 26(3), 298-303.

- Vrieling, A. H., van Keeken, H. G., Schoppen, T., Otten, E., Hof, A. L., Halbertsma, J. P., & Postema, K. (2008). Balance control on a moving platform in unilateral lower limb amputees. *Gait Posture*, 28(2), 222-228.
- Watve, Sachin, Dodd, Greg, MacDonald, Ruth, & Stoppard, Elizabeth R. (2011). Upper limb prosthetic rehabilitation. *Orthopaedics and Trauma*, 25(2), 135-142.
- Winter, D. A. (1992). Foot trajectory in human gait: a precise and multifactorial motor control task. *Phys Ther*, 72(1), 45-53; discussion 54-46.
- Winter, David A. (1991). *The Biomechanics and Motor Control of Human Gait: Normal, Elderly and Pathological*, 2nd Edition.
- Winter, David A. (2009). *Biomechanics and Motor Control of Human Movement*, Fourth Edition Mechanical Engineering - Design: Wiley.
- Winter, David A. (2009). *Kinematics Biomechanics and Motor Control of Human Movement* (pp. 45-81): John Wiley & Sons, Inc.
- Winter, David A., & Sienko, Susan E. (1988). Biomechanics of below-knee amputee gait. *Journal of Biomechanics*, 21(5), 361-367.
- Wu, Sai-Kit, Waycaster, Garrett, & Shen, Xiangrong. (2011). Electromyography-based control of active above-knee prostheses. *Control Engineering Practice*, 19(8), 875-882.
- Zach, L., Kuncicka, L., Ruzicka, P., & Kocich, R. (2014). Design, analysis and verification of a knee joint oncological prosthesis finite element model. *Comput Biol Med*, 54, 53-60.
- Ziegler-Graham, K., MacKenzie, E. J., Ephraim, P. L., Travison, T. G., & Brookmeyer, R. (2008). Estimating the prevalence of limb loss in the United States: 2005 to 2050. *Arch Phys Med Rehabil*, 89(3), 422-429.

LIST OF PUBLICATIONS

- Bhuiyan, M. S. H., I. A. Choudhury and M. Dahari (2015). Development of a control system for artificially rehabilitated limbs: a review. *Biological Cybernetics* 109(2): 141-162.
- Bhuiyan, M. S. H., Choudhury, I. A., Dahari, M., Nukman, Y. and Dawal, S. Z. An investigation into a gear based knee joint designed for lower limb prosthesis. *Applied Bionics and Biomechanics* doi.org/10.1155/2017/7595642.
- Bhuiyan, M. S. H., Choudhury, I. A., Dahari, M., Y. Nukman. and Dawal, S. Z. A review on limb defects and corresponding control systems for assistive devices. *Journal of Rehabilitation Research & Development* (Under review).
- Bhuiyan, M. S. H., Choudhury, I. A., Dahari, M., Nukman, Y. and Dawal, S. Z. An investigation into a spring based ankle joint designed for lower limb prosthesis. *Gait & Posture* (Under review).
- Bhuiyan, M. S. H., Choudhury, I. A., Dahari, M., Nukman, Y. and Dawal, S. Z. Gait Performance analysis of a mechanically controlled prosthesis in resolving the difficulties of the above knee amputee. *Journal of Rehabilitation Research and Development* (Under Review).
- Bhuiyan, M. S. H., Choudhury, I. A., Dahari, M., Nukman, Y. and Dawal, S. Z. Stability Performance analysis of a mechanically controlled prosthesis in resolving the difficulties of the above knee amputee. *Journal of Rehabilitation Research and Development* (Under Review).